THE UNIVERSITY OF TEXAS AT AUSTIN
CENTER FOR TRANSPORTATION RESEARCH

TECHNICAL REPORT 0-7070-1
TxDOT PROJECT NUMBER 0-7070

Develop Guidelines and Best Practices for Bonding Hot-Mix Asphalt to Portland Cement Concrete Pavement: Final Report

Satyavati Komaragiri, Ph.D.
Thanos Drimalas, Ph.D.
Darren Hazlett, P.E.
Zahra Sotoodeh-Nia, Ph.D.
Kevin Folliard, Ph.D.
Amit Bhasin, Ph.D., P.E.
Gamal Mabrouk, Ph.D.
Samer Dessouky, Ph.D.

August 2022
Published October 2022

https://library.ctr.utexas.edu/ctr-publications/0-7070-1.pdf

Technical Report Documentation Page

1. Report No. FHWA/TX-22/0-7070-1	2. Government Accession No.	3. Recipient's Catalog No.
4. Title and Subtitle Develop Guidelines and Best Practices for Bonding Hot-Mix Asphalt to Portland Cement Concrete Pavement: Final Report		5. Report Date Submitted: August 2022 6. Performing Organization Code
7. Author(s) Satyavati Komaragiri, Thanos Drimalas, Darren Hazlett https://orcid.org/0000-0002-8360-0022, Zahra Sotoodeh-Nia, Kevin Folliard https://orcid.org/0000-0003-3080-5486, Amit Bhasin https://orcid.org/0000-0001-8076-7719, Gamal Mabrouk, and Samer Dessouky		8. Performing Organization Report No. 0-7070-1
9. Performing Organization Name and Address Center for Transportation Research The University of Texas at Austin 3925 W. Braker Lane, 4th Floor Austin, TX 78759		10. Work Unit No. (TRAIS) 11. Contract or Grant No. 0-7070
12. Sponsoring Agency Name and Address Texas Department of Transportation Research and Technology Implementation Division 125 E. 11th Street Austin, TX 78701		13. Type of Report and Period Covered Technical Report September 2020 – August 2022 14. Sponsoring Agency Code
15. Supplementary Notes Project performed in cooperation with the Texas Department of Transportation and the Federal Highway Administration.		
16. Abstract Proper bonding between diferent layers of a composite pavement is the major factor in ensuring that the entire structure acts as a monolithic layer under loading. This bonding is provided by a thin layer of tack coat that is applied between the pavement layers. This project studied the bonding between hot mix asphalt (HMA) and concrete layers of a composite pavement using tack coats. The goals of this study were to: (i) identify, develop, and validate a test method(s) that can be used on a routine basis to screen and/or field-test the quality of the bond between the asphalt and the concrete layer; (ii) use the method to evaluate the impact of various factors on the performance of the bond, including but not limited to type of tack coat or membrane, application rate, surface texture (including cost-effective and innovative ways to prepare concrete surfaces), and surface moisture; and (iii) propose guidelines for future selection of surface preparation techniques and materials that will meet the requirements for adequate bonding at the interlayer surfaces. This study developed two test procedures. One test is a direct shear test using roadway cores or laboratory manufactured samples for use in the laboratory. The second is a pull-of test that can be conducted in-situ on a project site. Laboratory and field testing allowed development of suggested limits for these tests to indicate adequate bond strength. Pavement preparation for the concrete pavement for tack and HMA overlay were also suggested.		
17. Key Words Hot Mix Asphalt (HMA) Pavement, Portland Cement Concrete (PCC) Pavement, Tack Coat, Seal Coat, Bond, Shear Test, Pull-Off Test	18. Distribution Statement No restrictions. This document is available to the public through the National Technical Information Service, Alexandria, Virginia 22312; www.ntis.gov.	

19. Security Classif. (of report)	20. Security Classif. (of this page)	21. No. of pages	22. Price
Unclassified	Unclassified	172	

Form DOT F 1700.7 (8-72) Reproduction of completed page authorized

THE UNIVERSITY OF TEXAS AT AUSTIN
CENTER FOR TRANSPORTATION RESEARCH

Develop Guidelines and Best Practices for Bonding Hot-Mix Asphalt to Portland Cement Concrete Pavement: Final Report

Satyavati Komaragiri, Ph.D.
Thanos Drimalas, Ph.D.
Darren Hazlett, P.E.
Zahra Sotoodeh-Nia, Ph.D.
Kevin Folliard, Ph.D.
Amit Bhasin, Ph.D., P.E.

Center for Transportation Research
The University of Texas at Austin
Austin, Texas 78712

Gamal Mabrouk, Ph.D.
Samer Dessouky, Ph.D.

The University of Texas at San Antonio
San Antonio, Texas 78249

CTR Technical Report:	0-7070-1
Report Date:	Submitted: August 2022
Project:	0-7070
Project Title:	Develop Guidelines and Best Practices for Bonding Hot-Mix Asphalt to Portland Cement Concrete Pavement
Sponsoring Agency:	Texas Department of Transportation
Performing Agency:	Center for Transportation Research at The University of Texas at Austin

Project performed in cooperation with the Texas Department of Transportation and the Federal Highway Administration.

Center for Transportation Research
The University of Texas at Austin
3925 W. Braker Lane, 4th floor
Austin, TX 78759

http://ctr.utexas.edu/

DISCLAIMERS

Author's Disclaimer: The contents of this report reflect the views of the authors, who are responsible for the facts and the accuracy of the data presented herein. The contents do not necessarily reflect the official view or policies of the Federal Highway Administration or the Texas Department of Transportation (TxDOT). This report does not constitute a standard, specification, or regulation. Mention of trade names or commercial products does not constitute endorsement or recommendations for use.

Patent Disclaimer: There was no invention or discovery conceived or first actually reduced to practice in the course of or under this contract, including any art, method, process, machine manufacture, design or composition of matter, or any new useful improvement thereof, or any variety of plant, which is or may be patentable under the patent laws of the United States of America or any foreign country.

ENGINEERING DISCLAIMER

NOT INTENDED FOR CONSTRUCTION, BIDDING, OR PERMIT PURPOSES.

Project Engineer: Amit Bhasin
Professional Engineer License State and Number: Texas No. 126265
P.E. Designation: Research Supervisor

ACKNOWLEDGMENTS

The authors acknowledge the financial support of Texas Department of Transportation, RTI project 7070. The authors acknowledge support from the project monitoring committee members, Aido Madrid, Arash Motamed, Enad Mahmoud, Marta Stephens, Travis Patton, and RTI project manager Tom Schwerdt.

The authors thank Thomas Blackmore, Brenda Guerra, Steven Schmidt, Jacob Wells from Austin District; Soojun Han and Ben Mebarkia from Houston District; Andres Gonzalez, Diana Rogerio from San Antonio District; Kevin Grissom, Kenneth Wiemers, Ashley Dubose, Mark Kelley, Joe Seago, John Sudela, Keith Horn from Beaumont District; Bill Compton, Jeff Jackson from Waco District; Lacy Peters from Atlanta District for their help in coordinating with field testing.

Authors would also like to thank Chuck Fuller for his help in accessing a TOM mix for overlay testing. Finally, the authors would like to acknowledge Mr. Si-Yoon Woo for his help with the laboratory testing, and Mr. Tyler Seay and Dr. Angelo Filonzi for helping develop and carry out the field test procedure.

ABSTRACT

Proper bonding between different layers of a composite pavement is the major factor in ensuring that the entire structure acts as a monolithic layer under loading. This bonding is provided by a thin layer of tack coat which is applied between the pavement layers. This project studied the bonding between hot mix asphalt (HMA) and concrete layers of a composite pavement using tack coats. The goals of this study were to: (i) identify, develop, and validate a test method(s) that can be used on a routine basis to screen and/or field-test the quality of the bond between the asphalt and the concrete layer; (ii) use the method to evaluate the impact of various factors on the performance of the bond, including but not limited to, type of tack coat or membrane, application rate, surface texture (including cost-effective and innovative ways to prepare concrete surfaces), and surface moisture; and (iii) propose guidelines for future selection of surface preparation techniques and materials that will meet the requirements for adequate bonding at the interlayer surfaces. This study developed two test procedures. One test is a direct shear test using roadway cores or laboratory manufactured samples for use in the laboratory. The second is a pull-off test that can be conducted in-situ on a project site. Laboratory and field testing allowed development of suggested limits for these tests to indicate adequate bond strength. Pavement preparation for the concrete pavement for tack and HMA overlay were also suggested.

EXECUTIVE SUMMARY

Problem

Proper bonding between different layers of a composite pavement is the major factor in ensuring that the entire structure acts as a monolithic layer under loading. This bonding is provided by a thin layer of tack coat which is applied between the pavement layers. The primary function of a well-performing tack coat is to provide a strong adhesive bond between the existing pavement layer and its overlying surface so that the pavement does not experience rapid surface failures causing a reduction in service life. Measuring this bond to ensure its efficacy is critical for the successful performance of the overlay and is the goal of this study.

Objectives

The objectives of this study were to:

- determine the influencing factors on the performance of the hot mix asphalt (HMA) - Portland cement concrete (PCC) interface layer (tack coat),
- develop test(s) and investigate the influencing factors' effects on the functioning of the tack coat, and
- provide guidelines on requirements and best practices,

all to ensure the efficacy of the tack coat bond between the HMA and PCC.

Methodology

A literature review presented some of the most recent advancements and findings on bonding HMA to PCC. Important factors found in the literature that substantially influence the shear performance and bond strength of tack coats include:

- Tack coat material,
- Tack coat application rate,
- Concrete surface texture,
- Concrete cleanliness, and
- Concrete moisture.

Tests were evaluated for measuring the interfacial bond of test specimens. A modification of a direct shear test with confinement force, and a pull-off test were chosen for evaluating the above factors and their influence the bond.

A computer simulation using finite element analysis was performed to evaluate the stresses and strains at various locations in the composite pavement structure.

A set of laboratory experiments was designed and executed to evaluate the aforementioned factors on the bond effectiveness. A partial factorial test matrix was developed to use:

- four different tack coat types (Trackless tack #1, Trackless tack #2, Asphalt Rubber Binder, and PG 70-22),
- four levels of application rate for two different tack coat types,
- four different concrete surface textures (tined-polished, sand blasted, hydro-demolition, and polished),
- two levels of concrete cleanliness (clean and dirty [using aggregate fines as a surface contaminant]), and
- three levels of surface moisture (wet, moist, and dry).

Field evaluations of direct shear and pull-off tests were conducted at several field projects to validate the test procedures and to aid in setting shear and pull-off limits.

Conclusions

The following conclusions can be drawn based on this study.

- Some tack coat materials exhibit higher pull-off strength and shear strength and others (e.g. AR binder) exhibit more ductility.
- The influence of application rate on strength is not significant. However, ductility improved for Trackless tack #2 with an increase in application rate.
- Sandblasting and hydro-demolition are best performing surface texture both in terms of strength and ductility.
- The influence of PCC surface cleanliness and PCC surface moisture on PCC-HMA bond is not significant. However, good construction practices should be followed to ensure surfaces of PCC are as clean and dry as possible.
- A good correlation is observed between shear strength and pull-off strength obtained from direct shear test and pull-off test, respectively. This means that a field pull-off test could be used to ensure adequate bond of the HMA to the PCC.
- Most of the identified field sections exhibited a pull-off strength higher than 25 psi, which can be used as a frame of reference for acceptable performance.

Recommendations

Tests and Limits

This study recommends the modification of the existing direct shear test method to incorporate a newer type of loading jig that has the provision to apply a compressive load while conducting a shear strength test. This study also recommends the use of the field pull-off test for forensic purposes as needed as well as for QA purposes on newly placed overlays.

Data from both laboratory and field components using the shear and pull-off tests suggests the minimum shear strength between the HMA and concrete pavement should be 40 psi and corresponding pull-off strength of 25 psi. Field testing also indicates 20 psi as adequate, but the field tests were not performed on materials where failures had occurred, except in Waco. The results of lab and field studies both point to the use of the pull-off-test for evaluation of the tack coat bond for HMA overlays of concrete pavement in the field.

Both direct shear and pull-off strengths are typically higher when using trackless tack materials as compared to the use of a hot applied binder with aggregates (chip seal type) interface.

Implementation

The study recommends either to:

- use an evaluation procedure to study tack coat for a specific project using field conditions of concrete texture (using cores or manufactured concrete specimens), project proposed HMA, and tack coat type and application rate, in direct shear and correlate this with pull-off measurements, followed by the use of the pull-off test on the project to verify adequate bond, OR
- conduct pull-off tests in the field on the project to ensure that a minimum pull-off strength of 20 psi is attained.

To enhance bond, the concrete surface must be cleaned and free of debris before placing the tack coat and hot mix asphalt. If the concrete surface is new (as in the case when HMA on new concrete is required to match existing profile during expansion), it is vital to ensure that any curing compounds from the concrete surface are removed.

The following steps are highly recommended for surface preparation.

- Diamond grind the deck by approximately 1/16 inch to remove any contaminants.

- Pressure wash surface with water and allow the surface to dry or clean with compressed air.
- Apply tack coat.

TABLE OF CONTENTS

List of Figures xvi

List of Tables xxii

1 Introduction 1

1.1 Problem Statement . . . 1
1.2 Study Objectives . . . 1
1.3 Structure of the Report . . . 1

2 Comprehensive Documentation of Current Practices and Specifications 3

2.1 Materials . . . 3
2.1.1 Tack coat types . . . 3
2.1.1.1 Asphalt emulsions . . . 5
2.1.1.2 Asphalt binders . . . 6
2.1.1.3 Asphalt cutbacks . . . 6
2.1.1.4 Summary . . . 6
2.2 Failure Modes . . . 7
2.3 Numerical modeling . . . 7
2.3.1 FEM to simulate pavement responses under FWD loading . . . 8
2.3.2 FEM to simulate pavement responses under moving vehicular loading . . . 10
2.3.3 FEM to study pavement distresses and structural capacity . . . 10
2.3.4 FEM to study the PCC-HMA interface bonding characteristics 12
2.4 Laboratory performance and evaluation of tack coats . . . 14
2.4.1 Specimen preparation in the lab . . . 14
2.4.2 Tack coat evaluation . . . 15
2.4.3 HMA-PCC interlayer bonding evaluation . . . 16
2.4.4 Field performance measurement and validation . . . 18
2.4.5 Application of tack coats . . . 19
2.5 Design factors . . . 19
2.5.1 Effect of application temperature on the tack coat performance 19

2.5.2 Effect of testing temperature on the tack coat performance . 19
2.5.3 Effect of concrete surface texture on the tack coat performance 20
2.5.4 Effect of application rate 22
2.5.5 Effect of PCC cleanliness 24
2.5.6 Effect of wetness on the tacked surface and on the PCC surface 24
2.6 Summary 25

3 Selection of Methods, Materials, and Protocols 26
3.1 PCC Surface Preparation Techniques 26
3.1.1 Tining 26
3.1.2 Diamond grinding 27
3.1.3 Next-Generation Concrete Surface (NGCS) 28
3.1.4 Milling 28
3.1.5 Sandblasting 29
3.1.6 Hydro-demolition 29
3.1.7 Summary 30
3.2 HMA-PCC interfacial layer evaluation 31
3.2.1 Test 1: Direct Shear Test 33
3.2.2 Test 2: Pull-Off Test 34
3.2.3 Test 3: Torsional Shear Test 38
3.2.4 Arcan Test 40
3.2.5 Summary 40
3.3 Established Protocols 42
3.3.1 Protocol for Direct Shear to Evaluate Tack Coat 42
3.3.2 Protocol for pull-off test 44
3.4 Materials and application rates 49
3.4.1 Emulsion tack coats 49
3.4.2 PG binder Tack Coat 49
3.4.3 AR Tack Coats 49
3.4.4 Application rates 50

4 Finite Element (FE) Modeling and 3-D Computational Simulation 51
4.1 Overview and task objectives 51
4.2 Explicit FE dynamic simulation of the pavement structures 51

4.2.1 Modeling the pavement structure . . . 51
4.2.2 Modeling of wheel load . . . 55
4.2.3 FEM interactions and boundary conditions . . . 57
4.3 Simulation results . . . 58
4.3.1 Longitudinal shear stress at HMA-PCC interface . . . 58
4.3.2 Longitudinal shear strain at the HMA-PCC interface . . . 60
4.3.3 Transverse shear stress at HMA-PCC interface . . . 61
4.3.4 Transverse shear strain at the HMA-PCC interface . . . 63
4.4 Findings . . . 64

5 Finalizing test procedures to measure PCC-HMA bonding and evaluating influence of different factors on quality of bond 65
5.1 Influence of tack coat type . . . 65
5.1.1 Application of AR binder . . . 66
5.1.2 Application of other tack coats . . . 67
5.2 Influence of application rate . . . 67
5.3 Influence of PCC surface texture . . . 68
5.4 Influence of surface cleanliness . . . 70
5.5 Influence of surface moisture . . . 71
5.6 Sample preparation and testing . . . 72
5.6.1 PCC sample preparation . . . 72
5.6.1.1 Polished . . . 72
5.6.1.2 Tined-polished . . . 72
5.6.1.3 Sandblasting . . . 73
5.6.1.4 Hydro-demolition . . . 73
5.6.2 Application of tack coat . . . 73
5.6.3 Compaction of asphalt mix on PCC sample . . . 74
5.6.4 Testing . . . 75
5.6.4.1 Direct shear test . . . 75
5.6.4.2 Pull-off test . . . 77
5.7 Results . . . 78
5.7.1 PCC-HMA without tack coat . . . 78
5.7.2 Tack coat type . . . 78

5.7.3 Application rate . . . 80
5.7.4 PCC surface texture . . . 84
5.7.5 Surface cleanliness . . . 88
5.7.6 Surface moisture . . . 92
5.7.7 Pull-off strength vs direct shear strength . . . 96
5.8 Conclusions . . . 96

6 Evaluation of Field Sections **98**
6.1 Identified Sections . . . 98
6.2 Specimen Coring . . . 100
6.2.1 Procedure . . . 101
6.3 HMA-PCC Interfacial layer Evaluation . . . 103
6.3.1 Test 1: Direct Shear Test . . . 103
6.3.2 Test 2: Pull-Off Test . . . 105
6.4 Results and Discussion . . . 106
6.4.1 Direct Shear Test . . . 106
6.4.1.1 AUS SH130 . . . 107
6.4.1.2 HOU IH69 . . . 108
6.4.1.3 HOU SH225 . . . 109
6.4.1.4 SAT IH35 . . . 111
6.4.1.5 SAT I410 . . . 112
6.4.2 Pull-off test . . . 113
6.4.2.1 AUS SH130 . . . 114
6.4.2.2 HOU IH69 . . . 114
6.4.2.3 HOU SH225 . . . 115
6.4.2.4 Waco . . . 115
6.4.2.5 SAT IH35 . . . 117
6.4.2.6 SAT I410 . . . 118
6.5 Conclusions . . . 119

7 Conclusions and Recommendations **120**
7.1 Conclusions . . . 120
7.2 Recommendations . . . 121
7.2.1 Test and limits . . . 121

7.2.2 Implementation 121

References **122**

Appendix A **133**

Appendix B **139**

Appendix C **147**

LIST OF FIGURES

Figure 2.1. Schematic showing major distress modes at the interface layer (Raab and Partl, 2004) . . . 7
Figure 2.2. Schematic showing test modes for evaluation of tack coats (Wang et al., 2017) . . . 17
Figure 3.1. Specimen fabrication in the laboratory using a vibratory compactor . . . 32
Figure 3.2. Specimen fabrication using the Marshall compactor . . . 32
Figure 3.3. Interfacial layer shear strength device . . . 33
Figure 3.4. Tack coat shear strength tester (Gilson Inc.) . . . 34
Figure 3.5. Tack coat pull-off test (TxDOT designation:Tex-243-F) . . . 35
Figure 3.6. Direct pull-off test device . . . 36
Figure 3.7. A metal plate glued to the HMA surface . . . 37
Figure 3.8. Metal plates placed on the tack coat, and left under weights to achieve proper bonding with the tack coat . . . 38
Figure 3.9. Top Left: Aluminum disc sample in the shearing jig; Bottom Left: Disc sample in the shearing jig with confining plates and the compressive pressure in loading frame; Top Right: Tack coat joint between the shearing discs; Middle Right: Disc sample in the shearing jig with confining plates; Bottom Right: Failed samples . . . 44
Figure 3.10. Thermoelectric temperature control system that can be used in the field . . . 45
Figure 3.11. Coring of the asphalt overlay and concrete sub-surface by approximately 1/4" . . . 46
Figure 3.12. Metal caps on two specimens for pull-off test . . . 47
Figure 3.13. Tests conducted using multiple adhesives to determine the best adhesive for this application . . . 47
Figure 3.14. The pull-off device being locked on to the sample and the test being conducted using a force-controlled mode at a rate of 1 N/sec . . . 48

Figure 3.15. The pull-off test after completion; the figure also shows the epoxy system that was successful 48
Figure 4.1. FE modeled pavement structure (Mabrouk et al., 2021) . . 53
Figure 4.2. $|E^*|$ master curve at a reference temperature of 70°F and phase angles (ϕ) for a typical Type B HMA 53
Figure 4.3. FE modeling of the tire components (Mabrouk et al., 2021) 56
Figure 4.4. FE models assembly: (a) super single tire, (b) dual tires, and (c) tandem tire configuration 58
Figure 4.5. Longitudinal shear stress (X-X) at the HMA-PCC interface for a load level: (a) 6000 on a dual half axle, (b) 6000 lb on a super single half axle, and (c) 6000 lb on a tandem half axle 59
Figure 4.6. Longitudinal shear stress (X-X) at HMA-PCC interface for a load level: (a) 8000 lb on a super single half axle, (b) 8000 lb on a tandem half axle 59
Figure 4.7. Longitudinal shear stress (X-X) at HMA-PCC interface for a load level: (a) 10,000 lb on a super single half axle, (b) 10,000 lb on a tandem half axle 60
Figure 4.8. Longitudinal shear strain (X-X) at HMA-PCC interface for a load level: (a) 6000 on a dual half axle, (b) 6000 lb on a super single half axle, and (c) 6000 lb on a tandem half axle 60
Figure 4.9. Longitudinal shear strain (X-X) at HMA-PCC interface for a load level: (a) 8000 lb on a super single half axle, (b) 8000 lb on a tandem half axle 61
Figure 4.10. Longitudinal shear strain (X-X) at the HMA-PCC interface for a load level: (a) 10,000 lb on a super single half axle, (b) 10,000 lb on a tandem half axle 61
Figure 4.11. Transverse shear stress (X-Z) at the HMA-PCC interface for a load level: (a) 6000 on a dual half axle, (b) 6000 lb on a super single half axle, and (c) 6000 lb on a tandem half axle 62
Figure 4.12. Transverse shear stress (X-Z) at the HMA-PCC interface for a load level: (a) 8000 lb on a super single half axle, (b) 8000 lb on a tandem half axle 62

Figure 4.13. Transverse shear stress (X-Z) at the HMA-PCC interface for a load level: (a) 10,000 lb on a super single half axle, (b) 10,000 lb on a tandem half axle 63
Figure 4.14. Transverse shear strain (X-Z) at the HMA-PCC interface for a load level: (a) 6000 on a dual half axle, (b) 6000 lb on a super single half axle, and (c) 6000 lb on a tandem half axle 63
Figure 4.15. Transverse shear strain (X-Z) at the HMA-PCC interface for a load level: (a) 8000 lb on a super single half axle, (b) 8000 lb on a tandem half axle 64
Figure 4.16. Transverse shear strain (X-Z) at the HMA-PCC interface for a load level: (a) 10,000 lb on a super single half axle, (b) 10,000 lb on a tandem half axle 64
Figure 5.1. Precoated aggregates for creating chip seal 66
Figure 5.2. A PCC sample with AR binder as chip seal 67
Figure 5.3. A PCC sample with Trackless tack #2 applied on it 67
Figure 5.4. Procedure for preparation of a composite PCC-HMA sample for shear testing 74
Figure 5.5. Procedure for direct shear testing in laboratory 76
Figure 5.6. A typical stress-strain curve obtained from direct shear test showing the two parameters (1) shear strength and (2) brittleness factor 77
Figure 5.7. Procedure for pull-off testing in laboratory 78
Figure 5.8. Pull-off strength for different tack coat types 79
Figure 5.9. Shear strength for different tack coat types 80
Figure 5.10. Brittleness factor in shear for different tack coat types . . . 80
Figure 5.11. Pull-off strength at different application rates for (top) Trackless tack #2, (bottom) AR binder 81
Figure 5.12. Shear strength at different application rates for (top) Trackless tack #2, (bottom) AR binder 82
Figure 5.13. Brittleness factor at different application rates for (top) Trackless tack #2, (bottom) AR binder 83

Figure 5.14. Pull-off strength for different PCC surface textures for two different types of tack coats: (top) Trackless tack #2, (bottom) AR binder 85
Figure 5.15. Shear strength for different PCC surface textures for two different type of tack coats: (top) Trackless tack #2, (bottom) AR binder 86
Figure 5.16. Brittleness factor for different PCC surface textures for two different types of tack coats: (top) Trackless tack #2, (bottom) AR binder 87
Figure 5.17. Pull-off strength based on surface cleanliness for different PCC surface textures for two different types of tack coats: (top) Trackless tack #2, (bottom) AR binder 89
Figure 5.18. Shear strength based on surface cleanliness for different PCC surface textures for two different types of tack coats: (top) Trackless tack #2, (bottom) AR binder 90
Figure 5.19. Brittleness factor based on surface cleanliness for different PCC surface textures for two different types of tack coats: (top) Trackless tack #2, (bottom) AR binder 91
Figure 5.20. Pull-off strength based on surface moisture for different PCC surface textures for two different types of tack coats: (top) Trackless tack #2, (bottom) AR binder 93
Figure 5.21. Shear strength based on surface moisture for different PCC surface textures for two different types of tack coats: (top) Trackless tack #2, (bottom) AR binder 94
Figure 5.22. Brittleness factor based on surface moisture for different PCC surface textures for two different types of tack coats: (top) Trackless tack #2, (bottom) AR binder 95
Figure 5.23. Pull-off strength versus direct shear strength for all the combinations of different parameters in this study 96
Figure 6.1. Cores from HOU SH225 with failure at the interface during coring 100
Figure 6.2. Cores from SAT US90 with significant stripping at the bottom of HMA layer 101

Figure 6.3. Cores from BMT US87 Beaumont district where the HMA debonded from PCC during coring . . . 101
Figure 6.4. Procedure for obtaining 6-inch cores for the laboratory shear test . . . 102
Figure 6.5. Procedure for obtaining 2-inch pull-off samples for in-situ field test . . . 102
Figure 6.6. Schematic of shear loads applied on 6-inch specimens (a), and combination of shear and normal loads on 6-inch specimens (b) . . . 103
Figure 6.7. Tack coat shear strength tester (Gilson Inc.) . . . 104
Figure 6.8. In-situ pull-off test procedure (from top-left clockwise: cleaning of cores using an air jet; application of high strength epoxy to glue pull-off plate; use of a temperature control chamber to cure and condition the test specimen; pull-off test being conducted on one of the four replicates; image after completion of all four replicate pull-off tests) . . . 105
Figure 6.9. Comparison of maximum shear strength for the five identified field sections . . . 106
Figure 6.10. Comparison of the area under the load-displacements curves for the five identified field sections . . . 107
Figure 6.11. Load-displacement curves for AUS SH130 cores . . . 108
Figure 6.12. Top view from AUS SH130 cores after shear test . . . 108
Figure 6.13. Load-displacement curves for Hou IH69 cores . . . 109
Figure 6.14. Top view from Hou IH69 cores after shear test . . . 109
Figure 6.15. Load-displacement curves for Hou SH225 core . . . 110
Figure 6.16. Top view from Hou SH225 core after shear test . . . 110
Figure 6.17. Load-displacement curves for SAT IH35 cores . . . 111
Figure 6.18. Top view from SAT IH35 cores after shear test . . . 111
Figure 6.19. Side view from SAT IH35 cores after shear test . . . 112
Figure 6.20. Load-displacement curves for SAT I410 core . . . 112
Figure 6.21. Side and top view from SAT I410 core after shear test . . . 113
Figure 6.22. Comparison of pull-off strength for the five identified field sections and the Waco project . . . 113

Figure 6.23. Pull-off test on SH130 using AR Type II as tack coat 114
Figure 6.24. Pull-off test on IH69 using AR Type III as tack coat 114
Figure 6.25. Pull-off test on SH225 using trackless tack as tack coat . . 115
Figure 6.26. Waco NB widening section- diamond ground- No Treatment- Hot-applied trackless tack 116
Figure 6.27. Waco SB existing deck with treatment 116
Figure 6.28. Waco SB widening- no treatment- no diamond grinding- hot-applied trackless tack- 1st spot 117
Figure 6.29. Waco SB widening- no treatment- no diamond grinding- hot-applied trackless tack- 2nd spot 117
Figure 6.30. Pull-off test on I35 118
Figure 6.31. Pull-off test on I410 118
Figure C.1. Parameters used for economic analysis for VOR. 149
Figure C.2. Illustration of the NPV over a period of 20 years. 150

LIST OF TABLES

Table 2.1. Number of US and Canadian agencies using PG binders as tack coat (Gierhart and Johnson, 2018) 4
Table 2.2. Number of US and Canadian agencies using emulsions as tack coat (Gierhart and Johnson, 2018) 4
Table 2.3. Number of US and Canadian agencies using reduced-tracking emulsions as tack coat (Gierhart and Johnson, 2018) 5
Table 2.4. Recommended tack coat application rates 23
Table 3.1. Comparison of different surface preparation techniques (1 least preferred and 5 most preferred) 31
Table 3.2. Comparison of different test methods for characterizing the bonding performance of tack coats (1 is most preferred and 5 is least preferred) 41
Table 4.1. FE modeled pavement layer characteristics 54
Table 4.2. Prony series parameters for the modeled Type B HMA overlay thickness 54
Table 4.3. Material properties for the tire models (Alshukri et al., 2019) 56
Table 4.4. Simulated FE load levels for each axle configuration 57
Table 5.1. Test matrix to evaluate the influence of application rate . . 68
Table 5.2. Four different PCC surface textures evaluated in this study . 69
Table 5.3. Clean and dirty conditions for different PCC surface textures 71
Table 6.1. Identified field sections 99
Table C.1. Functional Areas for Project 0-7057 147

CHAPTER 1. INTRODUCTION

1.1 PROBLEM STATEMENT

It has been reported throughout Texas that the poor bond of a hot mix asphalt (HMA) with the underlying Portland cement concrete (PCC) layers has caused deformation or delamination of the HMA layer. Proper bonding between different layers of a composite pavement is the major factor in maintaining the entire structure acting as a monolithic layer under loading. This bonding is provided by a thin layer of tack coat which is applied between the pavement layers. The primary function of a well-performing tack coat is to provide strong adhesive bond between the existing pavement layer and its overlying surface so that the pavement does not experience rapid surface failures causing the reduction in service life. The failure to achieve a good bond between the HMA and PCC layers seems to be related to several factors such as properties of the tack coat, presence of moisture in the concrete, thickness of the HMA layer, cleanliness of the PCC surface, concrete surface preparation, etc. The failures due to poor bonding include, but are not limited to slippage cracking, top-down cracking, potholes, and fatigue cracking.

1.2 STUDY OBJECTIVES

The objective of this study is to investigate the effect of several influencing factors on the performance of HMA-PCC interface layer. To this end, factors of interest were identified based on a thorough literature review and recommendations from experts/agencies, and the influence of these variables on the interlayer shear performance and the bond strength was assessed.

1.3 STRUCTURE OF THE REPORT

This report includes seven chapters. Chapter 1 provides problem statement and objectives. Chapter 2 presents background on the current practices and specifications and literature review on the recent advancements on bonding of hot mix asphalt to Portland cement concrete by using different tack coats. Chapter 3 evaluates the most promising methods for evaluation of tack coat bond strength. This chapter also dis-

cusses various concrete surface preparation techniques for application of tack coat and materials for tack coat. Chapter 4 performs numerical simulation of a pavement with asphalt and concrete layers under moving traffic loads and evaluates the influence of overlay thickness, wheel load, traffic speed and axle configuration on the HMA-PCC interface. Chapter 5 develops a procedure to produce laboratory HMA-PCC samples and test bonding between the PCC and HMA layer. This chapter also evaluates the influence of several factors on the PCC-HMA bond. Chapter 6 evaluates the performance of field sections that have shown issues in the past or sections that have shown no distresses after several years of application. Chapter 7 provide conclusions based on the findings of this research study. This chapter also includes a list of recommendations to implement the present research.

CHAPTER 2. COMPREHENSIVE DOCUMENTATION OF CURRENT PRACTICES AND SPECIFICATIONS

According to American Society for Testing and Materials (ASTM), tack coat can be defined as a light application of asphalt emulsion or liquid asphalt on an existing HMA or PCC layer to enhance the adhesion between the existing layer and the HMA overlay. Tack coats are used between an existing pavement layer (HMA or PCC) and a new HMA overlay to enhance the bonding of the two layers. The traffic loads applied to the pavement source are transmitted through different layers within the pavement structure. A good bonding between pavement layers is essential to ensure efficient transfer of such loads. Lack of adequate interlayer bond typically results in rapid or premature failure such as cracking, debonding, and shoving (Mohammad, 2012).

It has been reported by many researchers that the mechanistic responses in the HMA layer such as tensile, compressive, and shear stress are significantly influenced by the HMA-PCC interfacial bonding conditions (Hu and Walubita, 2011). Therefore, it is of great significance to enhance the bonding conditions between the PCC and the HMA layers by utilizing the most promising surface preparation techniques and materials. Although many test procedures have been developed to evaluate the performance of tack coats, there are no standard specifications that can be used to evaluate their quality in the laboratory or on the field (Mohammad et al., 2008). The rest of this chapter provides a summary of the findings regarding the best practices, the most promising materials, and the effect of various factors on the HMA-PCC interlayer performance in terms of shear and tensile strength.

2.1 MATERIALS

2.1.1 Tack coat types

Two types of tack coats have been commonly used in the pavement industry: PG binders, and asphalt emulsions. As a result of a discussion in TRB standing committee AFK20 on the immediate need of a summary document regarding the state of practice of tack coats, NCHRP conducted a survey in 2018 with the objective to compile information on the specifications, materials, construction practices, testing

and acceptance, and the current state of practice for tack coats. All US DOTs, as well as Canadian provinces and territories through the Transportation Association of Canada were surveyed with a response rate of 100% and 54%, respectively. A summary of the number of agencies using certain tack coat materials is shown in Figures 40-42 of the NCHRP report (Gierhart and Johnson, 2018) reproduced here in Tables 2.1 through 2.3.

Table 2.1. Number of US and Canadian agencies using PG binders as tack coat (Gierhart and Johnson, 2018)

Binder grade	Number of agencies
PG 58-22	3
PG 58-28	3
PG 64-16	1
PG 64-22	6
PG 64-28	3
PG 67-22	2

Table 2.2. Number of US and Canadian agencies using emulsions as tack coat (Gierhart and Johnson, 2018)

Emulsion grade	Number of agencies
CQS-1h	4
CRS-1	5
CRS-2	5
CRS-2p	3
CSS-1	14
CSS-1h	26
HFMS-1	1
HFMS-2h	1
MS-1	2
RS-1	9
RS-2	1
SS-1	18
SS-1h	23
Non-standard emulsion	26

Table 2.3. Number of US and Canadian agencies using reduced-tracking emulsions as tack coat (Gierhart and Johnson, 2018)

Reduced-tracking emulsions	Number of agencies
AE-NT	1
CBC-1HT	1
CBC-1H	1
CNTTC	2
CRS-1h	1
EM-50-TT	3
LTBC	1
NTCQS-1hM	1
NTCRS-1HM	2
NTCRS-1HSP	2
NTHAP	1
NTQS-1HH	2
NTSS	1
NTSS-1HM	12
PATT	1
PennDOT non-tracking	1
Ultrafuse	2
Ultratack	1

2.1.1.1 Asphalt emulsions

NCHRP report (Gierhart and Johnson, 2018) presents a list of AASHTO specified emulsions that are currently being used as tack coat in US and Canadian agencies. It has been reported that due to some advantages such as ease of handling, reduced energy consumption, and environmental impacts, emulsified asphalt tack coats are preferable to use. Some disadvantages such as the potential for tracking and the time needed for the emulsion to break and set are also reported in the literature (Techbrief, 2016).

To address the tracking issue, the use of reduced-tracking (or non-tracking) tack coats have gained considerable attention over the past few years. This material hardens quickly, thus minimizing adhesion to tires. Research conducted for NCHRP project 9-40 in 2011 evaluated the bond strength of various emulsion tack coats among which trackless tack exhibited the highest shear strength, while CRS-1 exhibited the lowest

(Mohammad, 2012).

Dilution of emulsions is another practice that some agencies allow at the supplier's terminal or at the project site. The most common dilution rate is 1:1 (undiluted emulsion: additional water). One major benefit of the dilution practice is that the diluted emulsion will flow more easily from the distributor, thus allowing for a more uniform application. However, they require additional time to break, and the quality and temperature of water needs to be controlled (Gierhart and Johnson, 2018).

2.1.1.2 Asphalt binders

One advantage of asphalt binder as a tack coat over emulsified tack coat is that in terms of bond strength, they typically perform better than the emulsified asphalt tack coats (Mohammad et al., 2009, 2002). Another advantage is that asphalt binders require no time to break. Also, asphalt binder tack coats can sometimes be in the form of polymer-modified asphalts which are shown to perform better than unmodified ones in places where substantial stopping or turning traffic is experienced by the HMA overlay (Mohammad, 2012). However, the main disadvantage of these types of tack coats is the high temperature involved in the spraying process, which is a safety concern and requires more energy to heat the tack coat (Gierhart and Johnson, 2018).

2.1.1.3 Asphalt cutbacks

Due to the environmental concerns associated with the evaporation of petroleum solvents into the atmosphere, the use of asphalt cutbacks as tack coat materials has now been restricted or prohibited by many agencies. A survey included in NCHRP synthesis 516 in 2018 reported that only one agency (Illinois) was using cutbacks (RC-70) as a tack coat. In a 2012 survey, Kansas was reported as the only state using cutbacks as tack coats, but, in the 2018 survey they reported using only slow-setting emulsions and emulsion bonding liquid (EBL).

2.1.1.4 Summary

Due to aforementioned pros and cons for each type of tack coat materials, the material types are selected based on a combination of materials properties, availability and the project requirements.

2.2 FAILURE MODES

Generally, the rapid failure at the interface is attributed to shear and tension stress modes (Raab and Partl, 2004). Figure 2.1 illustrates these two major distress modes at pavement interface. The mechanistic pavement responses at the interface can be measured through either numerical modeling, laboratory measurements, or field measurements. The combination of all these can provide a good estimation of the required shear strength and bond strength as well as a validation of the measurements at different locations.

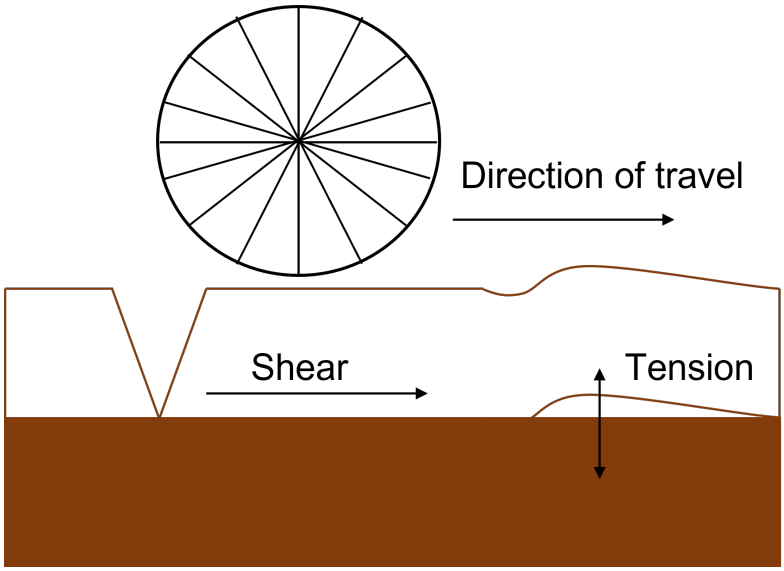

Figure 2.1. Schematic showing major distress modes at the interface layer (Raab and Partl, 2004)

2.3 NUMERICAL MODELING

Over the years, researchers have utilized different simulation techniques to numerically capture the pavement response under various loading and environmental conditions. Among these different simulation methodologies, the most common techniques utilized by researchers were the multi-layer elastic (Scullion et al., 1990) and viscoelastic analysis (Bai et al., 2021; Nielsen, 2019) (LEA and LVEA), and the finite element (FE) analysis (Al-Qadi et al., 2008b). Asphalt pavements exhibit viscoelastic and viscoplastic behaviors in their responses under the traffic loading and environmental conditions.

Due to this complexity in pavement response, along with the FE wide capabilities in modeling different structures and materials, FE analysis has gained increasing popularity over the decades in studying the mechanistic responses of pavement structures. Several research studies were published utilizing finite element models (FEM) to simulate pavements for different purposes, such as simulating the pavement responses under the falling weight deflectometer (FWD) loads (Tang and Yang, 2013; Xu and Prozzi, 2015; Hamim et al., 2018) and under the moving vehicular loads (Patil et al., 2013; Zhang et al., 2016; Eghbalpoor et al., 2019), studying pavement distresses and pavement structural capacity (Bekheet et al., 2001; Hu and Walubita, 2009; Ban et al., 2013; Alae et al., 2019), and modeling the pavement structural response and bonding characteristics at different layer interfaces (Ling et al., 2019; Davids, 2001). In the following subsections, some of these studies are summarized.

2.3.1 FEM to simulate pavement responses under FWD loading

The FWD testing technique is currently utilized by many transportation agencies in the United States and in many other countries for back calculating the pavement layers moduli to evaluate the structural capacity of existing pavements (Xu and Prozzi, 2014). FWD is a non-destructive testing (NDT) technique that is normally performed by dropping a known load from a certain height to impact the pavement surface. The pavement surface deflections due to this impact load pulse are measured with a set of geophones at different lateral offsets, with the first geophone located just under the dropped load (Al-Qadi et al., 2004). The typical output from the FWD test is a pavement deflection basin (i.e., the values of the surface deflections at the different lateral offsets). These values of surface deflections are typically used for back-calculating the layers mechanical properties, such as the pavement layer moduli. The main concept of the back-calculation analysis depends upon matching the measured FWD deflection basins with numerically estimated deflection basins based on assumed moduli (Hadidi and Gucunski, 2010). This is typically performed in an iterative procedure by assuming seed values for the layer properties, and using computer applications such as Modulus (Scullion et al., 1990) or ELMOD (Dynatest 2020) (Dynatest, 2020), until both of the deflection basins are matched. Once the two basins are matched with an acceptable Root Mean Square Error (RMSE), it can be assumed that the trial pavement moduli are equal to the measured pavement moduli (Chatti et al., 2004).

The current back-calculation techniques associated with the FWD are based on Layer Elastic Analysis (LEA) solutions that simplistically consider the asphalt as a linear elastic material. In addition, the software and mathematical expressions used to perform the back-calculation analysis use different algorithms. This may sometimes lead to potentially different results if different software or analysis models are used. Moreover, it is mandatory to know beforehand the thicknesses (h_i) and Poisson ratios (μ_i) of the layers that make up the existing pavement structure, which might not be available/accessible at the time of testing. In addition, convergence to a local optima due to the use of 'seed' moduli values during the back-calculation analysis may lead to erroneous final modulus results.

In addition to the numerical challenges associated with the current back-calculation algorithms, several researchers have utilized different FE algorithms to simulate the pavement responses under the FWD loading due to the wide acceptance of the FWD testing among pavement professionals. The main aim of most of these studies was to find a more accurate numerical solution to supplement/replace the LEA in back-calculating the pavement layers moduli.

Khan and Tarefder (2019) utilized FEM to determine the viscoelastic properties of asphalt pavements depending on numerical interconversion techniques to convert pavement response field data to the asphalt relaxation modulus. In addition, a comparative study was implemented to correlate the FE simulated pavement response to the actual pavement response under the FWD loading. Xu and Prozzi (2014) also developed a FE technique to inverse compute the multi-layer moduli, including the viscoelastic properties of the asphalt pavement layer, utilizing a Newton-Raphson iteration procedure. Hamim et al. (2018) carried out a comparative study to optimize a structural FE modeling technique for simulating the FWD static and dynamic back-calculation methodologies. The results of their study shed the light upon the best practices for developing FE models/algorithms to simulate the pavement responses under the FWD loading.

Furthermore, Li et al. (2017) performed a parametric analysis to study the nonlinear pavement responses under the FWD. The study also incorporated the viscoelastic behavior of the asphalt layer and its influence on the generated FWD deflection basin. Hamim et al. (2020) used a hybrid research approach, depending on the FE and the Artificial Neural Networks (ANNs) to back-calculate the viscoelastic properties of

asphalt layers as a function of the time-history FWD deflection data. Tang and Yang (2013) also utilized the dynamic FEM and Genetic Algorithms (GA) to evaluate the structural capacity of pavement structures utilizing the FWD deflections.

2.3.2 FEM to simulate pavement responses under moving vehicular loading

Utilizing the FEM in pavement research was also extended to studying the pavement responses under realistic moving traffic loadings. Realistic loading condition modeling is as important as accurately representing the material characteristics in order to capture an accurate pavement structure response.

Assogba et al. (2021) carried out a FE study to simulate the pavement responses under realistic dynamic moving loads. The study was implemented to simulate an instrumented pavement structure, and the field data collected from the pavement sensors were used to validate the models. Wang and Li (2016) also performed a FE study to correlate the pavement response under the FWD loading to actual pavement responses under moving vehicular loading. Their study incorporated both axisymmetric FE models and (3D) FE models to simulate both the FWD and the moving vehicular loading, respectively. Moreover, Patil et al. (2013) utilized the FEM to study the vehicle-pavement interaction effects. The study presents a simplified FEM to capture the vehicle-pavement interactions under moving loads while incorporating realistic pavement material and soil characteristics. Eslaminia and Guddati (2016) performed a Fourier-Finite Element (FFE) analysis to predict the pavement structural responses under regular traffic loads. Eghbalpoor et al. (2019) performed an implicit FE analysis to characterize the influence of moving traffic loads on pavement damage and healing mechanisms.

2.3.3 FEM to study pavement distresses and structural capacity

The accurate quantification of the structural capacity of a damaged pavement is a salient step for making an appropriate rehabilitation decision and for funds allocation. Different research studies have incorporated FEM to investigate the structural capacity of damaged pavements. Viscoelastic, viscoplastic, elasto-viscoplastic, and fracture mechanics concepts have been used to model and study the influences of permanent deformations and fatigue cracking on the structural capacities of pavements.

Abu Al-Rub et al. (2012) carried out a comparative study to investigate the merits and demerits of FEM and the constitutive modeling techniques for predicting asphalt structures permanent deformations. Their study was focused on evaluating the effect of various FEM techniques and material characterizing constitutive models on expected rutting in pavements under normal traffic conditions. Both 2D and 3D FEM were investigated and compared for predicting asphalt rutting. In addition, the study was extended to comparing the rutting performance indicators utilizing various constitutive behaviors. Their study emphasized the FE capabilities in predicting the damaged pavement responses under repeated traffic loading. Ali et al. (2009) also analyzed the rutting distresses of urban pavements using FEM. The nonlinear characteristics of pavement structures and the realistic traffic conditions were incorporated in the modeling approaches. In their study, the performance from the numerical model was correlated to pavement responses from a full-scale pavement testing to characterize the urban loading effects on the pavement distresses. Results conclude that urban traffic loading is detrimental for pavements and the study recommends the use of high resistance asphalt concrete as an efficient alternative for urban pavement rehabilitation. Saad et al. (2006) developed a 3D FE model to investigate the rutting of flexible pavements reinforced with geosynthetics. Leonardi (2015) utilized the FEM to study the airfield rutting of asphalt pavements. This study incorporated a numerical representation of the aircrafts impact loading on the pavement structures and used an elasto-viscoplastic material characterization. Alimohammadi et al. (2021) investigated the asphalt overlays rutting in a comparative analysis between the FEM and the Mechanistic-Empirical Pavement Design (MEPD) methods.

Furthermore, several researchers studied the effects of fatigue cracking on the pavement structural responses. Gajewski and Sadowski (2014) performed a sensitivity analysis to study the crack propagation mechanisms in asphalt pavements and to characterize the influences of crack severity on the pavement stresses in different layers. The study utilized a hybrid research methodology depending on FEM and ANNs. Sun et al. (2019) developed a 2D-microstructure FEM to investigate and analyze the load-induced top-down cracking initiation in asphalt pavements, and to simplify the consideration of these cracks effect in pavement design procedures. Ameri et al. (2011) utilized the general concepts of fracture mechanics, including the stress intensity factors (SIFs) and the T-stresses, in 3D-FEM to characterize the loading

effects on the asphalt crack propagation rates and loss of structural capacities. Kim and Buttlar (2009) also used the concepts of fracture mechanics and cohesive fracture modeling to study the detrimental effects of low temperatures on airport pavements. Gajewski and Sadowski (2014) carried out a sensitivity analysis, using FEM and ANNs, to characterize the influential parameters on crack propagation for bituminous layered structures.

In summary, it can be observed from the aforementioned studies that FEM is a powerful tool in assessing pavement distresses.

2.3.4 FEM to study the PCC-HMA interface bonding characteristics

As a result of construction time and traffic severity constraints, constructing asphalt overlays on top of existing damaged PCC pavements and vice-versa have become common rehabilitation trends among transportation agencies over the past few decades. One of the major challenges associated with these practices is the lack/loss of bonding between the HMA and the PCC. For the aforementioned purpose, several research efforts were extended to study the bonding characteristics at the interface between the PCC and the HMA. However, limited studies utilized the FEM to characterize the bonding characteristics at the interface between the PCC and the HMA.

Ling et al. (2019) performed a full-scale study, using accelerated pavement testing and FEM, to determine the critical responses of airfield composite pavements. This study was focused on quantifying the effects of three influential parameters (namely: temperature, interface bonding, and load level) on the responses of airfield pavements that are composed of HMA overlay and PCC pavement. The results of this study indicated that longitudinal strain is more critical than the transversal strain in HMA overlays when subjected to moving loads. In addition, it was also emphasized by the authors that a good interface bonding could be able to significantly reduce the critical strain in HMA overlays. The results from this study also implied that the bonding strength is highly affected by the application rate of tack coat application. Li and Vandenbossche (2013) used a finite element methodology supported by field measurements to study the different failure modes of the thin and ultra-thin whitetopping (concrete overlay on a distressed asphalt pavement). The study findings summarized the performance of in-service whitetopping overlays and indicated that the failure mode is dictated by concrete slab size and that the critical tensile stresses are in the

wheel-paths and at the bottom of the PCC layer.

Ozer et al. (2013) evaluated the interface shear strength between two HMA layers under moving vehicular loads using a 3D FEM based on frictional Mohr-Coulomb-based plasticity model. The interfacial response was captured at two different loading states: pure shear and shear with compression. The effectiveness of different tack coat materials was also investigated using a laboratory direct shear testing program. The measured laboratory interface shear stresses were compared to those predicted from FEM vehicular loading in a typical thick pavement structure. The results captured from the FEM and the laboratory experimentation clarified the effect of two influential parameters on the intensity of shear stress at the pavement layer interface. These parameters were found to be load related parameters (load and tire inflation pressure) and maneuvering related parameters (braking and acceleration). They also developed a fracture-based FEM to characterize the behavior of tack coat at the interface between the PCC and HMA layers (Ozer et al., 2008). This study incorporated an elastoplastic fracture-based constitutive relationship for frictional interface modeling.

Vandenbossche et al. (2017) carried out a FE analysis to review the mechanistic-empirical (ME) design procedures of the concrete overlays over damaged pavement structures. The traditional thought was based on the assumption that the failure mechanism is a function of the overlay thickness. Nevertheless, the study results emphasized that the critical stress at the overlay bottom, which is a function of the concrete slab dimensions, concrete modulus of rupture, traffic load level, and temperature variations are more significant to failure than the overlay thickness. Findings from this study were also supported by a sensitivity analysis to quantify the significance of the aforementioned parameters over the newly proposed design procedures.

Mu and Vandenbossche (2011) used the FEM along with dynamic strain data collected from instrumented pavement sections at the Minnesota Road Research Facility (MnROAD) to investigate the effect of temperature and traffic on the interface bonding for whitetopping overlays. Failure mechanisms were investigated by examining the pavement response to actual dynamic loads. The load-related pavement responses (i.e., stresses and strains) were, interestingly, found to be higher under thicker concrete overlays than under thinner ones. This was found to be true for all environmental conditions except for the summer season. It was observed that with an increase in the temperature the degree of bonding as well was the HMA stiffness was decreased, as

a result, large increase in strains were measured. Therefore, it was concluded in their research that a proper prediction of the whitetopping performance should account for seasonal variation of the HMA stiffness as well as the seasonal characteristics of bonding strength (Mu and Vandenbossche, 2011).

Hu and Walubita (2011) utilized a 3D-FE algorithm for modeling the mechanistic responses (i.e., stresses and strains) in the asphalt concrete (AC) layers by simulating the bonding conditions between pavement layers. Two different bonding conditions were investigated: fully bonded and fully debonded. The fully bonded characteristics were simulated by assuming zero slippage at the pavement layer interface, and hence represented with tie constraints, while the fully debonded were represented by identifying just the frictional characteristics between the layers. In addition, the 3D-FE modeling incorporated actual measured vertical tire-pavement contact pressure and investigated the effect of the vehicle acceleration and deceleration on the critical pavement responses. Results showed that the interfacial layer bonding condition has a significant effect on some pavement mechanistic responses such as the tensile, compressive, and shear stresses/strains in AC pavement structures. Moreover, layer debonding or separation was numerically found to have a significant effect on reducing the entire pavement section's structural capacity and exacerbating pavement distresses such as slippage cracking, fatigue cracking, shoving, shear deformation, and rutting.

Having introduced a summary of the literature that incorporated FEM in pavement studies, it can be concluded that the finite element method is a powerful tool that can be utilized to accurately capture the pavement behavior/response under different loading and environmental conditions. In addition, utilizing the FEM has a great potential of minimizing the field/lab testing efforts while, at the same time, pavement professionals can still capture reasonable pavement characteristics.

2.4 LABORATORY PERFORMANCE AND EVALUATION OF TACK COATS

2.4.1 Specimen preparation in the lab

Specimen preparation could be either by using field PCC cores or fabricating cylindrical PCC specimens in the lab. After obtaining PCC specimens, a thin layer of tack coat can be applied to the surface, followed by compacting HMA on top of the PCC

specimens.

Tack coat can be applied on the PCC surface by using a roller instead of paint brushes to ensure uniform distribution. To ensure accurate tack coat application rate, duct tapes can be wrapped around the PCC core. Tack coat application rate can be measured by weighing the PCC core before and after the application of tack coat.

Ozer and Rivera-Perez (2017) extracted 4 in. diameter PCC cores from PCC slabs and after cleaning and drying, applied seven different types of tack coats at the designated application rate. After 24 hours of curing, HMA mix was compacted on top of the PCC layer using a portable gyratory compactor. The HMA layer was initially compacted at 7% air void content and 4 in. thickness which resulted in significant variations in the number of gyrations (over 150). Later, they changed the target density to 10% air void and the thickness of the HMA to 2 in., this resulted in more consistent number of gyrations based on the compaction curves.

McDaniel et al. (2018) used 6 in. concrete cylinders fabricated in lab and moist cured for 45 days. To account for the difference in diameter of the plastic molds and the gyratory molds, they lined the plastic molds with flexible plastic sheeting. At the end of the curing period, the specimens were air-dried for 24 hours, and the tack coat was applied to the surface and cured for 2 hours. The HMA layer was preheated for 2 hours and compacted on top of the PCC specimen using a Pine gyratory compactor.

Leng et al. (2008) found that the interface skew caused by the slight difference in the diameter of PCC and the HMA layer affected repeatability of direct shear test results. They resolved this issue by placing the skewed surface in the horizontal plane during testing.

2.4.2 Tack coat evaluation

Previous studies on the performance evaluation of tack coats have almost exclusively focused on the ability of these materials to provide adequate bonding between the pavement layers. However, recent studies indicate that tracking of the tack coats is another key aspect that requires considerable attention. Tracking of asphalt emulsions can occur in two stages: tracking of the wet, uncured emulsion, and tracking of the emulsion residue after curing (Musselman et al., 2020). To prevent/mitigate tracking during the first stage, the emulsion shall be given enough time to break and cure. Tracking in the second stage is dependent on the pavement temperature and the

stiffness of the residue at the prevailing climatic conditions.

A variety of tests exist to evaluate the quality of tack coats in terms of tracking and moisture loss. The most common ones are summarized below:

- ASTM D6372 (2015) used a loaded wheel tester to measure the stability and resistance to compaction and displacement of multilayered cold mixes. Bahia et al. (2019) developed a modified version of this Loaded Wheel Tracking Test (LWTT) to evaluate the tracking resistance of emulsion tack coats. The LWTT test is conducted at 6°C intervals and the wheel is evaluated for tracking after each test. The authors compared the trackless temperature of two tack coats with their rutting parameter as G*/sin δ and concluded that this rutting parameter could be a good predictor of the tracking behavior of a tack coat. However, their study was limited to only two samples, and further investigation was needed to find a relationship between rheological properties of the tack coats and their tracking performance.
- In a later study, Sufian (2020) investigated the relationship between log G*/sin δ and the trackless temperature for a larger number of emulsion residues, and recommended that the G*/sin δ value of 30 kPa can be used as the lower limit of transition to trackless behavior.
- Clark et al. (2012) conducted a study to evaluate the laboratory performance of tack coats and proposed a modified version of ASTM D6372 (2015) to determine the no-pick-up time of tack coat. The test uses a metal cylinder with rubber O-rings which are repeatedly rolled down a ramp over a freshly applied tack coat film until there is no transfer of the tack coat to the rubber rings. The elapsed time from tack coat application to no transfer of the material was called the no-pick-up time.
- The moisture loss of the tack coat can be evaluated by a simple procedure developed by Bahia et al. (2019) which measures the water evaporation of the tack coat at different temperatures and humidity conditions.

2.4.3 HMA-PCC interlayer bonding evaluation

It has been found by researchers that testing the pavement layers under shear mode is the most useful way to evaluate the effectiveness of different types of tack coats (Al-Qadi et al., 2008a). Some test parameters such as shear failure are of significant

interest when comparing different types of tack coats and assessing their performance. The bond strength of the HMA-PCC interlayer can also be evaluated through various tensile and torque tests. Figure 2.2 illustrates the different modes of mechanical testing which are appropriate for the evaluation of tack coats (Wang et al., 2017). A review of some of the most common laboratory performance tests/apparatus is summarized below. Overall, all these tests can be listed as either direct shear tests, pull-off tests, or torsional shear tests with variations in loading, specimen size, etc.

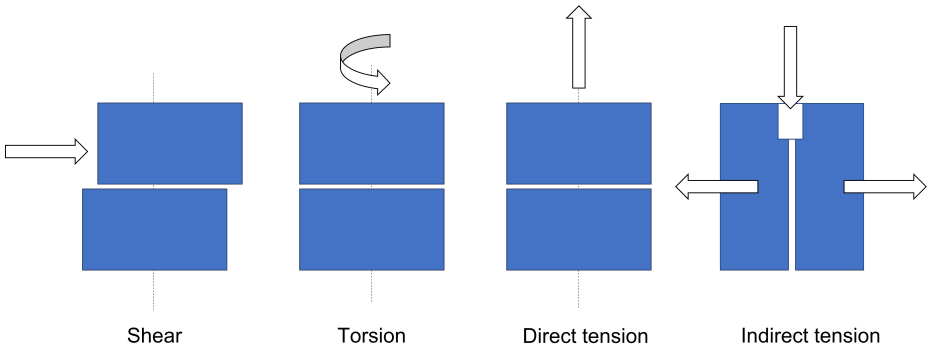

Figure 2.2. Schematic showing test modes for evaluation of tack coats (Wang et al., 2017)

- Florida Direct Shear Test: Florida DOT developed this test to measure the shear strength of a tack coat interlayer by applying a vertical shear load. Samples can be cored from roadways or fabricated in a laboratory.
- Louisiana Interlayer Shear Strength Tester (LISST): The LISST device was developed at the Louisiana Transportation Research Center for characterizing the interface shear strength of specimens in the laboratory (Mohammad et al., 2009). In this test, a vertical load is applied on a shearing frame holding part of the specimen, and it is increased until a shear failure occurs at the interface. The average coefficient of variation in the test results was found less than 10%.
- UTEP Pull-Off Test: This test was developed by University of Texas at El Paso and can be used either in lab or in-situ. The test applies a torque force to a tack-coated pavement and measures the tensile stress at the point of failure (Deysarkar, 2004). TxDOT designation: Tex-243-F also suggests this test procedure can directly measure the adhesive strength of a tack coat. A drawback of this test is the inability to control the rate of loading, which can influence

the repeatability (Gierhart and Johnson, 2018). The test is no longer utilized in Texas.

- NCAT Shear Test: This test was developed by NCAT to measure the interface shear strength by applying a vertical shear load on the specimen. The difference between this test and the Florida direct shear test is that this method applies a horizontal load as a normal pressure to determine the impact of surface texture on bond strength. Compared to the LISST test, this method applies a higher loading rate that may lead to unrealistic high bond strengths (Hachiya et al., 1997).

Among all different testing methods, the direct shear test performed in the laboratory has attracted considerable attention due to its relative simplicity, good repeatability, and quick results.

2.4.4 Field performance measurement and validation

According to past studies, laboratory-prepared specimens are likely to overestimate the actual interface shear strength in the field (Mohammad, 2012; Mohammad et al., 2010; Zhang, 2017). Therefore, it is essential to conduct field measurements to evaluate the shear and bond strength of the interfacial layer. There are a few field test methods that researchers have adopted to measure the field performance of tack coats. A review of these test methods is as follows:

- Torque Bond Test: Originally developed in Sweden, this test was first adopted in the UK for thin surfacing systems (Walsh and Williams, 2001). In this test, specimens are partially cored from an HMA-PCC slab or SGC compacted specimen to a depth that reaches into some portion of the PCC layer to expose the PCC-HMA bonding interface but without fully extracting or separating the core from the PCC base. A torque wrench is used to apply a torque on the specimens and measure the maximum torque at failure which is indicative of the shear strength of the tack coat. One major drawback of this test method is the high variability in the results, that is related to the difficulty in controlling the constant torque rate manually.
- Oregon Field Torque Tester (OFTT): Mahmoud et al. (2017) proposed a new low-cost technology that is capable of measuring the in-situ inter-facial layer shear strength. This test method uses cores that are 2.5 in. in diameter rather

than the laboratory shear tests which require cores of 6 in. in diameter. The bond strength of thin overlays can also be measured by using this device. They found high correlation between the peak in-situ torque values measured by the OFTT device and the measured laboratory shear strengths.

2.4.5 Application of tack coats

One important factor in the design and construction of tack coats is the proper application of tack coat in the field. Traditionally, tack coat was applied on the existing pavement surface by using asphalt distributor trucks. Today, most tack coats are applied using a special paver equipped with a tack coat tank and a spray bar. Several factors can affect the tack coat application quality in the field such as: uniformity of nozzle spray patterns, size of nozzles, height of spray bar, pressure of the application, and temperature of tack coat (Wang et al., 2017). The influence of these factors on the tack coat is not in the scope of this project, however, they can be studied and evaluated further in future studies.

2.5 DESIGN FACTORS

Full bonding between HMA and PCC layers depends on various factors to be optimized during the design of composite pavements. These factors include, but are not limited to tack coat type, tack coat application rate, asphalt overlay mix type and temperature, PCC surface material type and texture, and PCC cleanliness conditions. Therefore, prior to design of experiments, it is essential to identify the most influential factors and the effect of these factors on the overall performance of the interfacial layer.

2.5.1 Effect of application temperature on the tack coat performance

Different tack coat materials have different temperature ranges for application and storage. NAPA QIP 128 (Decker, 2013) provides a detailed guideline for application and storage temperatures of emulsion tack coats.

2.5.2 Effect of testing temperature on the tack coat performance

The testing temperature can be considered as a variable factor in this study because it can be related to the pavement temperature. In a study by Al-Qadi et al. (2008a), the

effect of testing temperature on the shear strength of tack coats was investigated and they found a statistically significant decrease in shear strength by increasing the test temperature in a range from 10°C to 30°C. Another study by Bahia et al. (2019) also showed the same trend for 25°C and 46°C. The testing temperatures for this project can be selected based on the high pavement temperature in the State of Texas.

2.5.3 Effect of concrete surface texture on the tack coat performance

A variety of concrete surface textures are available for pavements depending on different applications. Surface texture techniques are most commonly introduced while the concrete is in a fresh state to improve skid resistance. The most common surface application technique is known as tining. Surface textures can also be implemented onto concrete in its hardened state but these techniques are usually costly and can have negative environmental impact. This surface texture review will focus on tining, diamond grinding, milling, sandblasting, and hydro-demolition along with their bond strength behavior, costs, and environmental impacts they may impose.

Tining (transverse, longitudinal, or random) on concrete pavements is provided on the surface during its fresh state. Longitudinal tining has become more common since it increases ride quality. This is the most common surface texture and is probably the most often used texture to PCC pavements prior to tack coat application. Leng et al. (2008) reviewed smooth and tined (longitudinal and transverse) surfaces and they determined that tining increased the interface shear strength. Directional tining (transverse and longitudinal) had similar interface shear strength. Since tining is applied during the plastic state, the cost and environmental factors are very low for this texture.

Diamond grinding has become one of the most common methods of pavement surface texturing for new pavements, as well as for existing pavements. Diamond grinding roughens the concrete surface and can be used to level surfaces for enhanced ride quality and reduced noise. For new pavements, the depth of grinding is on the order of 0.125 in. to 0.1875 in., but higher grinding depths (e.g., up to 0.5 in.) may be needed when removing damaged or degraded concrete or to roughen the surface texture for tack coat application. Common costs for diamond grinding are between $3-5 per sq.yd. Diamond grinding does need a slight increase of tack residual rate due to its increased texture (Mohammad, 2012).

Milling removes the top layer of a pavement (HMA or PCC) through the use of rotating mandrels with sharp tips that chip or mill away the exposed surface. Due to the nature of cold milling, a rougher surface texture is produced, compared to less aggressive methods (e.g., sand or shot blasting). Similar to other concrete surface removals, there is an environmental concern with concrete disposal. In addition, a dust collection system needs to be in place for this surface preparation.

Sandblasting or shotblasting has been used to texture pavements for subsequent overlay applications. Sandblasting of larger roadway pavements is not as common as the other techniques. Sandblasting removes the smallest amount of concrete from the surface compared to the other hardened concrete surface treatments. Environmental impacts are of concern with this technique as it needs a dust collection system. Surface cleaning is needed after sandblasting to create dust proof surface for proper bonding.

Hydro-demolition has been used extensively in the construction of bonded concrete overlays, especially for bridge deck rehabilitation. This technique may prove to be more feasible since diamond grinding already requires the use of slurry removal after surface texturing. This technique requires proper collection systems to collect the runoff.

All of the above techniques can increase the interface bond strength compared to smooth concrete surface. However, it must be noted that the surface must not be dusty prior to tack coat application.

Regarding the effect of surface type, several studies have found a direct relationship between the roughness of the existing surface and the shear strength at the interface (Mohammad et al., 2010). These studies observed that the milled concrete surface provided greater interface shear strength for the interface than tined and smooth PCC surfaces for the same tack coat application rate (Bahia et al., 2019; Al-Qadi et al., 2008a; Tashman et al., 2006). Bahia et al. (2019) found that the existing surface texture is the most important factor controlling the inter-facial layer shear strength for newly compacted specimens.

In this study, four different types of surface textures were selected from the aforementioned textures and analyzed in Chapter 5.

2.5.4 Effect of application rate

According to many studies, another important factor in the design and construction of tack coats is the application rate. Proper application rate and uniformity during the application of tack coats are important to achieve the maximum bond between HMA and PCC layers. The tack coat application rate can vary from 0.03 gal/sq. yd. to up to 0.1 gal/sq. yd. based on the surface type. Table 2.4 shows the recommended tack coat application rates for different surfaces provided in NCHRP report 712 (Mohammad, 2012), FHWA Tech Brief on tack coats (Techbrief, 2016), and NAPA's QIP 128 (Decker, 2013), respectively.

Table 2.4. Recommended tack coat application rates

NCHRP Report 712			
Surface Type	Residual Application Rate (gal/sq. yd.)	Approximate Bar Rate Undiluted (gal/sq. yd.)	Approximate Bar Rate Diluted 1:1 (gal/sq. yd.)
New Asphalt	0.035	-	-
Existing Asphalt	0.055	-	-
Milled Surface	0.055	-	-
PCC	0.045	-	-
FHWA Tech Brief on Tack Coats			
Surface Type	Residual Rate (gal/sq. yd.)	Approximate Bar Rate Undiluted (gal/sq. yd.)	Approximate Bar Rate Diluted 1:1 (gal/sq. yd.)
New Asphalt	0.02-0.05	0.03-0.07	0.06-0.14
Existing Asphalt	0.04-0.07	0.06-0.11	0.12-0.22
Milled Surface	0.04-0.08	0.06-0.12	0.12-0.24
PCC	0.03-0.05	0.05-0.08	0.10-0.16
NAPA QIP 128			
Surface Type	Residual Asphalt Binder (gal/sq. yd.)	Applied Undiluted Emulsion (gal/sq. yd.)	Applied Diluted Emulsion (gal/sq. yd.)
New Asphalt	0.03-0.04	0.04-0.06	0.09-0.12
Existing Asphalt	0.04-0.06	0.06-0.09	0.12-0.18
Milled Surface	0.03-0.05	0.04-0.07	0.09-0.15
PCC	0.04-0.06	0.06-0.09	0.12-0.18

Although such tables provide promising values as a start point, it is still necessary to find an optimum value based on different materials used in different projects under different scenarios. An optimum application rate is desirable to ensure adequate material is available to bond the entire layers on one hand and avoid excessive material that may migrate into the new HMA and decrease the air void content on the other hand

(Mohammad, 2012). Mahmoud et al. (2017) used a slow setting emulsion tack coat at medium (0.07 gal/sq. yd.) and high (0.1 gal/sq. yd.) application rates and found higher shear strength at the medium application rate. Al-Qadi et al. (2008a) found an optimum application rate of 0.04 gal/sq. yd. for the slow setting emulsion tack coat that they used in their study. Leng et al. (2008) used a slow setting emulsion tack coat, a standard binder mix, and a cutback tack coat on smooth PCC surface, and found an optimum application rate of 0.04 gal/sq. yd.

In this study, different tack coat types and application rates were considered a factor and analyzed in Chapter 5.

2.5.5 Effect of PCC cleanliness

The PCC cleanliness plays an important role in HMA-PCC bonding. Numerous studies have recommended a clean surface for the application of tack coat (McDaniel et al., 2018; Leng et al., 2008; Wang et al., 2017). NCHRP report 712 (Mohammad, 2012) recommends a dry and clean pavement surface when using an asphalt cement tack coat or a cutback. Three cleaning operations mentioned in the literature are: mechanical brooming, flushing the surface with water, and using high-pressure air to blow off the debris (Gierhart and Johnson, 2018; Decker, 2013). Of these three methods, brooming is most commonly used.

In this study, two different cleanliness conditions are considered and analyzed in Chapter 5.

2.5.6 Effect of wetness on the tacked surface and on the PCC surface

The wet condition on the tacked surface can be simulated by uniformly spraying water before placement of the HMA overlay. Mohammad (2012) simulated wet weather conditions during construction of HMA overlay by using a small quantity of water on the tacked surface and found no statistically significant differences between the dry and wet conditions. In another study, they used different types of tack coats on PCC pavement and found that at wet conditions, the asphalt cement tack coat did not generate enough bond strength (Mohammad et al., 2010). Al-Qadi et al. (2008a) also found that moisture conditioning significantly decreased the interface shear strength. This reduction was more significant when a stripping-vulnerable binder was used as

the tack coat. Overall, they recommended a dry surface to avoid the negative effects of water on the bonding properties of the inter-facial layer.

In this study, three different surface moisture conditions are considered and analyzed in Chapter 5 in detail.

2.6 SUMMARY

This literature review presented some of the most recent advancements and findings on bonding hot mix asphalt (HMA) to Portland cement concrete (PCC) by using different type of tack coat materials. The important factors that substantially influence the shear performance and bond strength of tack coats were identified and considered in the design of experiments.

CHAPTER 3. SELECTION OF METHODS, MATERIALS, AND PROTOCOLS

In this chapter, most promising methods for PCC surface preparation and evaluation of tack coat bond strength were identified. A weighted scoring method was used to rank the candidate test methods in terms of factors including capital cost, testing time, repeatability, sensitivity, and the extent to which the test methods are used by other countries, states, and agencies in previous tack coat projects.

After the highest ranked methods were identified, detailed test protocols were developed. These protocols included factors such as specimen fabrication procedure, tack coat application rate, testing equipment, and testing conditions.

Finally, a list of candidate materials was provided based on previous projects and feedback from different districts of the receiving agency.

3.1 PCC SURFACE PREPARATION TECHNIQUES

The surface of the PCC slab can be prepared using different techniques that have been identified in the literature or existing highway agency practice. The selection of concrete pavement surface texture requires consideration of noise, environmental impact, safety, durability, and cost. Current surface preparation methods for application of tack coats include tining, diamond grinding, milling, sandblasting, and hydro-demolition. These methods are briefly described below, and a weighted scoring method was used to rank the candidate test methods, as shown in Table 3.1.

3.1.1 Tining

Tining (transverse, longitudinal, or random) is applied on concrete pavements during its plastic state. Longitudinal tining has become more common since it increases ride quality. This is the most common surface texture and is probably the most often used texture to PCC pavements prior to tack coat application. Since tining occurs during the plastic state, the cost and environmental factors are very low for this texture. FHWA specifies a spacing of 20 mm for both transverse and longitudinal tining. A width of 3 mm and a maximum depth of 3 mm are also recommended for both methods. Factors such as spacing, depth, width, and orientation of the

tine pattern have a significant influence on the surface noise characteristics of the completed surface.

A summary of advantages and disadvantages is presented below; a "*" indicates the advantage or disadvantage relevant in the context of surface preparation for tack coat.

Advantages:

- Low-cost method*
- Longitudinal tining has less variability in noise generation compared to transverse tining
- Longitudinal textures are among the quietest on the PCC pavements
- Hydroplaning reduction
- Reduced wet weather accidents
- Improved durability
- Improved resistance to lateral skidding

Disadvantages:

- Ensuring shallow, uniform grooves is critical to reducing pavement noise
- Can only be carried out in plastic state of the concrete*

3.1.2 Diamond grinding

Diamond grinding has become one of the most common methods of pavement surface texturing for new pavements, as well as for existing pavements. Diamond grinding roughens the concrete surface and can be used to level surfaces for enhanced ride quality and reduced noise. For new pavements, the depth of grinding is on the order of 0.125 in. to 0.1875 in. but higher grinding depths (e.g. up to 0.5 in.) may be needed when removing damaged or degraded concrete or to roughen the surface texture for tack coat application. According to FHWA, specific groove depth and spacing is dependent on hardness of the aggregate, but the typical values are 0.118 in. wide grooves, spaced at 0.197 - 0.236 in. intervals.

Common costs for diamond grinding are between $3-5 per sq. yd. Diamond grinding does result in a slightly increased application rate for the tack coat due to the increased texture of the underlying surface.

A summary of advantages and disadvantages is presented below; a "*" indicates the advantage or disadvantage relevant in the context of surface preparation for tack

coat.

Advantages:

- Enhances surface friction*
- Reduces splash and spray
- Reduced accident rates compared to un-ground surfaces (approximately 40-50%)
- Environmentally friendly*

Disadvantages:

- Higher costs and additional operation into the construction process compared to tining method*

3.1.3 Next-Generation Concrete Surface (NGCS)

Next-Generation Concrete Surface (NGCS) employs a combination of grinding and grooving in multiple passes. This technique is shown to provide good friction and quiet concrete textures. The cost of NGCS construction is considerably higher than the conventional methods due to the need for multiple equipment passes. TxDOT Houston district has incorporated this technology into several major highways, including I-10, and the I-610 Loop, and has constructed approximately 3 million square yards of NGCS as of 2018.

Advantages:

- Similar to Diamond Grinding

Disadvantages:

- Higher costs
- Timely process (multiple-pass operation)

3.1.4 Milling

Milling removes the top layer of a pavement (HMA or PCC) through the use of rotating mandrels with sharp tips that chip or mill away the exposed surface. Due to the nature of cold milling, a rougher surface texture is produced, compared to less aggressive methods (e.g., sand or shot blasting). Similar to other concrete surface removals, there is an environmental concern with concrete disposal. In addition, the dust collection system needs to be in place for this surface preparation.

Advantages:

- Improves bonding characteristics of the overlay to the existing pavement

Disadvantages:

- Increase in the amount of tack coat due to increase in the surface area
- High variability in the shear strength results of PCC-HMA interlayer due to difference in surface texture
- Additional cleaning procedure due to production of excess fine materials
- Residual microfractures on the surface of the concrete

3.1.5 Sandblasting

Sandblasting has been used to texture pavements for subsequent overlay applications. This technique is mostly used for repairing of joint seals. Sandblasting of longer roadway sections is not as common as the other techniques described in this section. Sandblasting removes a small amount of concrete from the surface. Environmental impacts are of concern with this technique as it needs a dust collection system. Surface cleaning is needed after sandblasting to create dust proof surface for proper bonding.

Advantages:

- Best suited for smaller construction projects

Disadvantages:

- Not advisable for larger sections
- Needs a dust collection system for collecting hazardous airborne particles
- Dust pollution

3.1.6 Hydro-demolition

Hydro-demolition has been used extensively in the construction of bonded concrete overlays, especially for bridge deck rehabilitation. This technique is usually utilized in the case of concrete restoration projects where embedded objects such as rebars need to be preserved. No previous use of this technique has been reported in the studies on PCC surface preparation practices. This technique requires proper collection systems to collect the runoff.

Advantages:

- Environment friendly (no dust pollution, reduced noise pollution)

- In some cases, the process-water can be cleaned and reused
- High-quality bonding surfaces
- No microfractures

Disadvantages:

- Surface preparation to collect water runoff properly

3.1.7 Summary

In general, tining is the most commonly used surface preparation technique as most pavements have an initial tined surface when paved. Although tining is not feasible on an existing / old concrete surface that is identified for an asphalt overlay, it is possible that existing surface presents some residual texture from the original tining that has not worn out over the years. Similarly, NGCS is an expensive surface restoration technique used to regain the skid resistance of a concrete pavement. Similar to tining, it is possible that a concrete surface with worn NGCS after several years of use may be identified for an asphalt overlay but by itself this may not be a procedure that is viable for surface preparation to receive an asphalt overlay.

The use of milling is a common practice for a surface preparation technique on a surface after it has hardened. Other than tining, most of the other surface preparation techniques require some form of an environmental collection system. In addition to environmental collection systems, noise pollution is a major problem with some of these techniques. Diamond grinding and milling could be managed on a larger overlay project whereas sandblasting and hydro-demolition would be more burdensome.

Table 3.1 shows the results of the surface preparation evaluation used to select the surface preparation conditions to use in this study.

Table 3.1. Comparison of different surface preparation techniques (1 least preferred and 5 most preferred)

	Diamond Grinding	Milling	Sand-blasting	Hydro-demolition
Level of practice in tack coat projects	2	3	3	3
Cost	2	5	3	5
Environmental Impact	2	3	4	4
Noise reduction	2	3	3	4
Friction	2	2	2	1
Construction time	2	4	3	2
Relative amount of tack coat used after surface prep	2	4	2	4
Overall Score	14	24	20	23

In this study, four different surface textures were evaluated in Chapter 5: (1) tined-polished, (2) sandblasted, (3) hydro-demoliton and (4) polished. Polished represents the worst case with a worn, untextured surface.

3.2 HMA-PCC INTERFACIAL LAYER EVALUATION

For laboratory evaluation, researchers developed three different specimen fabrication procedures. In the first procedure a PCC slab is cast, cured, and textured. The PCC slab is then coated by a layer of tack coat and allowed to cool before placing a layer of asphalt and compacting it. A vibratory compactor is used to compact the asphalt layer to target density (Figure 3.1).

Figure 3.1. Specimen fabrication in the laboratory using a vibratory compactor

In the second procedure, 4 inch diameter PCC cylinders are produced and textured using the selected surface preparation techniques in the previous section. The appropriate amount of tack coat is weighed, heated, and evenly applied on the PCC surface. The cylinders are then placed in the Marshall compactor mold, and a pre-weighed and pre-heated amount of loose HMA is placed over the tack coat to be compacted to the desired thickness (Figure 3.2).

Figure 3.2. Specimen fabrication using the Marshall compactor

In the third procedure, the tack coat is applied on a concrete cylinder and an asphalt mix is compacted on top of the concrete layer using a Superpave Gyratory Compactor (SGC). In this case, the desired density that would be representative of the first few years of the pavement life shall be achieved by specifying the compaction parameters in the SGC.

In either case, the tack coat is applied to the PCC surface at various application rates selected based on the literature review in Chapter 2 and presented later in this report.

The following is a list of tests and methods that were evaluated for consideration in this study.

3.2.1 Test 1: Direct Shear Test

Test 1: Direct Shear - Variation 1: Direct Shear: The shear bond strength between two bonded pavement layers can be determined by the direct shear test. The measuring device is capable of holding the test specimens and producing shear loads perpendicular to the specimens' vertical axis (TxDOT Designation: Tex-249-F (2019)). Figure 3.3 shows the interfacial layer shear strength device.

Figure 3.3. Interfacial layer shear strength device

During the test, shear load at a constant rate of displacement can be applied on the specimen, and the test can be terminated after the maximum shear load is

achieved. After testing, the maximum load and location of failure can be recorded. The maximum shear strength can be estimated for all specimens.

Advantages:

- Common method to evaluate the performance of tack coat at the PCC-HMA interlayer
- Relatively simple and easy to conduct

Drawbacks:

- Skewed interface between the PCC and HMA layers can cause large variability in the test results

Test 1: Direct Shear - Variation 1: Direct Shear with Normal Stress: Tex-249-F (2019) measured the shear strength between the PCC and HMA layers in the absence of any normal force. Figure 3.4 shows a testing jig commercially available that also allows for application of a normal stress while conducting the shear strength test. Real shear failures will always occur due to a combination of shear and normal stress acting on the interface between PCC and HMA.

Figure 3.4. Tack coat shear strength tester (Gilson Inc.)

3.2.2 Test 2: Pull-Off Test

Test 2: Pull-off - Variation 1: Tex-243-F: The pull-off test can measure the tensile strength of a tack coat before or after placement of the HMA overlay. TxDOT designation Tex-243-F (2009) suggests a test procedure which directly measures the adhesive strength of a tack coat allowed to cure for approximately 30 min (Figure

3.5). This shall also be considered as a candidate for further evaluation, particularly because it can also be carried out in the field. However, a drawback of this test is the inability to control the rate of loading, which can influence the repeatability. This shall be addressed by considering other candidate variations of this test.

Advantages:

- Simple procedure and easy to conduct
- The device is portable and can be used either in the laboratory or in the field

Drawbacks:

- This device can only be used on the tack coat surface
- Load application rate is manually controlled and can introduce high variability

Figure 3.5. Tack coat pull-off test (TxDOT designation:Tex-243-F)

Test 2: Pull-off - Variation 2: Portable Motorized Pull-Off Via HMA layer: In this approach, the pull-off strength of a tack coat is measured by using a motorized portable direct pull-off test device (Figure 3.6).

Figure 3.6. Direct pull-off test device

Specimens are partially cored from an HMA-PCC slab or SGC compacted specimen to a depth that reaches into some portion of the PCC layer to expose the PCC-HMA bonding interface but without fully extracting or separating the core from the PCC base. The top surface of the HMA is glued to a metal plate using high strength epoxy and allowed to cure (Figure 3.7). A portable motorized pull-off device is used to conduct a pull-off strength test to measure the tensile strength of the bond between PCC and HMA. The specimen is then inspected for the location of failure, whether it occurred at the bond, in the upper or lower layer, or at the glue interface.

Advantages:

- Enhanced repeatability and reproducibility compared to the manual pull-off test
- Simple and fast procedure

Drawbacks:

- Application of epoxy is time consuming
- If the failure occurs at the upper or lower layer, no determination of the interfacial layer bond strength can be made
- Tensile strength does not realistically directly represent the mode of failure (shear) in the field

Figure 3.7. A metal plate glued to the HMA surface

Test 2: Pull-off - Variation 3: Portable Motorized Pull-Off via Standard Metal Disc:

The pull-off test can also be used directly on the tack coat surface. In this procedure, a hot metal plate is placed on the tack coat film and allowed to cure and bond to the tack coat for couple of hours (Figure 3.8). As before, a portable motorized pull-off device is used to conduct a pull-off strength test to measure the tensile strength of the bond between PCC and HMA. The test configuration can be further refined to obtain more accurate and repeatable results.

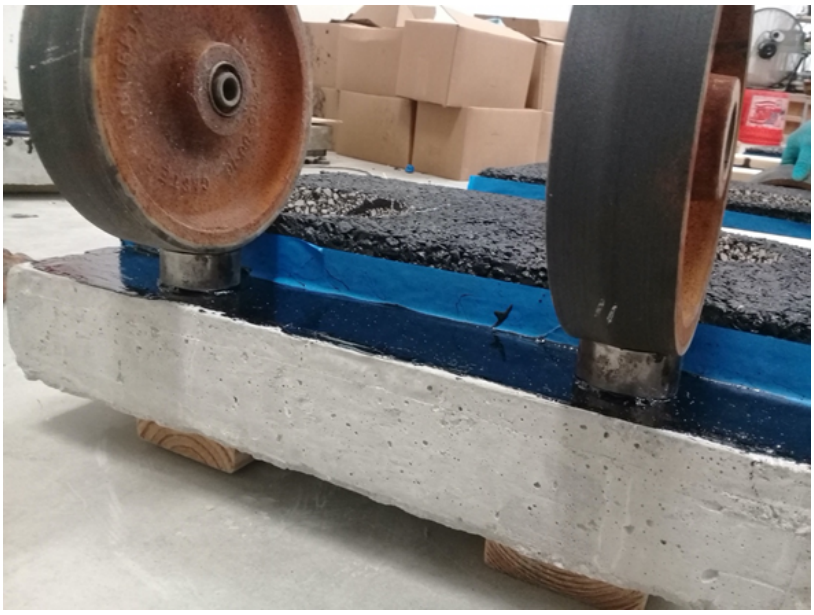

Figure 3.8. Metal plates placed on the tack coat, and left under weights to achieve proper bonding with the tack coat

3.2.3 Test 3: Torsional Shear Test

A variation of the direct shear test is the torsional shear test. The advantage of a torsional shear test is that it is a more accurate representation of the failure mode compared to a direct pull-off test (although the two may be correlated). However, a torsional shear apparatus also requires more site preparation work because the load frame must be anchored to prevent rotation (particularly when motorized) as opposed to the simplicity of a direct tension test that uses support reaction without the need for being anchored.

Test 3: Torsional Shear - Variation 1: Manual Torsion via Asphalt Sample: Based on the review of literature conducted, researchers examined the potential use of a manual torsional shear test to evaluate the bond strength between the asphalt mix and PCC. This test is similar to the direct pull-off test (Test 2) except the failure is measured in torsional shear and not in tension, which is a more accurate mode of failure in the field. As in the case of Test 2, specimens are partially cored from an HMA-PCC slab or SGC compacted specimen to a depth that reaches into some portion of the PCC layer to expose the PCC-HMA bonding interface but without fully extracting or

separating the core from the PCC base. The top surface of the HMA is glued to a metal plate using high strength epoxy and allowed to cure. The torque wrench is used to conduct a torsional shear strength test to measure the bond strength between PCC and HMA.

Advantages:

- Consideration of torsional shear stresses

Drawbacks:

- Inconsistent loading rate
- High variability in test results

Test 3: Torsional Shear - Variation 2: Manual Torsion via Metal Disc: This is very similar to the previous variation, except that a heated metal disc is placed and adhered directly to the tack coat instead of the asphalt mix. The advantage of this variation is that it can be conducted very rapidly, and it is independent of the asphalt mixture type and better controlled because of the use of metal disc for bonding.

Test 3: Torsional Shear - Variation 3: Motorized Torsion via Asphalt Sample and Variation 4 via Metal Disc: These two variations are exactly the same as the previous two variations except that a motorized setup is used to apply the torsional shear until failure. Based on the literature review, any ready-to-use commercial version to apply such loads either in the construction or other industries have not been identified. However, researchers explored two possibilities to include these variations as candidates for further validation.

The first possibility was to retrofit a commercial device for use in laboratory and field for such purposes. For example, the use of a motorized vane shear test apparatus could be retrofit for use a torsional test device to evaluate the bond strength between PCC and HMA. However, based on the available torque capacity of such devices and required torque with a reasonable sample size for the proposed application, this approach would require significant developmental work.

The second possibility was to build a custom device for such applications. For example, researchers explored the device used in Oregon for such purposes. However, this approach, similar to the previous approach would present significant challenges in terms of implementation and routine use by TxDOT.

Advantages:

- Less destructive (in-place measurements and smaller cores)

Drawbacks:

- Device is custom built

3.2.4 Arcan Test

The Arcan test can provide tensile load, shear load, and the combination of both simultaneously. In this test, a specimen is notched at the bond interface and the top and bottom surfaces are bonded to metal plates and fixed in a loading frame. The orientation of the sample with respect to the notch can be arbitrarily chosen so that it could be tested in direct tension, direct shear, or a combination of both.

Advantages:

- Simultaneous consideration of shear and tension loading mechanisms

Drawbacks:

- The test protocol has not been established well for HMA-PCC specimens
- Complicated installation
- Device is custom built

3.2.5 Summary

In summary, a weighted scoring approach was used to identify the best candidate methods for evaluating the bonding performance of tack coats (Table 3.2). Based on this scoring, the direct shear test was selected for evaluating the shear strength of tack coats. The motorized pull-off test was also selected to measure the bond strength of tack coats.

Table 3.2. Comparison of different test methods for characterizing the bonding performance of tack coats (1 is most preferred and 5 is least preferred)

	Direct shear	Direct Shear w/ Normal Stress	Pull-off (Tex-243-F)	Pull-off (via HMA)	Pull-off (on the tack coat)	Manual Torque Bond Test	Motorized Torsional Shear Device	Arcan
	Shear	Shear	Tension	Tension	Tension	Torsion	Torsion	Tension + Shear
Simplicity	1	1	1	1	1	1	2	2
Level of Practice in Tack Coat Projects	1	1	2	1	1	3	4	5
Representation of Field Condition	2	2	3	3	3	2	2	1
Capital Cost	3	3	3	3	3	1	4	2
Test Time (Prep+Test)	2	2	3	3	1	2	3	2
Repeatability	2	1	3	2	2	5	4	2
Sensitivity	2	1	3	2	2	4	3	3
Overall Score	13	11	18	15	13	18	22	17

3.3 ESTABLISHED PROTOCOLS

3.3.1 Protocol for Direct Shear to Evaluate Tack Coat

The direct shear test can also be used to evaluate the intrinsic shear strength and properties of the tack coat. In order to do so, it is important to control the nature and type of the substrate material to ensure repeatability and consistency across different testing sites and laboratories. The test described in the previous section involves a concrete specimen bonded to an asphalt mixture through the tack coat. Therefore, the test results also account for the influence of:

- concrete texture and physical chemistry of the concrete surface,
- intrinsic properties of the tack coat,
- effective tack coat film thickness (considering the texture of the underlying surface),
- asphalt mixture type including binder content and grade used in the mixture

In order to control all other variables except for the intrinsic properties of the tack coat, an alternative test method using aluminum discs was developed. In this approach, two aluminum discs are used instead of the asphalt mixture and concrete on either side. Each aluminum disc is one-inch thick each and four-inch in diameter. The discs are textured to allow for better uniform bonding. The texture is obtained by cutting fine groove lines that are 0.125" apart (c/c) and 0.025" wide and 0.01" deep.

The following protocol was developed for use with these discs and to carry out the direct shear tests.

1. The appropriate amount of tack coat material is weighed in a silicone container. This weight is based on the target application rate (typical 0.06 gallons/square yard for most tack coat materials and 0.40 gallons/square yard for AR binders). The loss of material in the texture is not accounted in this weight. In the case of an emulsion, the target amount of binder is adjusted based on the percentage of binder in the emulsion.
2. One of the two aluminum discs is cleaned using acetone and a masking tape is affixed to the disc with half the width of the tape adhering to the circumference of the disc near its top edge and the other half standing out.
3. The pre-weighed asphalt binder is heated to the target temperature (application

temperature based on manufacturer recommendation) and then poured on the surface of the aluminum disc.

4. Three metal ball bearings with a diameter that is closest to but no more than 0.01" smaller than the target film thickness are dropped at three corners of the tack coat surface.
5. The disc is immediately placed in an oven at 150°C for five minutes on a level platform to ensure that the binder has spread uniformly. The aluminum disc with the binder spread over it is then removed from the oven and allowed to cool to room temperature. This step is not required for emulsions. Instead, the emulsion shall be allowed to level and cure at room temperature by placing the disc over a flat surface.
6. Once the tack coat material has cooled or cured completely, the top aluminum plate is heated to 150°C in an oven and then immediately transferred onto the tack coat covered bottom plate, which is at room temperature.
7. A weight is placed on top of the top aluminum disc and the composite sample is allowed to cool to room temperature. The composite is then placed in a temperature control chamber set to the target test temperature and tested between 12 to 24 hours after placement.
8. The direct shear test is conducted using protocols similar to the shear test conducted using a concrete-asphalt composite specimen.

Figure 3.9 shows the test jig, samples for test and a failed sample.

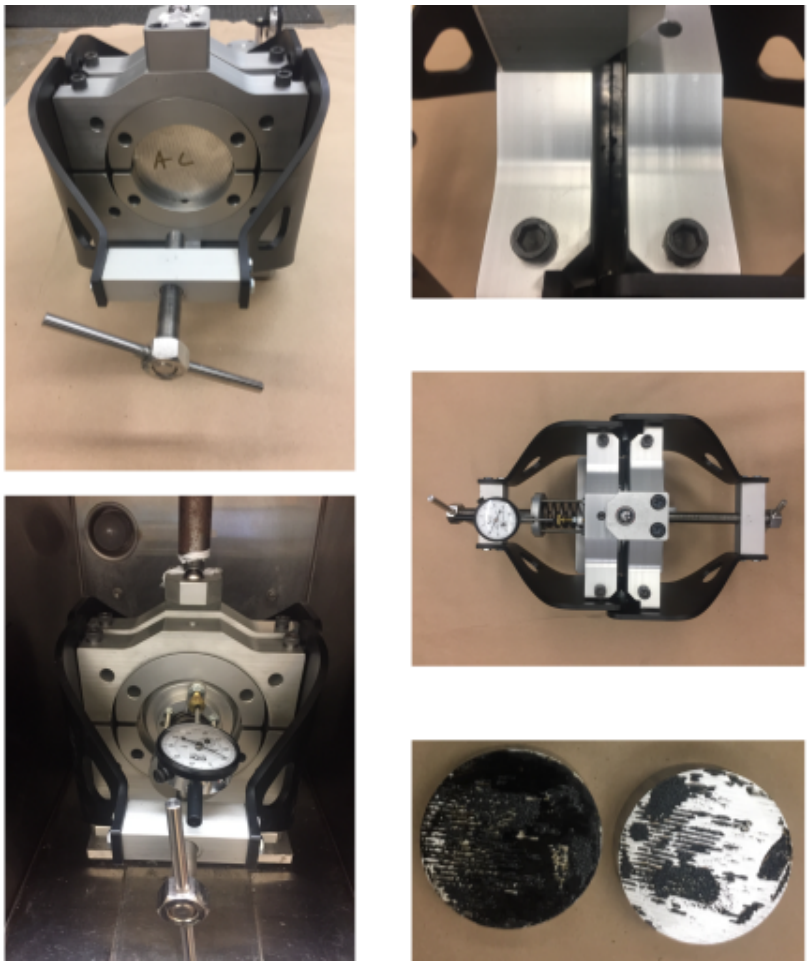

Figure 3.9. Top Left: Aluminum disc sample in the shearing jig; Bottom Left: Disc sample in the shearing jig with confining plates and the compressive pressure in loading frame; Top Right: Tack coat joint between the shearing discs; Middle Right: Disc sample in the shearing jig with confining plates; Bottom Right: Failed samples

3.3.2 Protocol for pull-off test

The pull-off test can be performed in the field without the need for coring through the depth of the entire concrete slab. This test can be conducted in the field and in the laboratory. From a field test point of view, it is important to control the temperature at which the test is conducted, which may be significantly different from the ambient temperature. Therefore, it was necessary to build a portable temperature control device. Figure 3.10 shows this device that was designed and built using a thermoelectric

heater-cooler. The device can be used to cool down or heat the environment around the test specimen by up to 15°C.

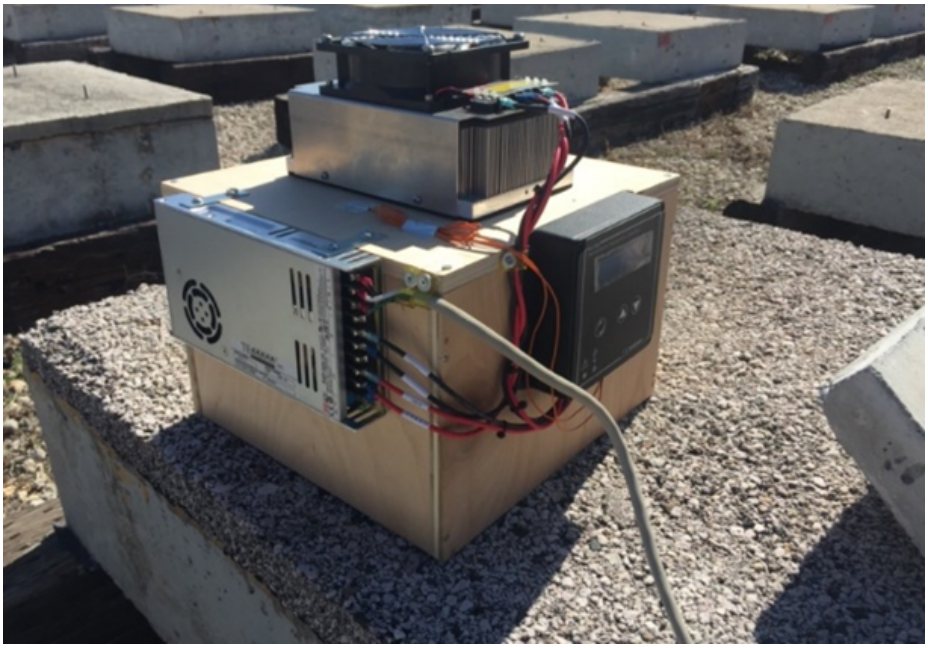

Figure 3.10. Thermoelectric temperature control system that can be used in the field

The following protocol was developed for conducting the direct pull-off tests.

1. A 2-inch diameter coring bit is used to core through the asphalt layer. The coring is continued until the bit encounters the concrete surface and approximately 1/4" below the concrete surface. Figure 3.11 shows the coring operation.

Figure 3.11. Coring of the asphalt overlay and concrete sub-surface by approximately 1/4"

2. The coring area is cleaned and dried for 10 minutes using a portable vacuum cleaner. The metal plate for the pull-off tester is adhered to the top of the asphalt surface. Figure 3.12 shows two samples in proximity with each other with the metal plates glued on the surface. Figure 3.13 shows trials that were conducted using several different epoxy and other adhesive systems to glue the metal plates to the asphalt surface. Only two specific types of epoxies worked successfully without adhesive failure after the pull-off test was completed.

Figure 3.12. Metal caps on two specimens for pull-off test

Figure 3.13. Tests conducted using multiple adhesives to determine the best adhesive for this application

3. The environmental chamber is placed over the metal plates and the temperature is set to 30°C to accelerate curing of the epoxy for 20 minutes. Subsequently, the temperature is set to 25°C, which is also the test temperature.

4. The pull-off device is placed over the test sample and the coupling mechanism is locked in. The device is manually set to applying a seating load of 5 psi. The test is then conducted by applying a load at a rate of 1 psi/second.

Figure 3.14. The pull-off device being locked on to the sample and the test being conducted using a force-controlled mode at a rate of 1 N/sec

Figure 3.15. The pull-off test after completion; the figure also shows the epoxy system that was successful

5. The peak strength data from the pull-off tester is recorded.

3.4 MATERIALS AND APPLICATION RATES

The three types of commonly used tack coats are hot paving asphalt cement (including PG-based binders and AR binders), cutback asphalt, and emulsions. Many agencies are reluctant to use cutbacks due to the environmental issues associated with the petroleum solvents. Asphalt emulsions and AR binders are the most widely used tack coat materials.

3.4.1 Emulsion tack coats

The most common types of emulsions used for tack coat applications are slow-setting emulsions. Recently, NTSS tack coats also known as trackless tack coats have been successfully used in tack coat projects. Emulsion bonding liquid (EBL) is also being used in some states as a promising tack coat material.

3.4.2 PG binder Tack Coat

PG binders are occasionally used as tack coat materials in some states. In studies that included emulsions and PG binders as tack coats, the PG binders yielded the highest tensile, torsional, and shear strengths (Mohammad, 2012; Tran et al., 2012; Mohammad et al., 2002).

3.4.3 AR Tack Coats

Feedback gathered from TxDOT districts shows that AR binder performs well as a tack coat material and in some cases, districts reported best bonding compared to other commonly used tack coats.

To evaluate the bonding characteristics of tack coats, the performing agency conducted a study on some of the most commonly used tack coats listed below, and found the highest shear strength for NTSS, and highest direct pull-off strength for ETAC. Also, in this study they found that although some tack coats can exhibit superior shear strength in displacement-controlled mode, in a load-controlled mode they might show a brittle behavior. Therefore, it is essential to conduct the tests on a variety of tack coats in order to better identify the best candidate materials for the field trials. Trackless tacks, PG binders and AR binders are proposed for initial evaluation.

3.4.4 Application rates

Based on the feedback from districts, a range of application rates between 0.04 and 0.06 gal/sq. yd. will be used for trackless tacks, PG binders and AR binders. For AR binders, a range between 0.2 and 0.5 gal/sq. yd. will be used. In either case, the optimum application rate will be selected based on the performance evaluation and visual observation.

CHAPTER 4. FINITE ELEMENT (FE) MODELING AND 3-D COMPUTATIONAL SIMULATION

4.1 OVERVIEW AND TASK OBJECTIVES

The primary objectives of this chapter are as follows:

1. To numerically simulate the pavement responses (i.e., stresses and strains) at the interface of the HMA and PCC pavement layers under real-life moving traffic loads.
2. To numerically identify the effect of a number of influencing parameters (including: overlay thickness, wheel load, traffic speed, and axle configuration) on the pavement responses at the HMA/PCC layer interface.

4.2 EXPLICIT FE DYNAMIC SIMULATION OF THE PAVEMENT STRUCTURES

This section details the methodology of modeling the pavement structures including an asphalt overlay layer on top of PCC layer. Additionally, it includes the information about the different simulated pavement structures and loading scenarios. All FE simulations were performed using ABAQUS.

4.2.1 Modeling the pavement structure

In this study, a typical freeway pavement structure was considered with a varying asphalt overlay thickness placed on top of the PCC layer. Figure 4.1 shows the model pavement structure and layers thicknesses. For the HMA overlay, 4 different thicknesses were considered in the analysis (2 inches, 4 inches, 6 inches, and 8 inches). All layers except for the HMA overlay were modeled as elastic-isotropic materials with the moduli (E and Poisson's ratio (μ) values shown in Table 4.1. The HMA overlay was modeled as a linear viscoelastic material (LVE) by considering the complex dynamic modulus $|E^*|$. Therefore, the $|E^*|$ values for a typical HMA mix was interconverted to a Prony Series (Generalized Maxwell Model) (Monk et al., 2003), represented by Equation 4.1. The $|E^*|$ can be numerically expressed as a function of the storage modulus, $E'(\omega)$, and the loss modulus, $E''(\omega)$, as shown in Equation 4.2, where

both the storage and loss moduli can be numerically determined using Equations 4.3 and 4.4, respectively. It is also known that the $|E^*|$ and the phase angle (ϕ) can be mathematically expressed as in Equations 4.5 and 4.6, respectively (Bai et al., 2021). Therefore, these mathematical expressions were used with the inter-conversion procedures explained in Park and Schapery (1999); Schapery (1974) to fit the $|E^*|$ master curve shown in Figure 4.2 to a mechanistic model (i.e., Prony Series) that is compatible with the FE software. The Prony Series parameters used in the FE simulations are shown in Table 4.2.

$$E(t) = E_0 + \sum_{i=1}^{N} e^{-T_r/\tau_i} \tag{4.1}$$

$$E^*(\omega) = E'(\omega) + i * E''(\omega) \tag{4.2}$$

$$E'(\omega) = E^*(\omega) * cos(\phi) = E_0 + \sum_{i=1}^{N} E_i \frac{(2\pi\omega T_i)^2}{1+(2\pi\omega T_i)^2} \tag{4.3}$$

$$E''(\omega) = E^*(\omega) * sin(\phi) = \sum_{i=1}^{N} E_i \frac{(2\pi\omega T_i)^2}{1+(2\pi\omega T_i)^2} \tag{4.4}$$

$$|E^*| = \sqrt{E'^2 + E''^2} \tag{4.5}$$

$$\phi = tan^{-1} \frac{E'}{E''} \tag{4.6}$$

where,

$E(t)$ = relaxation modulus

E_0 = modulus of each Maxwell spring

τ_i = relaxation time for each Maxwell element η_i/Ei

η_i = viscosity of each Maxwell dashpot

T_r = reduced time

N = number of Maxwell elements

$E'(\omega)$ = storage modulus at a specific frequency (ω)

$E''(\omega)$ = loss modulus at a specific frequency (ω

$E^*(\omega$ = complex dynamic modulus at a specific frequency (ω)

$i = \sqrt{-1}$

ϕ = phase angle

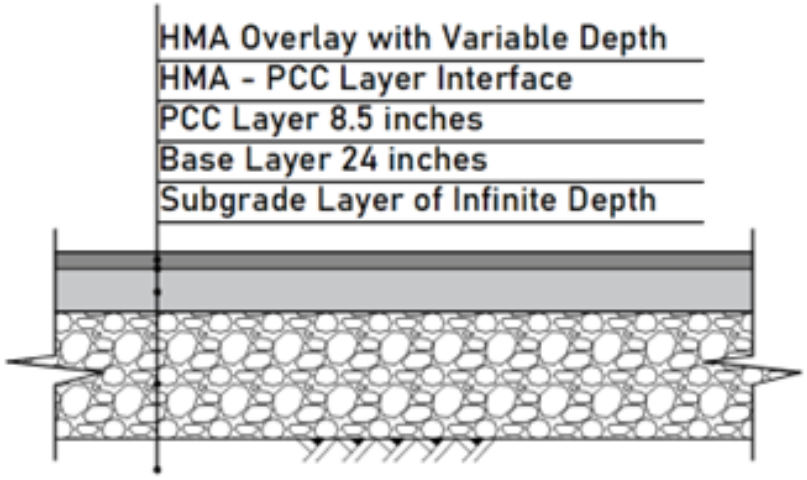

Figure 4.1. FE modeled pavement structure (Mabrouk et al., 2021)

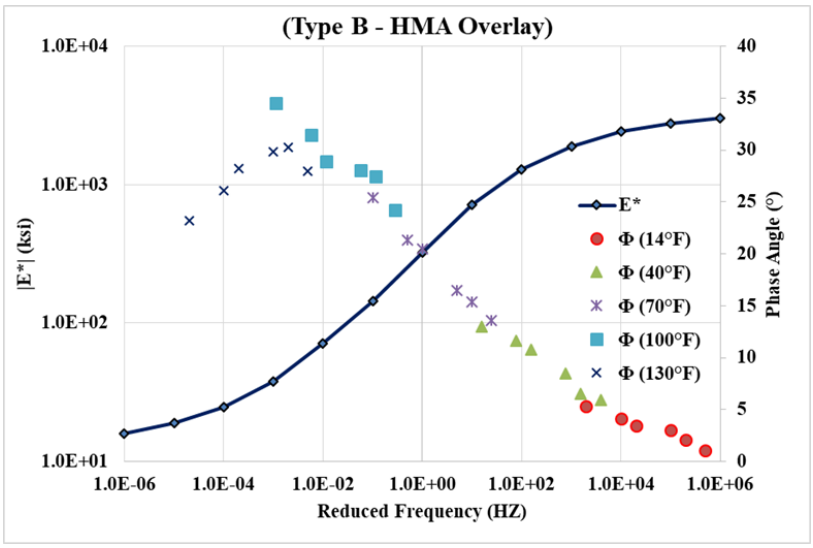

Figure 4.2. $|E^*|$ master curve at a reference temperature of 70°F and phase angles (ϕ) for a typical Type B HMA

Table 4.1. FE modeled pavement layer characteristics

Pavement layer	E (ksi)	μ (assumed)
HMA overlay	LVE - Prony series	0.35
PCC	4000	0.3
Granular base	35	0.4
Subgrade	7	0.45

Table 4.2. Prony series parameters for the modeled Type B HMA overlay thickness

No.	$E(i)$ (ksi)	τ_i, (sec)
E_0	3.00	–
E_1	289.88	0.000001
E_2	153.16	0.00001
E_3	558.94	0.0001
E_4	176.91	0.001
E_5	404.34	0.01
E_6	168.39	0.1
E_7	93.66	1
E_8	47.73	10
E_9	15.97	100
E_{10}	9.78	1000
E_{11}	4.76	10000
E_{12}	1.15	100000
E_{13}	9.18	1000000

After modeling each layer and assigning the material properties to these layers, the layers were assembled by defining "tie constraints" at the layer interfaces, assuming zero slippage between the layers, to ensure that the pavement layers will behave as a single structure under the applied loading and boundary conditions. Additionally, an

initial sensitivity check was performed to assign all the appropriate model dimensions, and the model dimensions were progressively reduced while monitoring the changes in results. The minimum dimensions that have no effects on the simulation results were specified for the model. Thus, the model width and length were assumed to be 12 ft. and 35 ft, respectively. Also, the subgrade was assumed to have an infinite depth (Bazi et al., 2020; You et al., 2018), to negate the effects of the model boundary conditions on the deflection results.

All the layers were meshed using explicit - hexahedral - 8 nodded - reduced integration linear bricks. The mesh sizes were assumed by specifying the minimum required number of elements, based on a convergence check to ensure mesh independency. Thus, the mesh sizes were specified as 1 inch for both the HMA overlay and the PCC layers, 2 inches for the base layer, and 3 inches for the subgrade layer.

4.2.2 Modeling of wheel load

In this study, three axle/tire configurations were considered (super single, dual, and tandem configurations). For the super single tire, a tire with the dimensions 445/50R/22.5 was considered. The 445 dimension represents the tire width in millimeters, the 50% is the aspect ratio which represents the tire wall height, measured from the top tread to the rim, as a percentage of the tire width, and the 22.5 is the rim diameter in inches. For the dual tire configuration, two tires with the dimensions 295/75R22.5 and a gap of 2 inches between each other were considered. For the Tandem axle/tire configuration two dual tire sets, of the same previous dimensions, spaced 17 inches center to center were considered.

All tires were modeled as three components, and the interactions between these components were defined, as exemplified in the literature (Mabrouk et al., 2021). The first component is the main rubber body of the tire. This part was used as a host layer for the other two reinforcing parts, which are the steel belt and the carcass plies. These two components were defined as "embedded reinforcing regions" inside the main rubber body to form the tire model, see Figure 4.3. Modeling the tire treads was ignored to reduce the model complexity. Additionally, the rim was modeled by assigning "rigid body constraints" to the rubber elements that should be contacting the rim from both sides. All the parts were modeled as elastic - isotropic materials and the material properties were assigned to them according to the values presented

in Table 4.3.

The rubber body was meshed with explicit - hexahedral - 8 nodded - reduced integration linear bricks, whilst the carcass plies and the steel belt were meshed with explicit - quadratic - 4 nodded - reduced integration linear shells. The mesh sizes for all the three parts were specified as 1 inch to ensure convergence (Walubita et al., 2014).

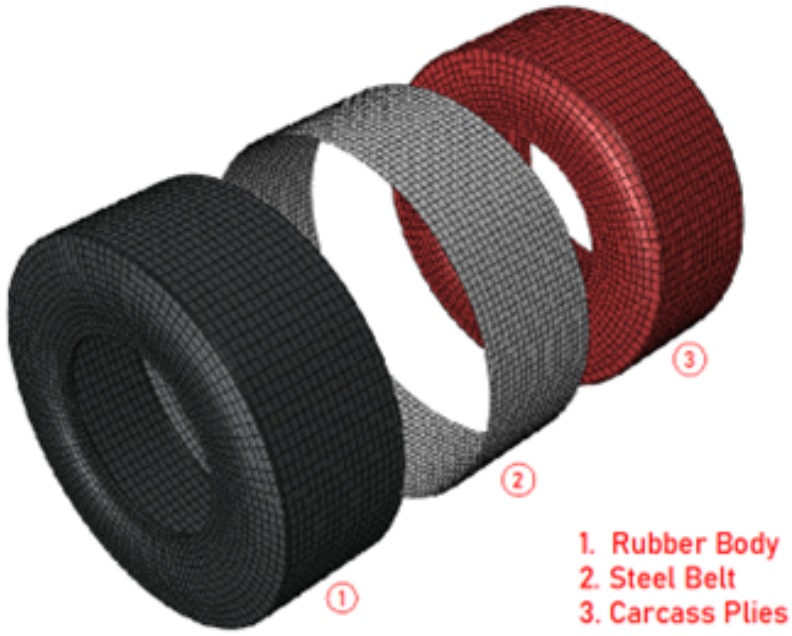

Figure 4.3. FE modeling of the tire components (Mabrouk et al., 2021)

Table 4.3. Material properties for the tire models (Alshukri et al., 2019)

Component	Density (lbs/ft^3)	E (ksi)	μ
Rubber	75	1.305	0.495
Steel belt	368	29.00 E+03	0.300
Carcass	93	58.00 E+01	0.300

In addition, different load levels were considered in the simulations according to Table 4.4. All the values shown in Table 4.4 are for half of an axle. Also, all the load levels were assumed to be lower than the federal load limit for each axle configuration.

Table 4.4. Simulated FE load levels for each axle configuration

Axle configuration	FE simulated load levels (lbs.)
Dual	6000 on half axle
Super single	6000, 8000, and 10000 on half axle
Tandem	6000, 8000, and 10000 on half axle

4.2.3 FEM interactions and boundary conditions

The interactions between the tires and the pavement surface were defined as a "surface to surface contact", and the "penalty method" was used to represent the tangential behavior of the friction between the tires and the pavement surface (Ong and Fwa, 2010; Peng et al., 2019). Also, the normal behavior of the contact property was represented by identifying the pressure - overclosure as a "Hard-Contact" in ABAQUS. Thereafter, all the vertical surfaces were restrained from displacement in both the longitudinal and the transverse directions, whilst the subgrade bottom surface was restrained from vertical displacement. Additionally, the vertical loads, according to the modeling scenarios, were applied to the center of wheels. Also, a uniform inflation pressure with two different values (100 psi and 120 psi) was considered in the simulations. The inflation pressure was applied radially to the inner surface of all the tire rubbers. Moreover, a radial as well as longitudinal speed boundary conditions were applied to the central point of the wheels, with their values varying depending on the analysis speed. Three different speed conditions were considered (namely 5 mph, 10 mph, and Stop/Go). The Stop/Go condition was modeled by applying an amplitude on the speed boundary condition to simulate the braking forces. Finally, the tires with their loads, constraints, and boundary conditions were placed on top of the pavement structure to make the model ready for the FE analysis - see Figure 4.4. Also, it is important to note that all analyses were "dynamic-explicit" with the non-linear geometry control (Nlgeom) turned on. The time incrementation was set as "Automatic" in ABAQUS, to ensure stability.

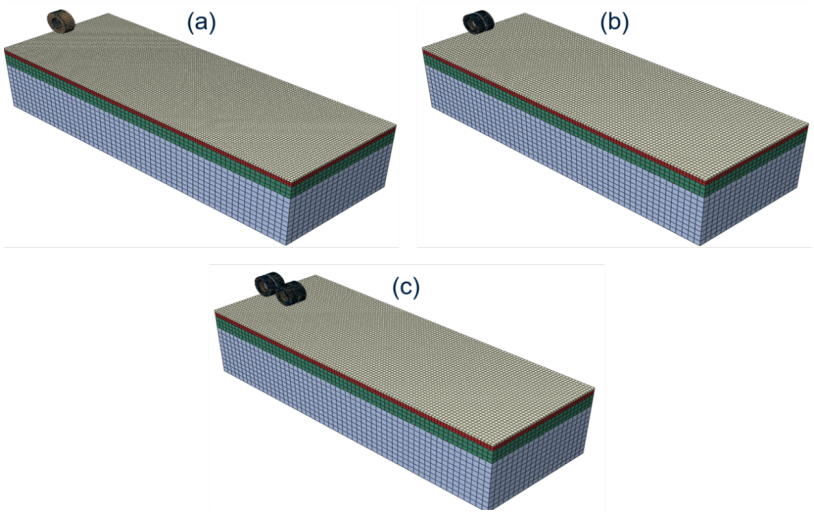

Figure 4.4. FE models assembly: (a) super single tire, (b) dual tires, and (c) tandem tire configuration

4.3 SIMULATION RESULTS

This section provides the detailed results of different FEM simulations performed in this study. To help understand the boding characteristics between HMA and PCC, pavement responses for different loading scenarios at the interface between HMA and PCC, in terms of shear stress and strains in two directions, were investigated. These responses are: longitudinal shear stresses and strains (i.e., in the direction of travel, indicated as X-X), and transverse shear stresses and strains (i.e., perpendicular to travel direction, indicated as X-Z). All these responses were investigated for all loading scenarios as previously mentioned, including the three load levels, three speeding conditions, two inflation pressures, and three axle configurations. The results of these pavement responses are shown in the following subsections.

4.3.1 Longitudinal shear stress at HMA-PCC interface

Figures 4.5 to 4.7 show the results obtained for longitudinal shear stress at the HMA-PCC interface.

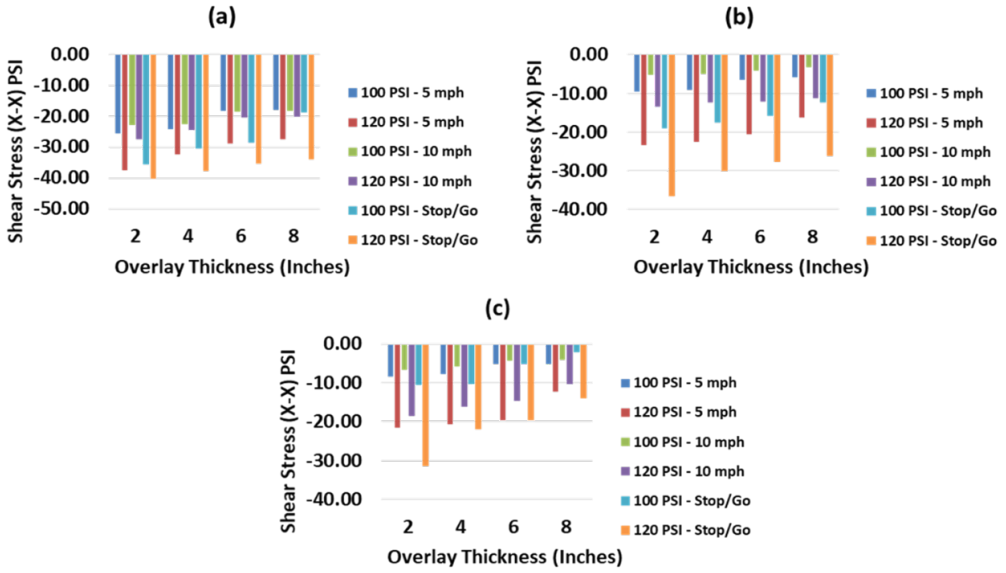

Figure 4.5. Longitudinal shear stress (X-X) at the HMA-PCC interface for a load level: (a) 6000 on a dual half axle, (b) 6000 lb on a super single half axle, and (c) 6000 lb on a tandem half axle

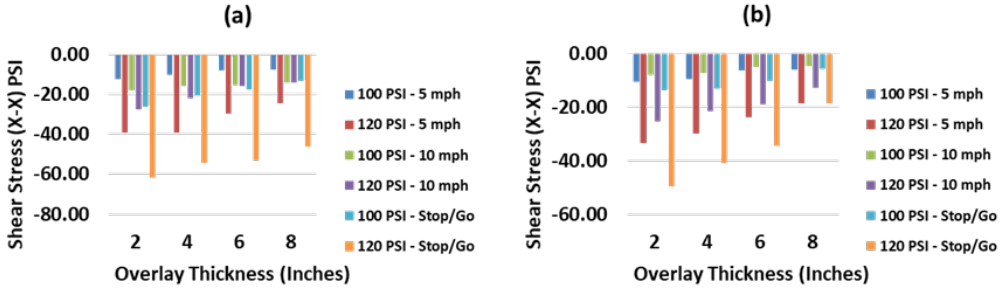

Figure 4.6. Longitudinal shear stress (X-X) at HMA-PCC interface for a load level: (a) 8000 lb on a super single half axle, (b) 8000 lb on a tandem half axle

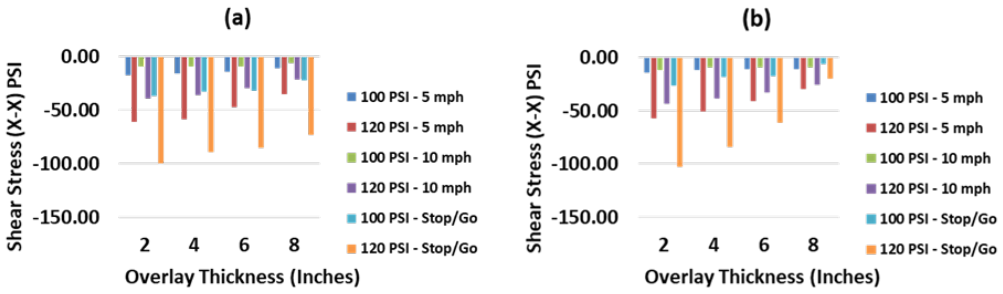

Figure 4.7. Longitudinal shear stress (X-X) at HMA-PCC interface for a load level: (a) 10,000 lb on a super single half axle, (b) 10,000 lb on a tandem half axle

4.3.2 Longitudinal shear strain at the HMA-PCC interface

Figures 4.8 to 4.10 show the results obtained for longitudinal shear strain at the HMA-PCC interface.

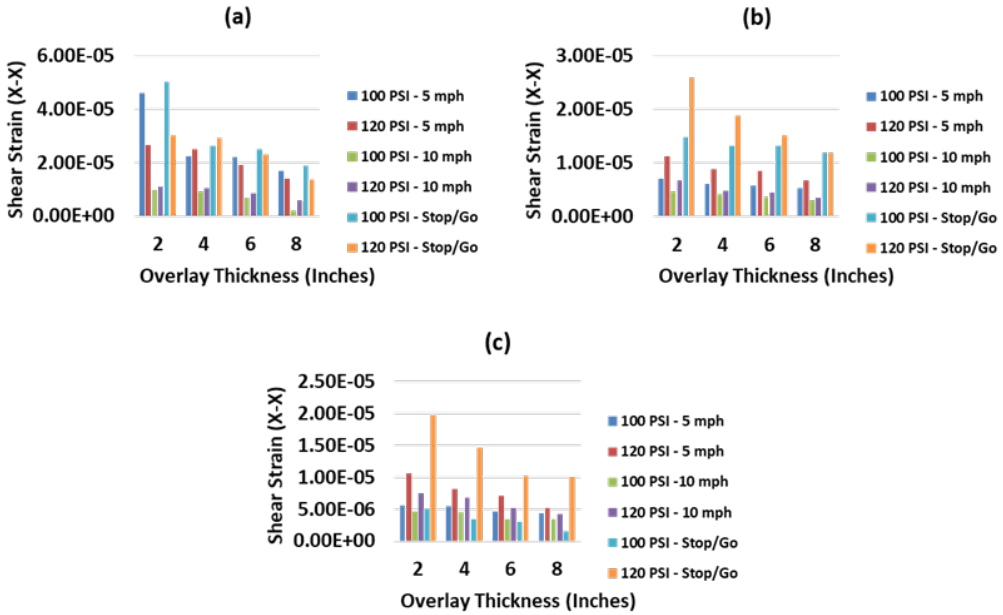

Figure 4.8. Longitudinal shear strain (X-X) at HMA-PCC interface for a load level: (a) 6000 on a dual half axle, (b) 6000 lb on a super single half axle, and (c) 6000 lb on a tandem half axle

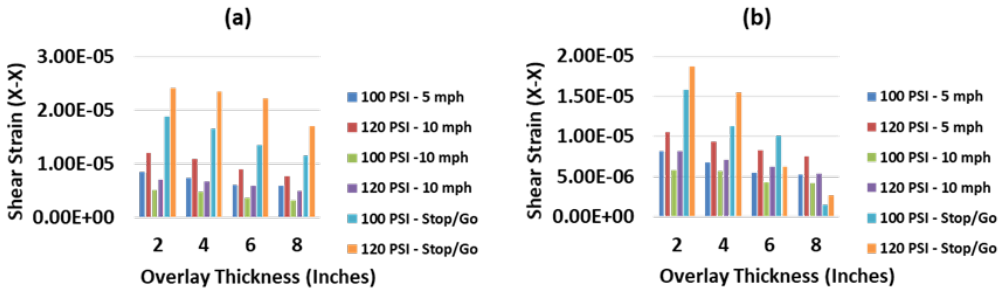

Figure 4.9. Longitudinal shear strain (X-X) at HMA-PCC interface for a load level: (a) 8000 lb on a super single half axle, (b) 8000 lb on a tandem half axle

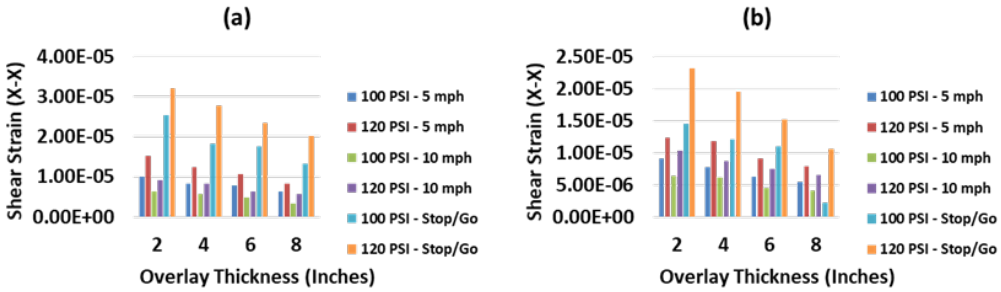

Figure 4.10. Longitudinal shear strain (X-X) at the HMA-PCC interface for a load level: (a) 10,000 lb on a super single half axle, (b) 10,000 lb on a tandem half axle

4.3.3 Transverse shear stress at HMA-PCC interface

Figures 4.11 to 4.12 show the results obtained for transverse shear stress at the HMA-PCC interface.

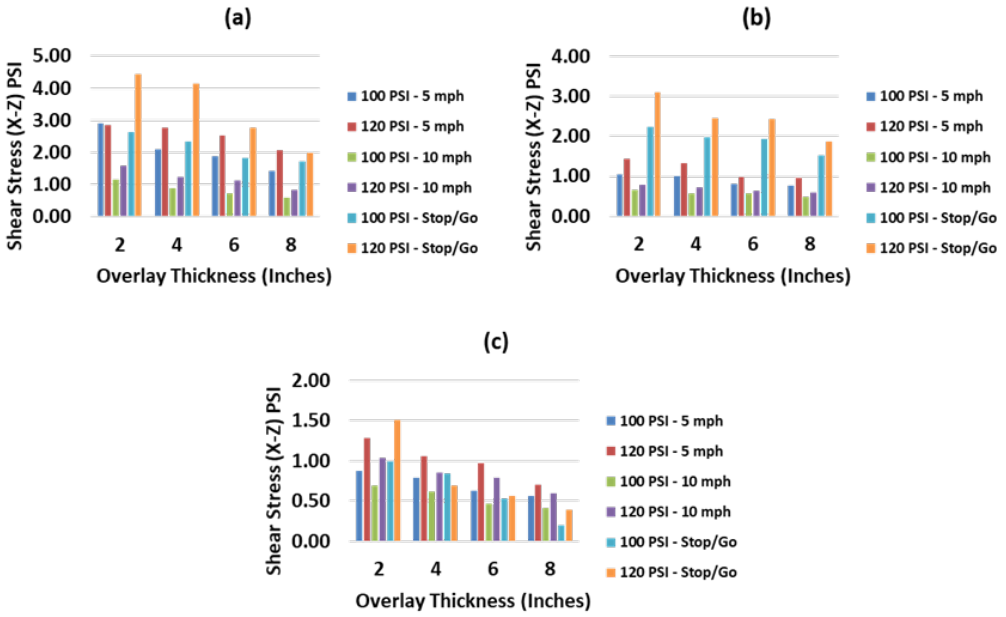

Figure 4.11. Transverse shear stress (X-Z) at the HMA-PCC interface for a load level: (a) 6000 on a dual half axle, (b) 6000 lb on a super single half axle, and (c) 6000 lb on a tandem half axle

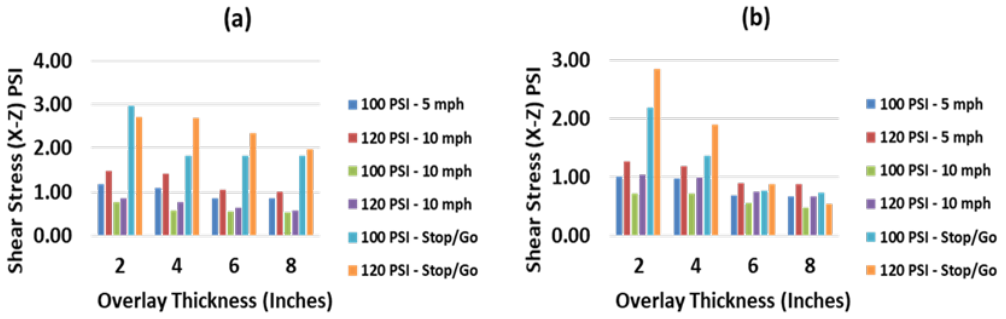

Figure 4.12. Transverse shear stress (X-Z) at the HMA-PCC interface for a load level: (a) 8000 lb on a super single half axle, (b) 8000 lb on a tandem half axle

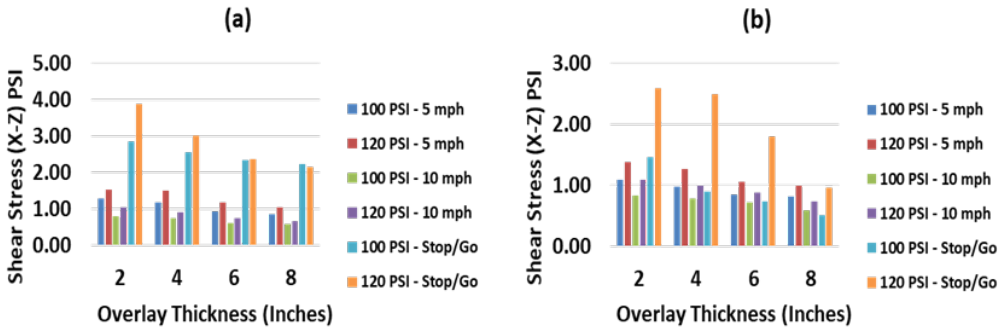

Figure 4.13. Transverse shear stress (X-Z) at the HMA-PCC interface for a load level: (a) 10,000 lb on a super single half axle, (b) 10,000 lb on a tandem half axle

4.3.4 Transverse shear strain at the HMA-PCC interface

Figures 4.14 to 4.16 show the results obtained for transverse shear strain at the HMA-PCC interface.

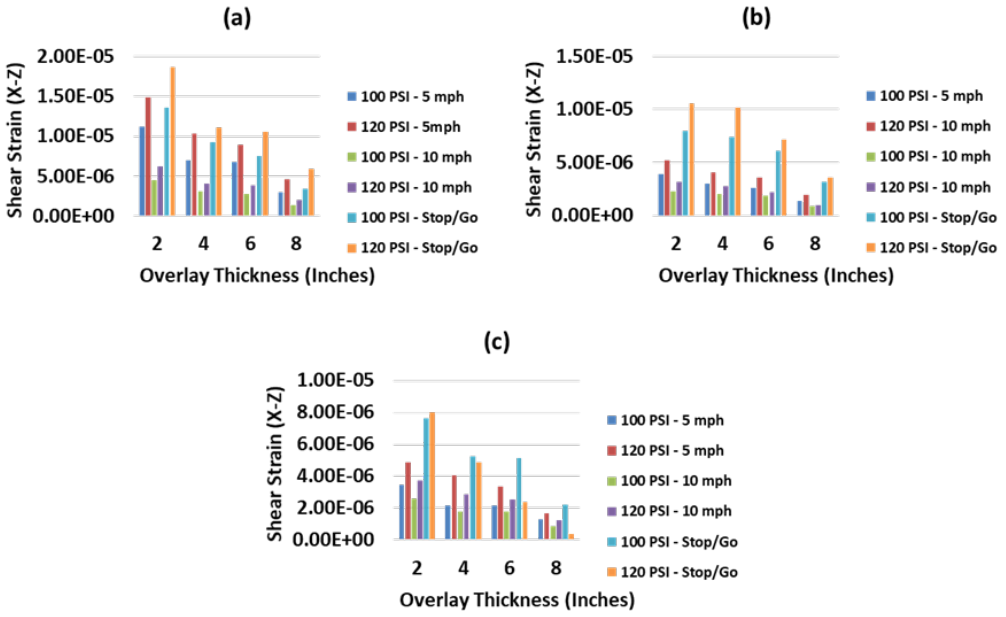

Figure 4.14. Transverse shear strain (X-Z) at the HMA-PCC interface for a load level: (a) 6000 on a dual half axle, (b) 6000 lb on a super single half axle, and (c) 6000 lb on a tandem half axle

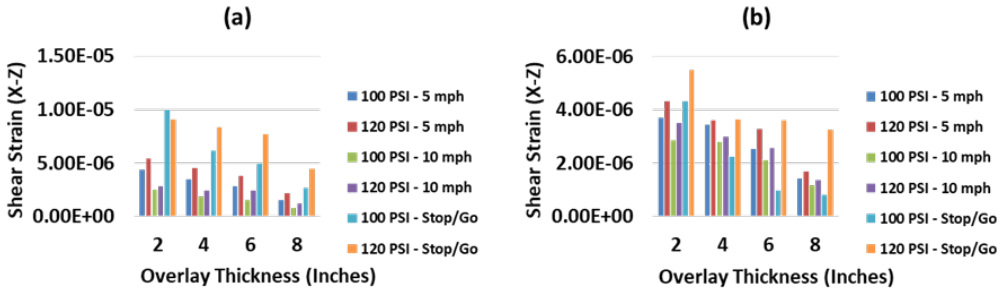

Figure 4.15. Transverse shear strain (X-Z) at the HMA-PCC interface for a load level: (a) 8000 lb on a super single half axle, (b) 8000 lb on a tandem half axle

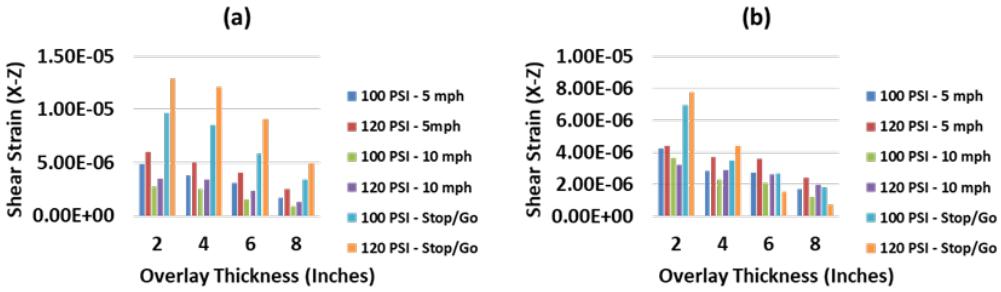

Figure 4.16. Transverse shear strain (X-Z) at the HMA-PCC interface for a load level: (a) 10,000 lb on a super single half axle, (b) 10,000 lb on a tandem half axle

4.4 FINDINGS

From the previous results, as it was expected, the shear stresses/strains at the HMA-PCC interface is highly affected by the loading scenario. The most influencing parameter was found to be the braking forces, represented in the simulation by the Stop/Go condition as previously explained. Also, the overlay thickness was found to be highly influential, as the stress/strain magnitudes reduces significantly with the increase of the overlay thickness. Almost the same difference in the pavement responses magnitude was found with the increase of the inflation pressure in different loading scenarios. In addition, a similar pattern was found with the change of speed from 5 mph to 10 mph. Finally, the ranges of the shear stresses/strains at the HMA-PCC interface were found to be varying significantly based on the loading scenario.

CHAPTER 5. FINALIZING TEST PROCEDURES TO MEASURE PCC-HMA BONDING AND EVALUATING INFLUENCE OF DIFFERENT FACTORS ON QUALITY OF BOND

The main objectives for this task were to: (1) develop a procedure to produce PCC-HMA laboratory samples and test the bonding between the PCC and HMA layer, and (2) evaluate the influence of the following factors on the PCC-HMA bond:

- Tack coat type
- Application rate
- PCC surface texture
- Surface cleanliness
- Surface moisture

Two different test methods were evaluated in this study to evaluate the quality of the PCC-HMA interfacial bond: (1) a direct shear test, and (2) a pull-off test. The direct shear test was intended so it can be used on laboratory prepared specimens as well as using field cores to evaluate the shear strength of the PCC-HMA bond. The pull-off test was developed primarily as a tool to evaluate the quality of the PCC-HMA bond in the field but without the need for taking cores and running the test in the laboratory. However, in order to validate the efficacy of this method, a version of this test was developed so it could be conducted on laboratory samples and allow for comparison of results from the direct shear and the pull-off tests.

This chapter presents a summary of the materials used, the sample preparation method that was developed to carry out the aforementioned tests in the laboratory, a description of the test method, and results. Appendices A and B present a description of the direct shear and pull-off test (field version) in a standard format.

5.1 INFLUENCE OF TACK COAT TYPE

Four different tack coats were evaluated in this part of the study:

1. Trackless tack #2
2. AR Binder
3. Trackless tack #1
4. PG 70-22

Different tack coats were used while keeping the other conditions constant. The tack coats were applied in two different ways: (1) as a chip seal for AR binder (2) applied directly with spatula for all other tack coats.

5.1.1 Application of AR binder

AR binder is applied as a chip seal on the PCC surface in this study. For chip seal, precoated aggregates were created by mixing Grade 4 igneous non-absorptive aggregates with 0.2% asphalt binder of grade PG 64-22. Figure 5.1 shows the precoated aggregates obtained from this procedure.

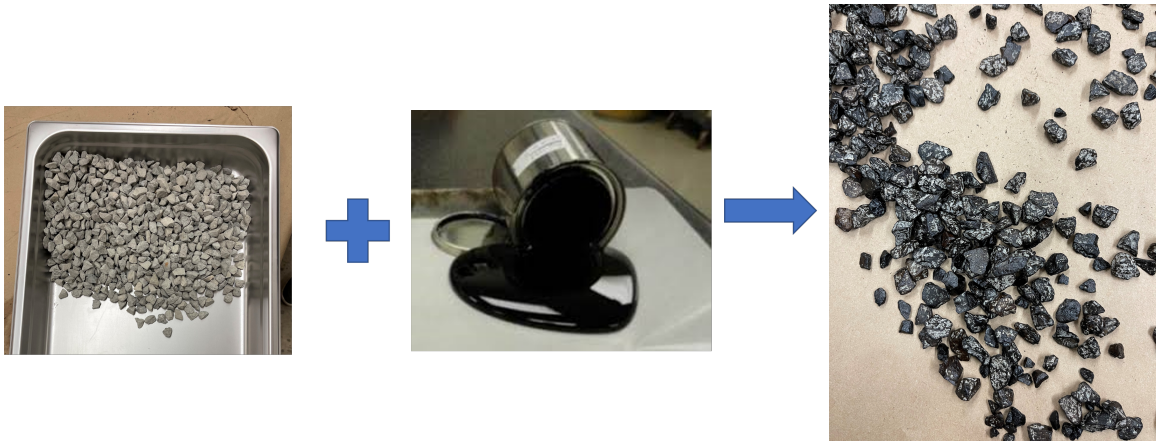

Figure 5.1. Precoated aggregates for creating chip seal

On the PCC surface hot AR binder was applied at a rate of 0.4 gallons/sq. yd. The precoated aggregates were placed on the hot applied binder so that approximately half the surface area was covered with the precoated aggregate particles. Figure 5.2 shows a PCC sample with chip seal applied on it.

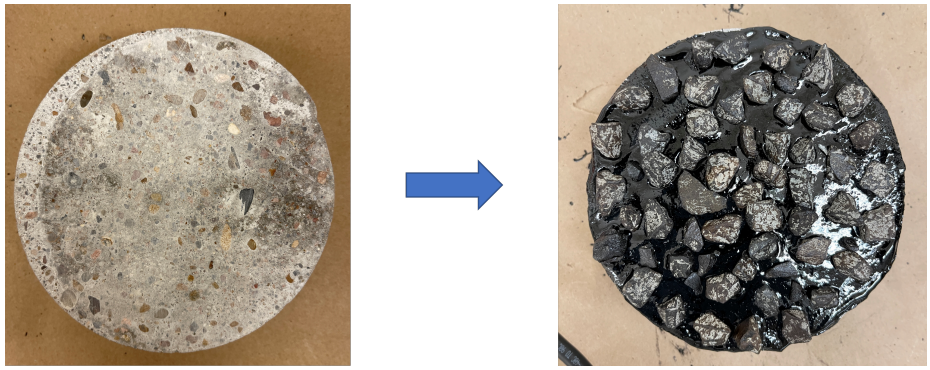

Figure 5.2. A PCC sample with AR binder as chip seal

5.1.2 Application of other tack coats

The three remaining tack coats: Trackless tack #1, Trackless tack #2 and PG 70-22, were directly applied on the PCC surface at a rate of 0.06 gallons/sq. yd. using a spatula and a heat gun.The target amount of binder was weighed and poured evenly over the surface of the concrete. The heat gun and a spatula were used to spread the tack coat uniformly over the surface of the concrete. A more detailed description of the sample preparation procedure is described in the subsequent section. Figure 5.3 shows a PCC sample with Trackless tack #2 applied on it.

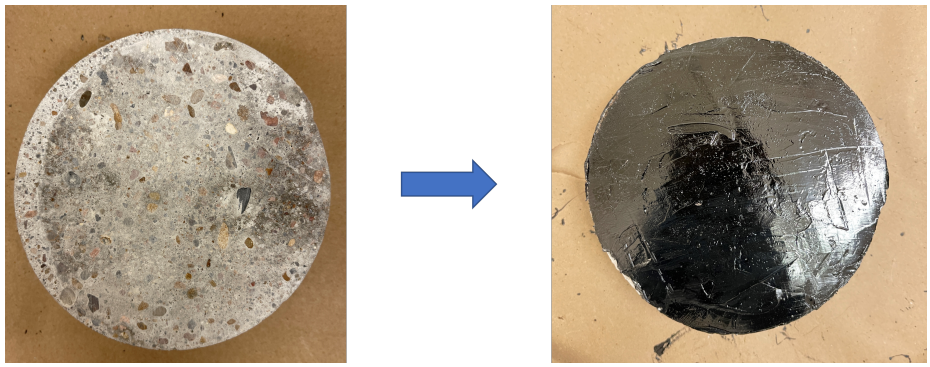

Figure 5.3. A PCC sample with Trackless tack #2 applied on it

5.2 INFLUENCE OF APPLICATION RATE

In order to evaluate the impact of application rate on the quality of the bond, four different application rates using two different tack coats were evaluated in this task

as shown in the Table 5.1. Recall that AR binder was applied as chip seal whereas Trackless tack #2 was applied directly on the concrete surface.

Table 5.1. Test matrix to evaluate the influence of application rate

Tack coat type	Application rate (gal./sq. yd.)
Trackless tack #2	0.04 0.05 0.06 0.07
AR binder	0.2 0.3 0.4 0.5

5.3 INFLUENCE OF PCC SURFACE TEXTURE

In order to evaluate the influence of PCC surface structure on the quality of the bond, four different PCC surface textures were evaluated using two different types of tack coats and one application rate: (1) tined-polished, (2) sandblasted, (3) hydro-demolition and (4) polished. These textures are shown in Table 5.2 and a summary of the process used to produce these textures is presented in the subsequent section.

Table 5.2. Four different PCC surface textures evaluated in this study

Tined-polished	
Sandblasted	
Hydro-demolition	
Polished	

5.4 INFLUENCE OF SURFACE CLEANLINESS

The influence of cleanliness of PCC surface on PCC-HMA bond was also examined in this study. Two different cleanliness conditions were considered: (1) clean and (2) dirty. The clean surface was obtained by wiping the PCC surface clean with a piece of dry paper towel prior to the application of the tack coat. In fact, this was the procedure used for all specimens except when a dusty surface was being evaluated by design. The dirty surface was obtained by spreading 0.1 g of fines of igneous material (passing sieve no. 200) over clean PCC surface to achieve a surface coating of fines. Table 5.3 shows clean and dirty surfaces for each PCC surface texture.

Table 5.3. Clean and dirty conditions for different PCC surface textures

PCC surface texture	Clean	Dirty
Tined-polished		
Sandblasted		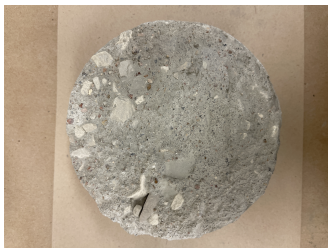
Hydro-demolition		
Polished		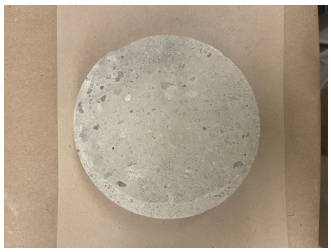

5.5 INFLUENCE OF SURFACE MOISTURE

Three different surface moisture conditions were used to evaluate the impact of surface moisture on PCC-HMA bond: (1) wet, (2) moist, and (3) dry. Post fabrication all PCC samples were stored under water. The three surface moisture conditions are based on the time that the PCC sample was in air in the lab conditions prior to the application of the tack coat. Samples out in air for 2-4 hours were considered as wet,

22-26 hours as moist, and 7 days as dry.

5.6 SAMPLE PREPARATION AND TESTING

5.6.1 PCC sample preparation

Four concrete surface textures were applied to concrete disks to determine how well an asphalt overlay would adhere to the surface. All of the samples began as 6-inch diameter concrete disks that were 2 inches thick. The concrete mixture design followed TxDOT Class P concrete specifications which included a maximum 520 lbs of cementitious material with a water to cement ratio of 0.45. This mix design was used for two different coarse aggregates (river gravel and limestone). The mixing procedure followed ASTM C192 (2015). After mixing, concrete was cast into the disk molds. The concrete was placed in two layers and rodded 25 times per layer. A wooden trowel was used to strike off the excess concrete. The samples were then covered with wet burlap and plastic to cure for 24 hours. After 24 hours, the samples were demolded and placed into the moist cure room. The following sections provide information on how the samples were created for each texture type.

5.6.1.1 Polished

Samples were polished to achieve a worst-case scenario. The intent was to replicate a rigid pavement surface that had experienced polishing over time due to the action of traffic. After 7 days of wet curing the concrete disks, the samples were removed from the moist cure room. The samples were ground on a wet 100 grit polishing wheel. Each sample was ground for 5 minutes with a hand applied pressure. Samples that may have had more surface irregularities from after casting took a few more minutes to polish. After reaching the desired polish, the samples were placed back into the moist cure room.

5.6.1.2 Tined-polished

A set of samples were tined initially after casting and then polished after seven days. The intent was to replicate a rigid pavement surface that had tining immediately after construction but had also experienced polishing over time due to the action of traffic.

The tining took place shortly after the wood trowel strike off. A quarter inch tine mark spaced every one inch was created on the surface of the disk. The samples were then wet cured for seven days which then followed the same procedure outlined in the polished section.

5.6.1.3 Sandblasting

Sandblasting equipment was used to increase the surface texture of the concrete disks. After seven days of moist curing, the samples were removed and placed on a table outside. A sandblasting gun with 70 grit blast sand was used to texture the surface of the disks. After sandblasting the surface, the samples were placed back into the moist cure room.

5.6.1.4 Hydro-demolition

Hydro-demolition was used to remove the top paste layer of each concrete disk. Hydro-demolition usually occurs after the concrete has hardened with the use of high-pressure water to remove layers of concrete. The concrete disks for this project were subjected to hydro-demolition after casting. An hour after casting the concrete disks, a water hose nozzle was used at intermittent blasts to remove the top layer of concrete. This procedure produced a hydro-demolition texture to the concrete samples. The samples were demolded at 24 hours and placed in the moist cure room for 28 days.

5.6.2 Application of tack coat

Different tack coats were applied to the PCC samples as discussed in Section 5.1. Note that the PCC samples were stored under water after the samples were fabricated and cured. The time period for which the samples were kept in air after being removed from water was based on the condition of the surface moisture, as discussed in Section 5.5. The tack coat was applied after this time period.

For hydro-demolition and sandblasted surfaces, a thin film of tack coat was applied on hot PCC surface for all tack coats except AR binder, as these surfaces were very rough to evenly spread the tack using a spatula. The PCC surface was heated to approximately 160°C using a temperature-controlled heat gun for a very short duration. Although the PCC surface is not heated in practice, this was done to compensate for

the cooling of the small amount of binder used in a laboratory environment and to ensure a good bond between tack coat and PCC surface. The tack coat film was created by pouring the desired quantity of hot tack coat on a parchment paper and spreading it in a circle of 150 mm diameter using a spatula and heat gun. This film was peeled off from the parchment paper after it was allowed to cool. In all other cases, hot tack coat was poured on the PCC surface and was spread using a spatula and a heat gun as described in Section 5.1. After applying the tack coat, the PCC sample was left overnight to cure.

5.6.3 Compaction of asphalt mix on PCC sample

A thin overlay mix (TOM) was used as the surface mix. A large sample of this mix was obtained from a hot mix plant in several small boxes and placed in cold storage. A sample of the loose asphalt mixture (as needed) was heated in the oven for about two hours at 165°C. The concrete sample with the tack coat on its surface is placed in the SGC mold. Note that the concrete specimen and the tack coat are at room temperature at this stage to closely replicate a realistic scenario in the field. An amount of 4.4 lbs. of the HMA (preheated to compaction temperature) was placed on top of the tack coat surface inside the mold. The sample was then compacted to 110 gyrations using the SGC using conditions as described in Tex-241-F (2019). Figure 5.4 shows the step-by-step procedure that was used to prepare laboratory specimens for testing. The prepared composite samples were left overnight prior to testing.

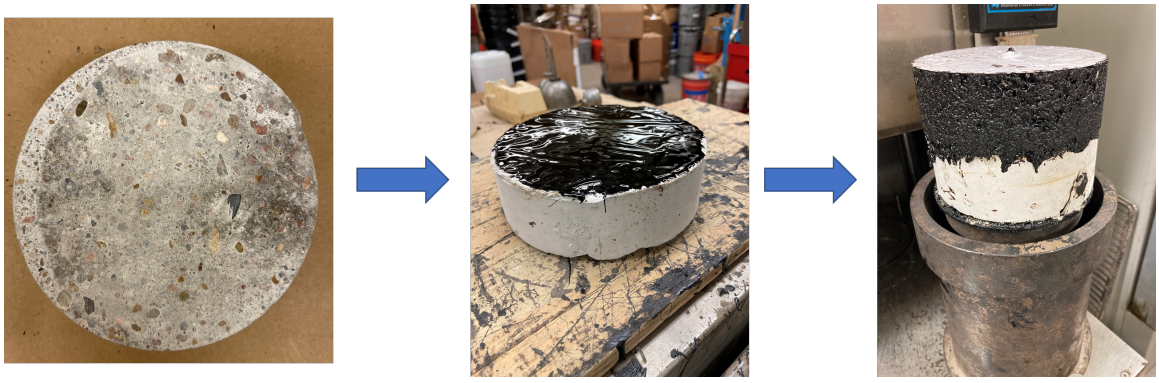

Figure 5.4. Procedure for preparation of a composite PCC-HMA sample for shear testing

5.6.4 Testing

Based on Task 3, two test methods were selected to evaluate the PCC-HMA bonding (i) direct shear test (ii) pull-off test. Three replicate specimens were created for testing each of the aforementioned factors. Two of these specimens were used with the direct shear test and one specimen was used for the pull-off test.

5.6.4.1 Direct shear test

The PCC-HMA samples were tested for direct shear by placing the sample in the jig and applying a confining pressure of 10 psi. The test method is a modification of Tex-249-F (2019) based on AASHTO TP-114 (2018). Preliminary tests showed that the use of confinement improved repeatability and reduced noise in the load-displacement response from the test. The modified Tex-249-F is included in Appendix A of this report. In summary, the sample was loaded in shear at a displacement rate of 0.2 inch/minute to obtain the stress-strain curve while retaining a confining pressure of 10 psi. Figure 5.5 shows the procedure for performing the direct shear test in the laboratory.

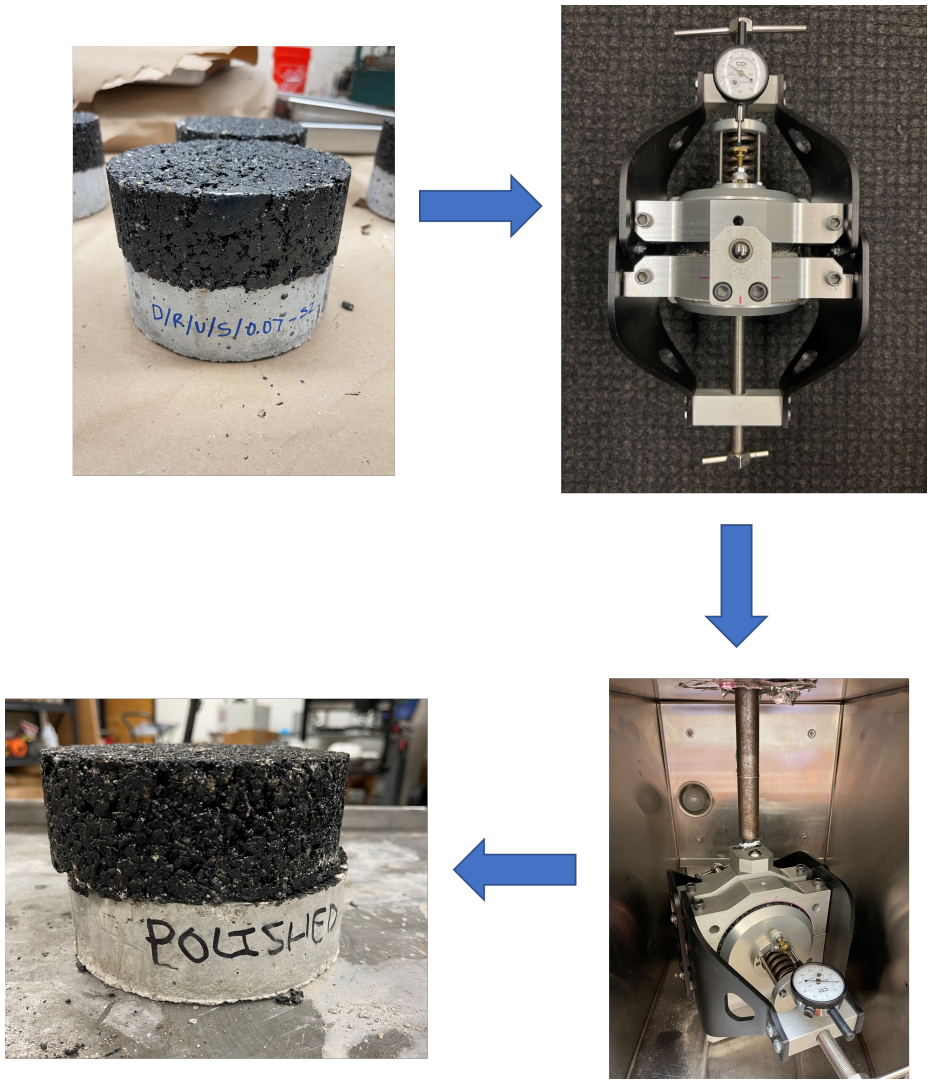

Figure 5.5. Procedure for direct shear testing in laboratory

From the stress-strain curve, two parameters were used to evaluate the bond between PCC and HMA: (1) shear strength, and (2) brittleness factor. Shear strength was defined as the maximum stress from the stress-strain response captured during the test. Brittleness factor was defined as a ratio of shear strength and stress at the strain of 1.2 times the strain at the maximum stress. This factor ranges from 1 to infinity. A higher value of this factor implies low ductility and a value close to 1 implies very high ductility. Figure 5.6 shows these two parameters in the stress-strain curve.

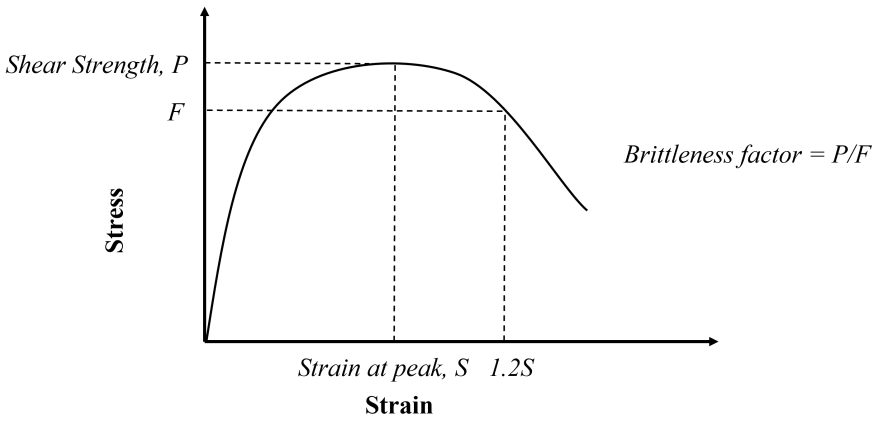

Figure 5.6. A typical stress-strain curve obtained from direct shear test showing the two parameters (1) shear strength and (2) brittleness factor

5.6.4.2 Pull-off test

A pull-off test was developed and used to evaluate the in-situ quality of tack coat. A more detailed description of this test along with field test results is provided in another chapter of this report. One of the goals of this task was to evaluate the accuracy of this method as a field test as compared to measurement of the bond strength using the direct shear test.

To perform the pull-off test on PCC-HMA samples, a 2-inch diameter coring bit was used to core through the asphalt layer. The coring continued into the concrete layer to a depth of approximately 0.125 to 0.25 inches to ensure that the asphalt core was completely detached from its surroundings. The compacted sample was cored at two locations to obtain two replicate sites for testing. The sample was then cleaned with water to remove any debris from the drilling process followed by compressed air. The sample was dried overnight before the pull-off tester was glued to the steel disk on top of the drilled asphalt surface. The glued sample was cured overnight before testing at a load rate of 1 psi/second with the pull-off tester to obtain the pull-off strength of the PCC-HMA bond. Note that the field process uses an environmental chamber to accelerate the drying and curing process to within one hour. Figure 5.7 shows the step-by-step procedure of performing the pull-off test.

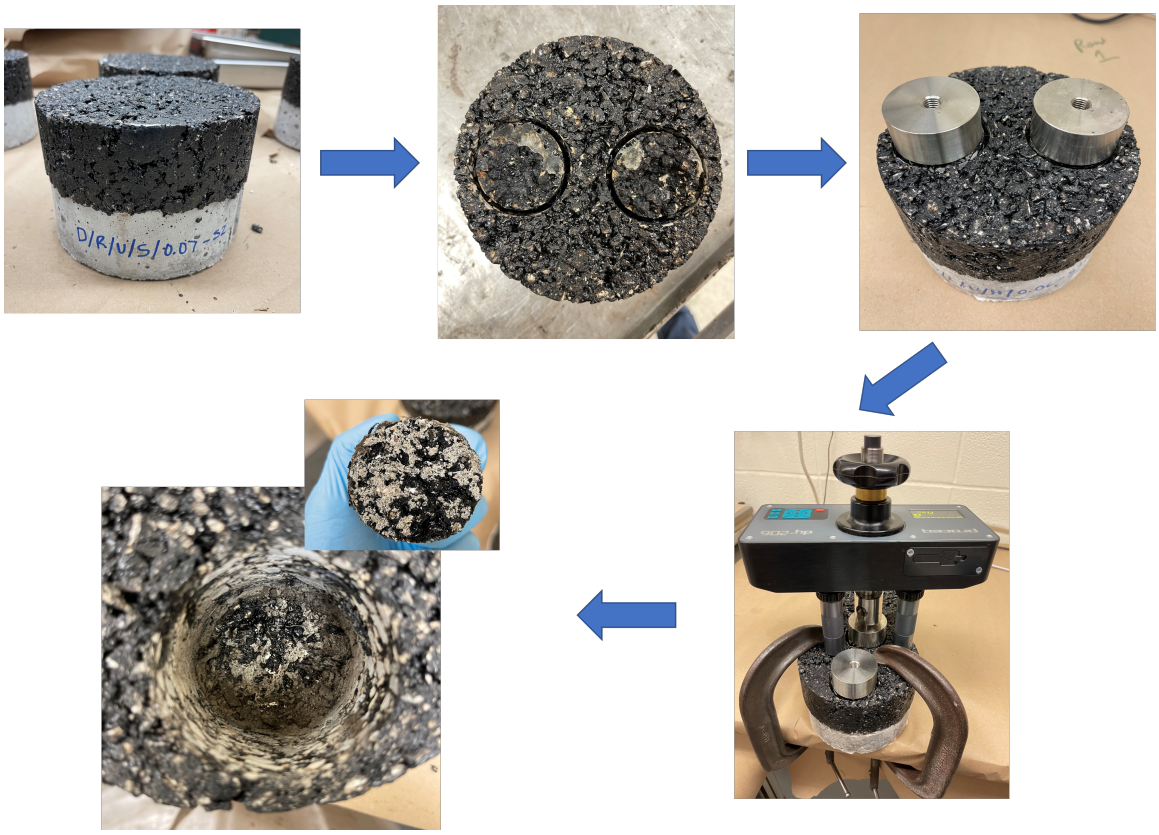

Figure 5.7. Procedure for pull-off testing in laboratory

5.7 RESULTS

5.7.1 PCC-HMA without tack coat

Direct shear testing was performed PCC-HMA samples without any tack coat. Note that in this case, the PCC samples had texture only from the casting of the concrete and no special surface texture was provided on them. River gravel concrete mix was used for these samples. Two replicates were tested and the average shear strength was 54 psi and the average brittleness factor was 1.61.

5.7.2 Tack coat type

Figures 5.8, 5.9 and 5.10 show the pull-off strength, shear strength and brittleness factor of the four different tack coats, respectively. It should be noted here that dry, clean, and polished PCC surface condition was used to evaluate these tack coats.

Three observations can be made from these figures. First, results from both direct shear test and pull-off test show the same trend. Second, Trackless tack #1 has the highest pull-off strength as well as shear strength followed by Trackless tack #2 whereas the AR binder has the least. Third, although Trackless tack #1 and Trackless tack #2 have high strength they also have high brittleness factor showing less ductile nature of failure whereas AR binder is more ductile in nature.

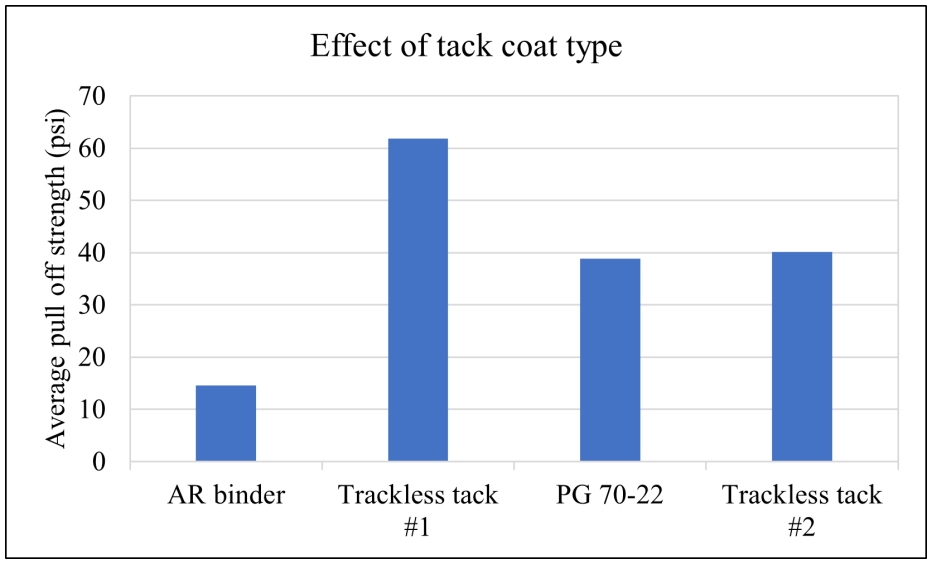

Figure 5.8. Pull-off strength for different tack coat types

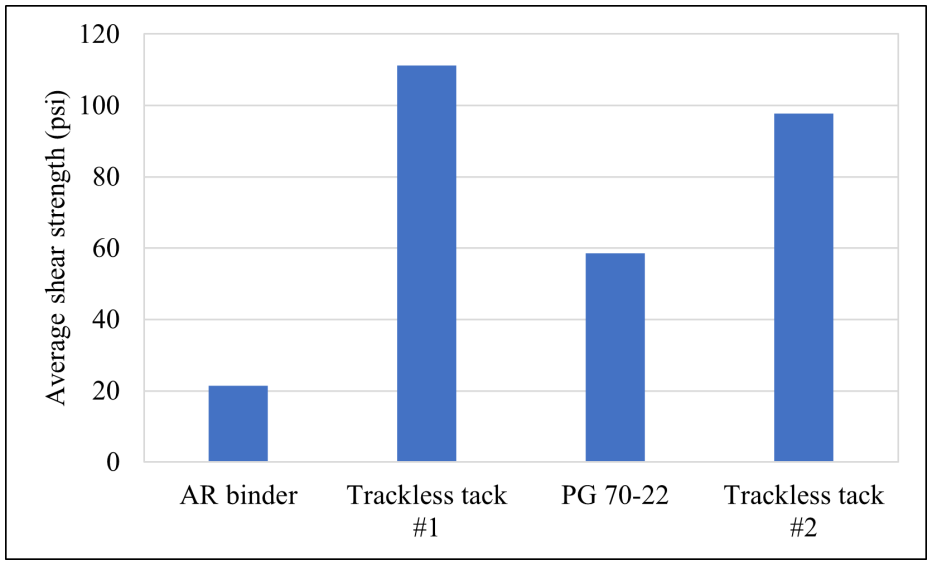

Figure 5.9. Shear strength for different tack coat types

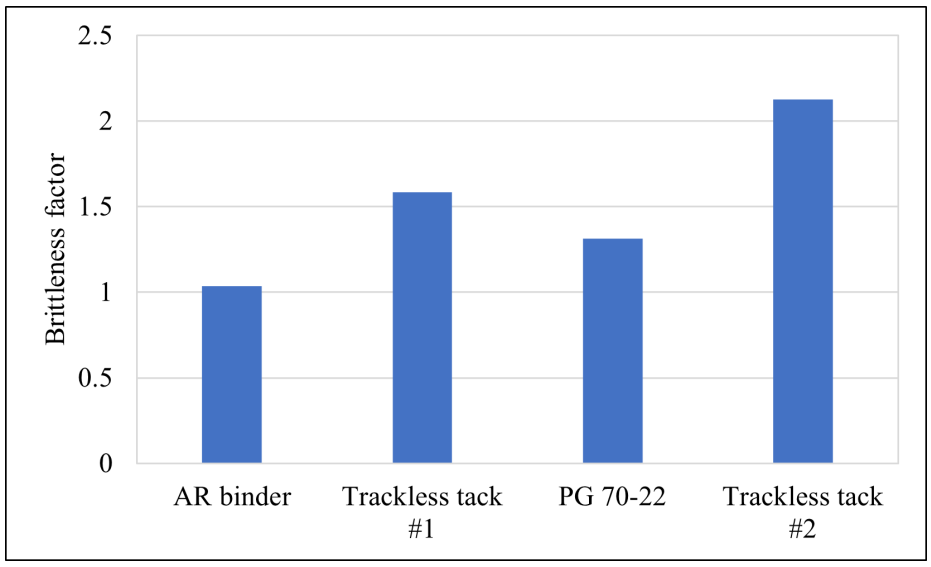

Figure 5.10. Brittleness factor in shear for different tack coat types

5.7.3 Application rate

Two different tack coats (1) Trackless tack #2 and (2) AR binder, were evaluated for four different application rates as described in Section 5.2. Dry, clean, and polished PCC surfaces were used to evaluate the application rate parameter. Figures 5.11, 5.12 and 5.13 show pull-off strength, shear strength, and brittleness factor for the

two tack coats, respectively. It can be seen from these figures that the influence of the application rate is not significant for both types of tack coats in terms of pull-off strength and shear strength. However, in the case of the Trackless tack #2, ductility improved with an increase in application rate. In the case of AR binder, the brittleness factor is close to 1 for all four application rates showing a good ductility for these four application rates.

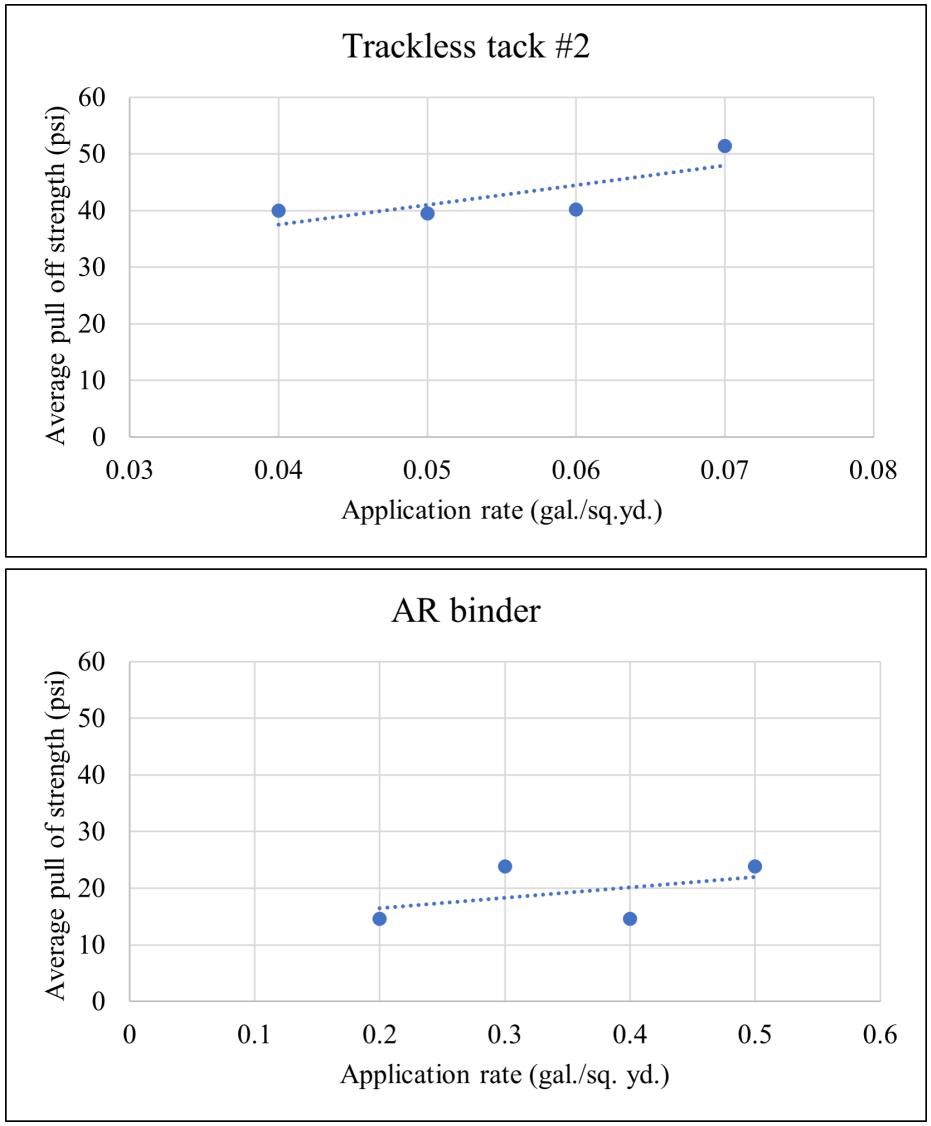

Figure 5.11. Pull-off strength at different application rates for (top) Trackless tack #2, (bottom) AR binder

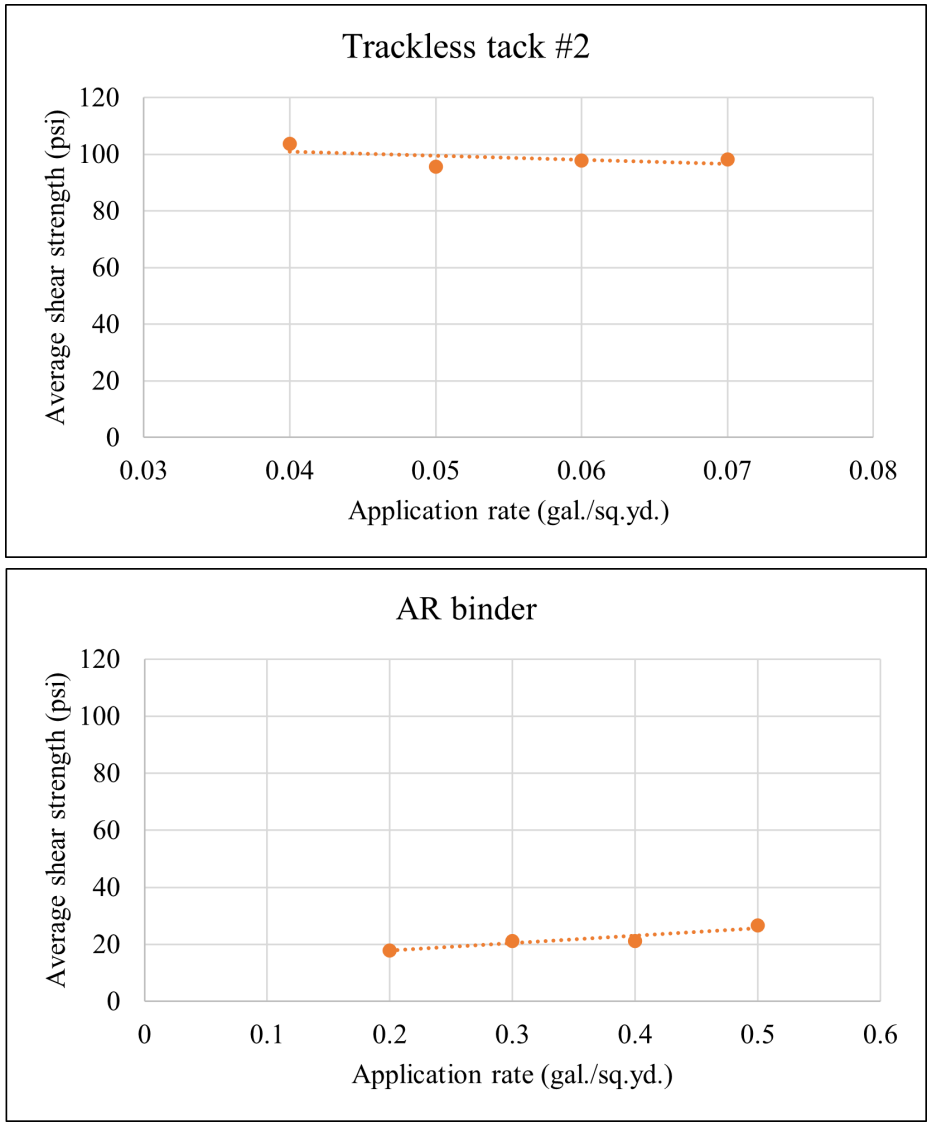

Figure 5.12. Shear strength at different application rates for (top) Trackless tack #2, (bottom) AR binder

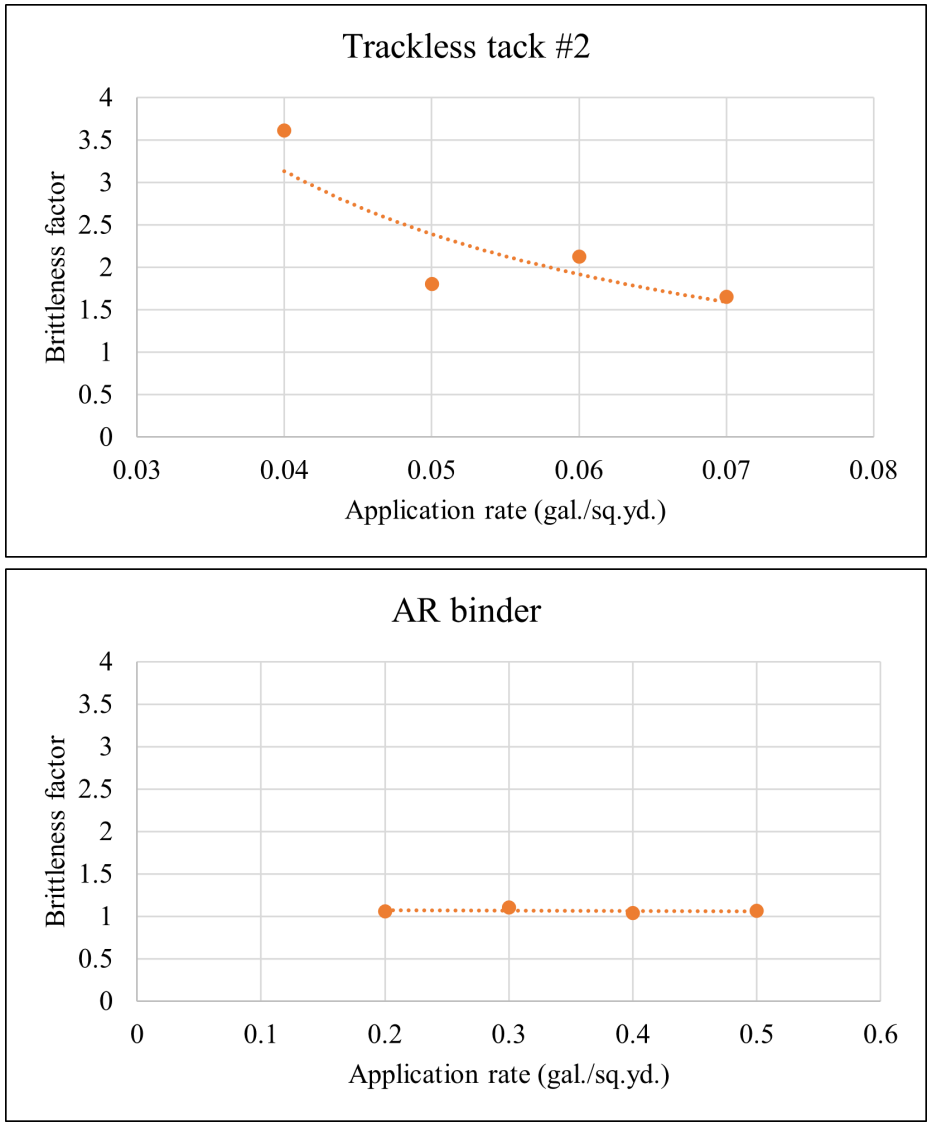

Figure 5.13. Brittleness factor at different application rates for (top) Trackless tack #2, (bottom) AR binder

5.7.4 PCC surface texture

The influence of PCC surface texture on PCC-HMA bond was evaluated for two different tack coats and two different application rates for each tack coat. Clean and dry PCC surface conditions were used. Figures 5.14, 5.15 and 5.16 show pull-off strength, shear strength and brittleness factor, respectively. Following observations can be made from these figures: (1) both pull-off strength and shear strength is higher for Trackless tack #2 for all four textures as compared to the AR binder, (2) higher shear strength and pull-off strength can be observed for sandblasted and hydro-demolition surfaces, and (3) hydro-demolition and tined-polished surfaces were more ductile in shear as compared to other surfaces. In most cases, sandblasting and hydro-demolition appear to be better performing PCC surface texture both in terms of strength and ductility.

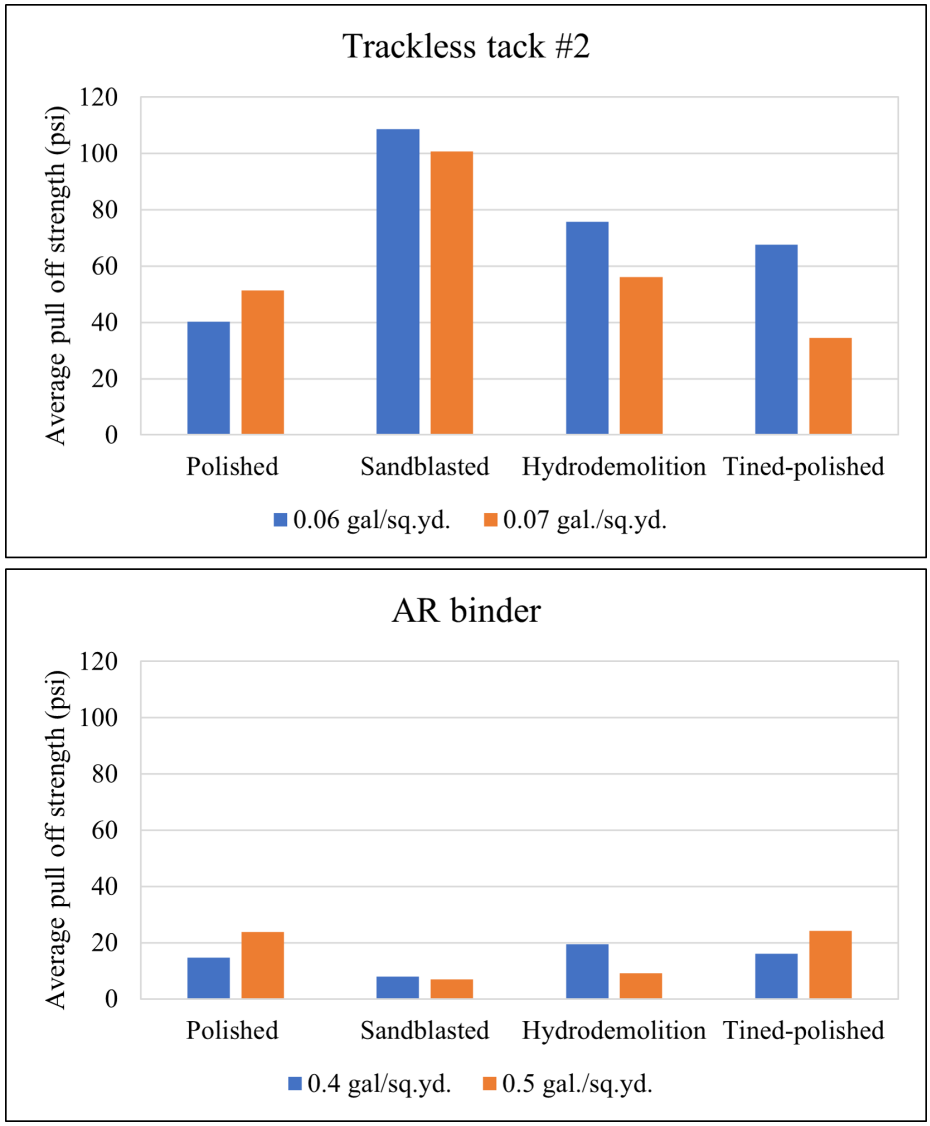

Figure 5.14. Pull-off strength for different PCC surface textures for two different types of tack coats: (top) Trackless tack #2, (bottom) AR binder

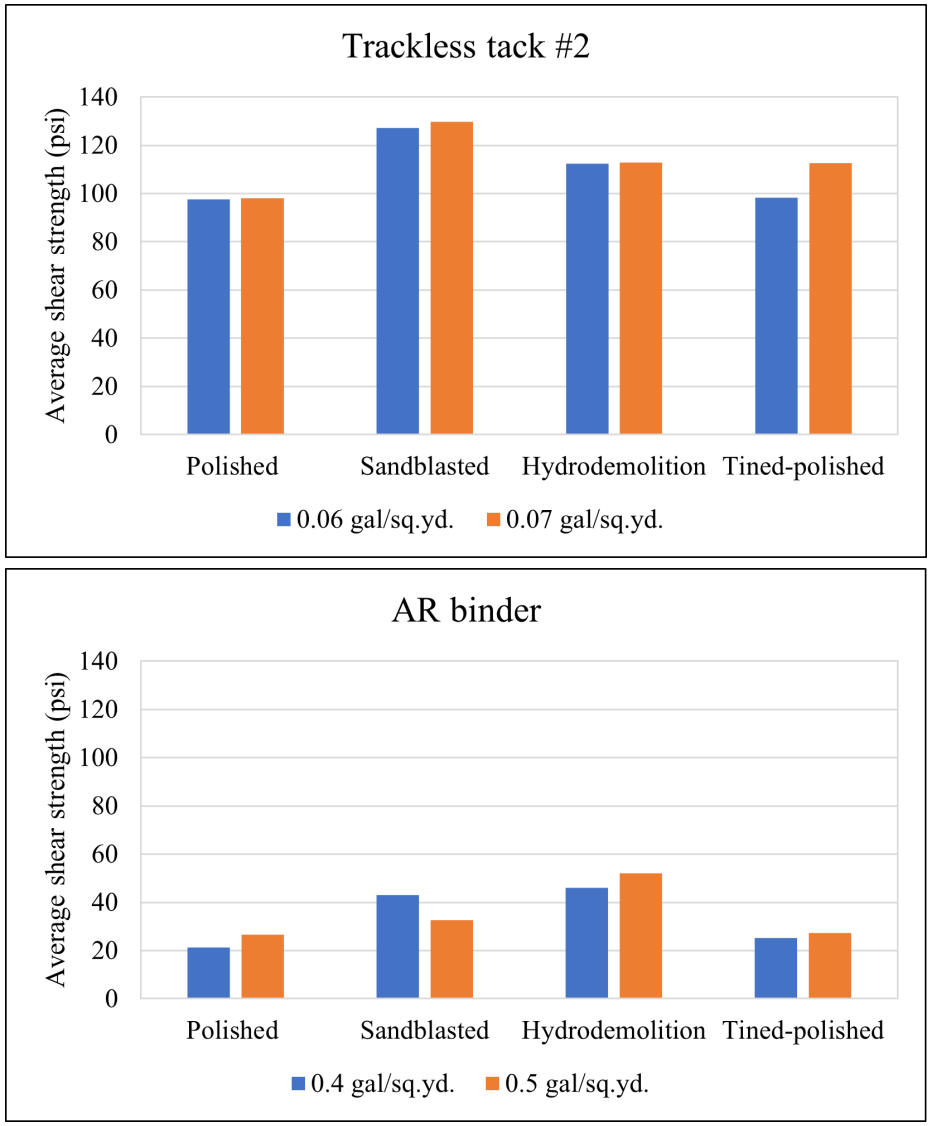

Figure 5.15. Shear strength for different PCC surface textures for two different type of tack coats: (top) Trackless tack #2, (bottom) AR binder

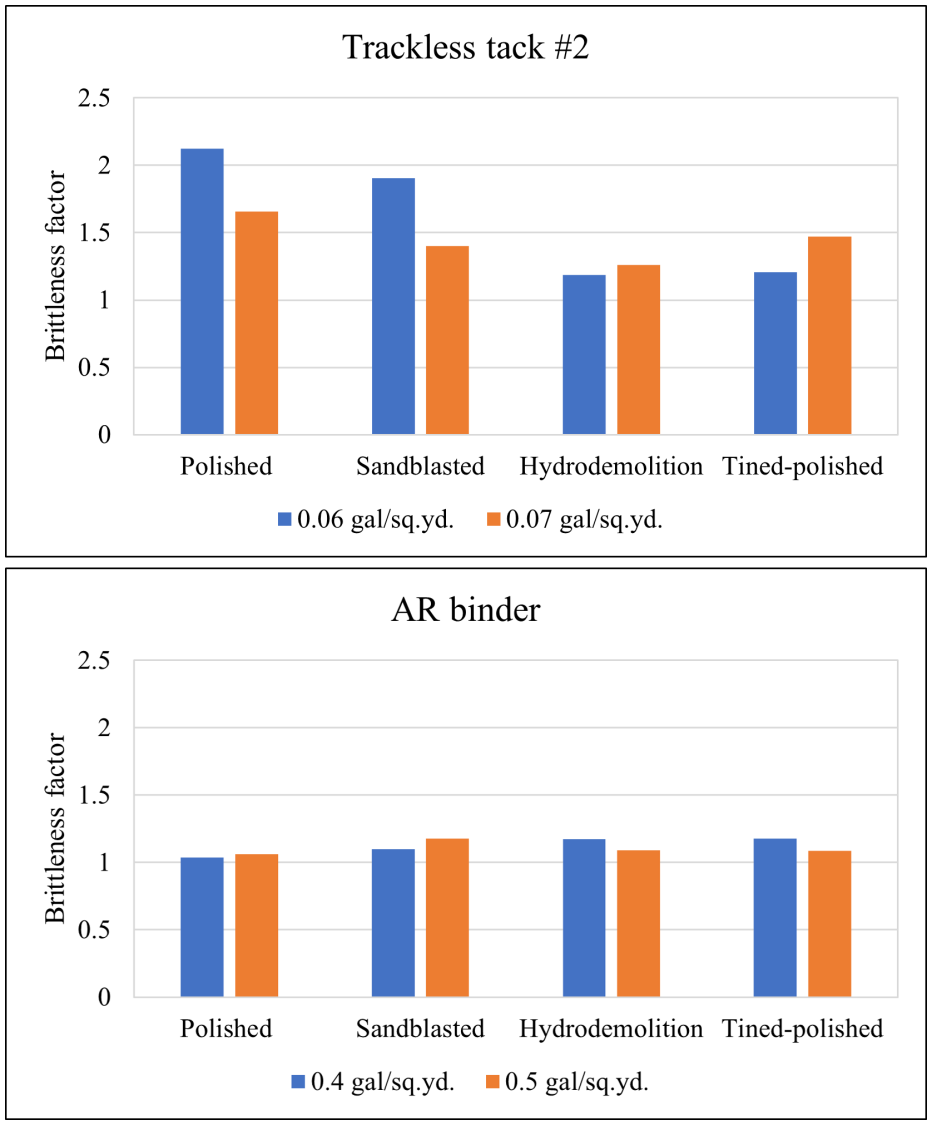

Figure 5.16. Brittleness factor for different PCC surface textures for two different types of tack coats: (top) Trackless tack #2, (bottom) AR binder

5.7.5 Surface cleanliness

Dry PCC surfaces with 4 different textures were used to evaluate the effect of surface cleanliness (1) hydro-demolition, (2) polished, (3) polished for limestone coarse aggregate concrete mix, and (4) sandblasted. Two different tack coats were also considered at an application rate of 0.06 gal./sq. yd. for Trackless tack #2 and 0.4 gal./sq. yd. for AR binder. Two surface cleanliness conditions were considered as described in Section 5.4. Figures 5.17, 5.18 and 5.19 show pull-off strength, shear strength and brittleness factor, respectively. It can be observed from these figures that there is no significant pattern on the basis of the cleanliness of the PCC surface that suggests its influence on the PCC-HMA bond. It is speculated that a slight increase in strength due to the presence of dust in some cases could be due to the increased friction resulting from the dust at the interface. In the field, cleanliness should be as good as can be obtained, possibly by air blowing the surface before tack coat application.

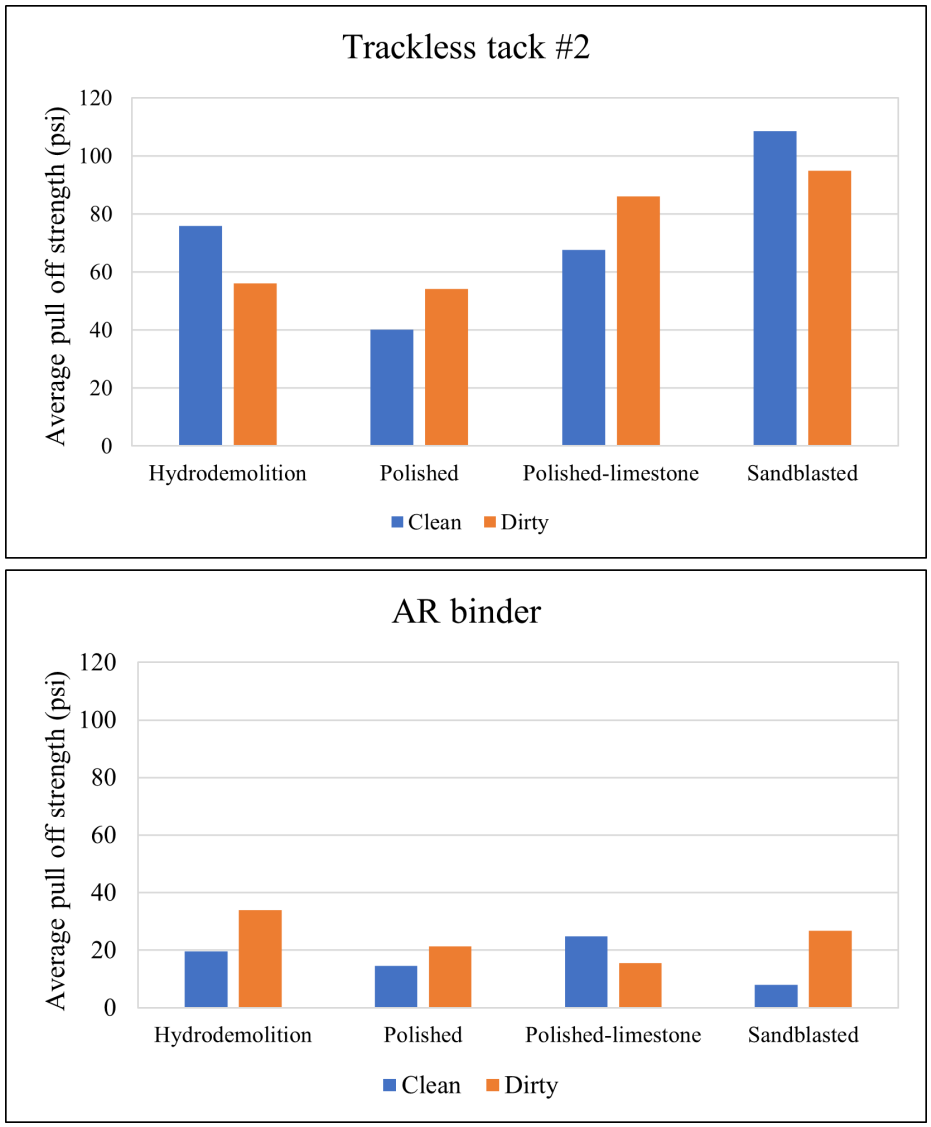

Figure 5.17. Pull-off strength based on surface cleanliness for different PCC surface textures for two different types of tack coats: (top) Trackless tack #2, (bottom) AR binder

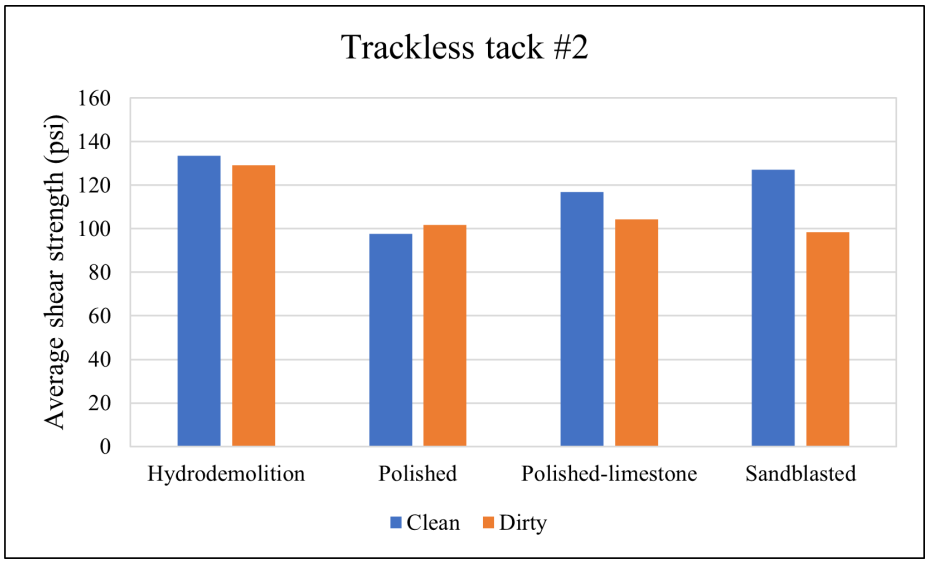

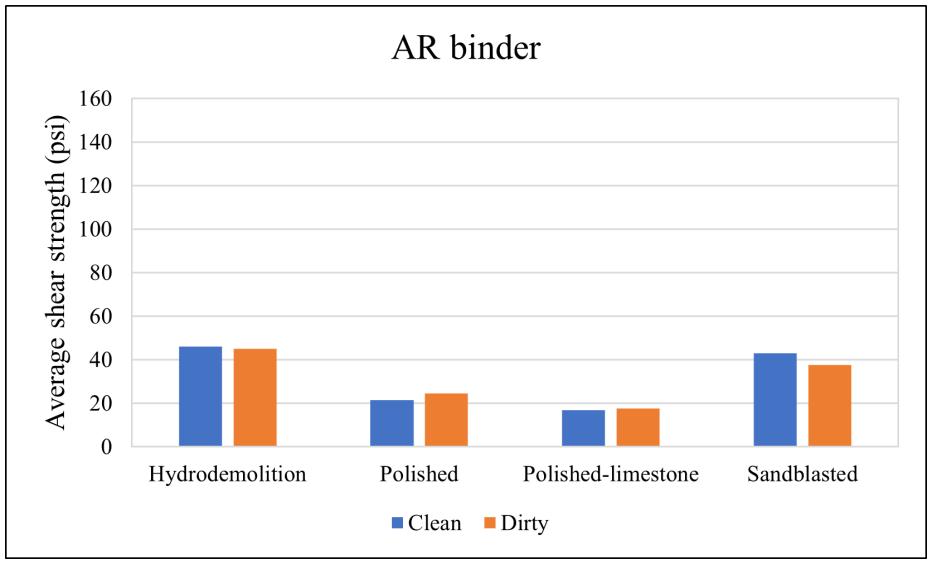

Figure 5.18. Shear strength based on surface cleanliness for different PCC surface textures for two different types of tack coats: (top) Trackless tack #2, (bottom) AR binder

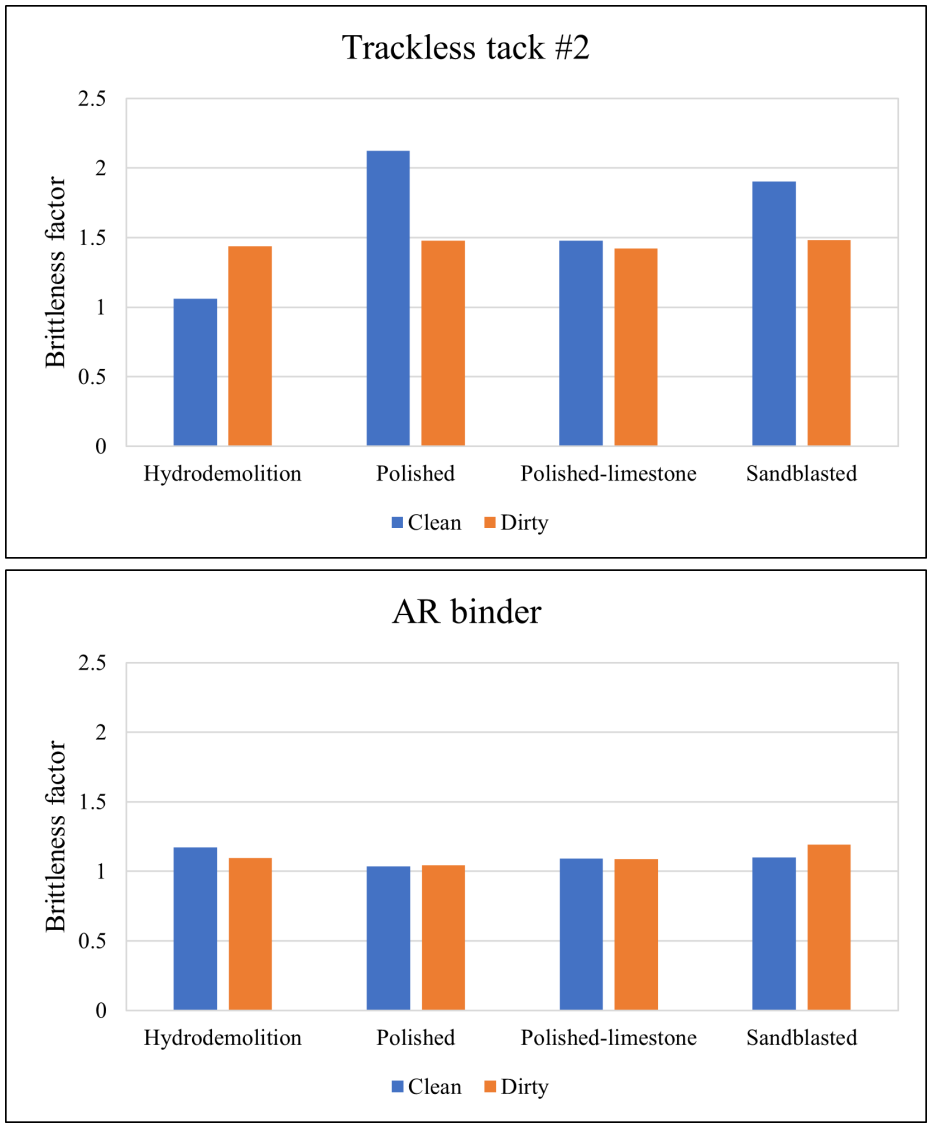

Figure 5.19. Brittleness factor based on surface cleanliness for different PCC surface textures for two different types of tack coats: (top) Trackless tack #2, (bottom) AR binder

5.7.6 Surface moisture

Three surface moisture conditions were evaluated as described in Section 5.5. Clean PCC surfaces with four different textures were used to evaluate the effect of surface moisture (1) hydro-demolition, (2) polished, (3) polished for limestone coarse aggregate concrete mix, and (4) sandblasted. Two different tack coats were considered with an application rate of 0.06 gal/sq. yd. for Trackless tack #2 and 0.4 gal./sq. yd. for AR binder. Figures 5.20, 5.21 and 5.22 show pull-off strength, shear strength and brittleness factor, respectively. It can be seen from these figures that near surface moisture may not be a significant variable affecting the PCC-HMA bond as no systematic pattern can be observed.

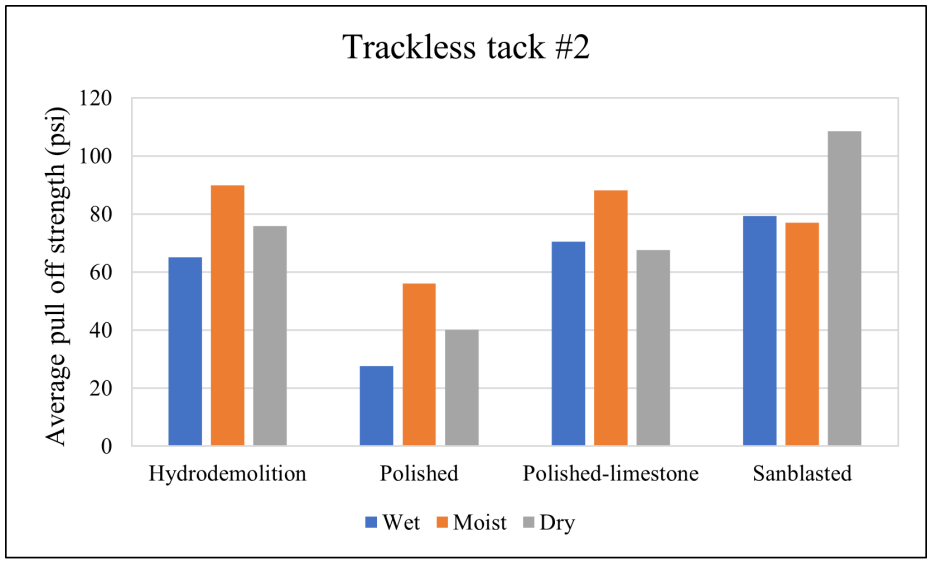

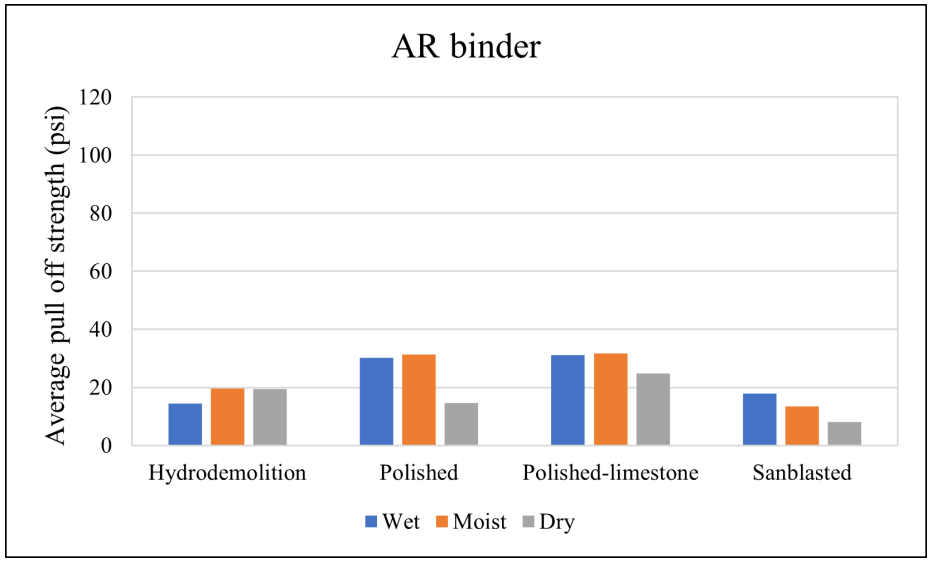

Figure 5.20. Pull-off strength based on surface moisture for different PCC surface textures for two different types of tack coats: (top) Trackless tack #2, (bottom) AR binder

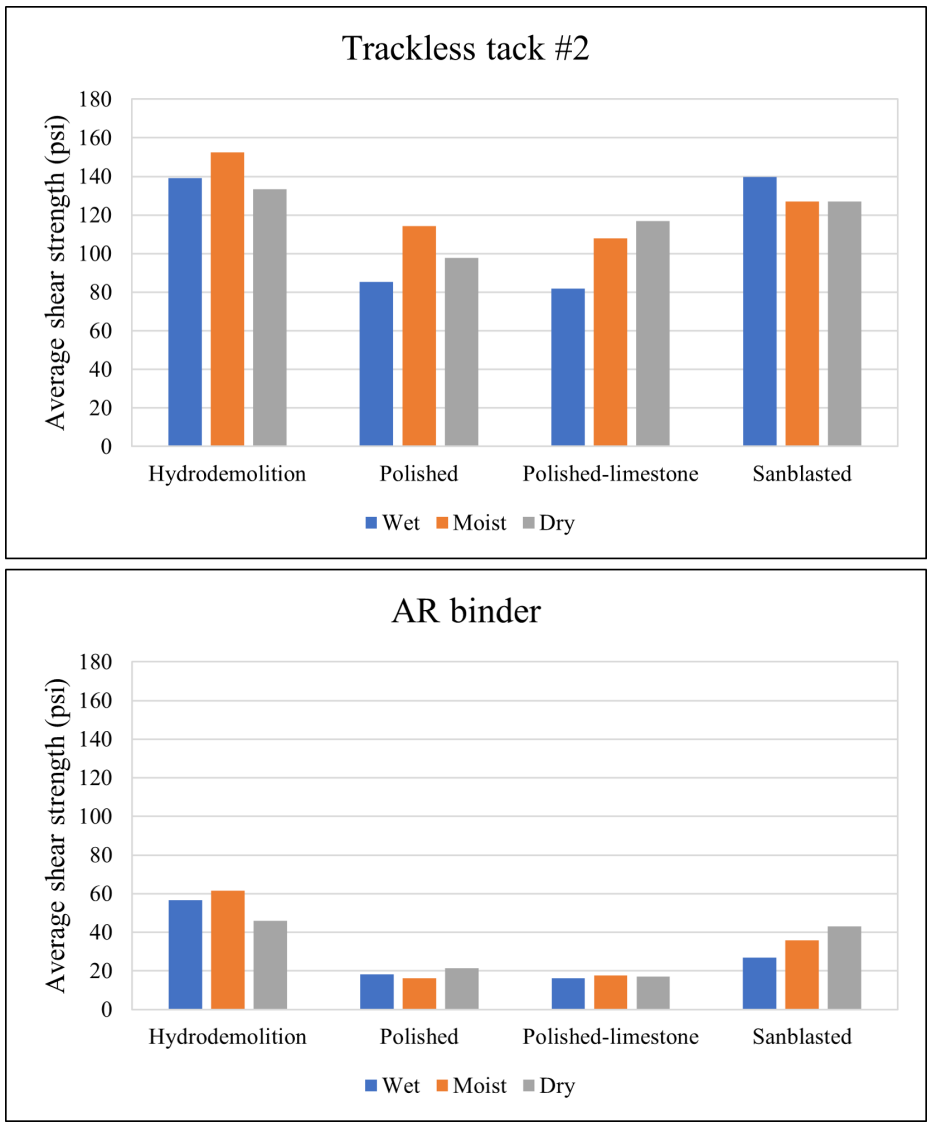

Figure 5.21. Shear strength based on surface moisture for different PCC surface textures for two different types of tack coats: (top) Trackless tack #2, (bottom) AR binder

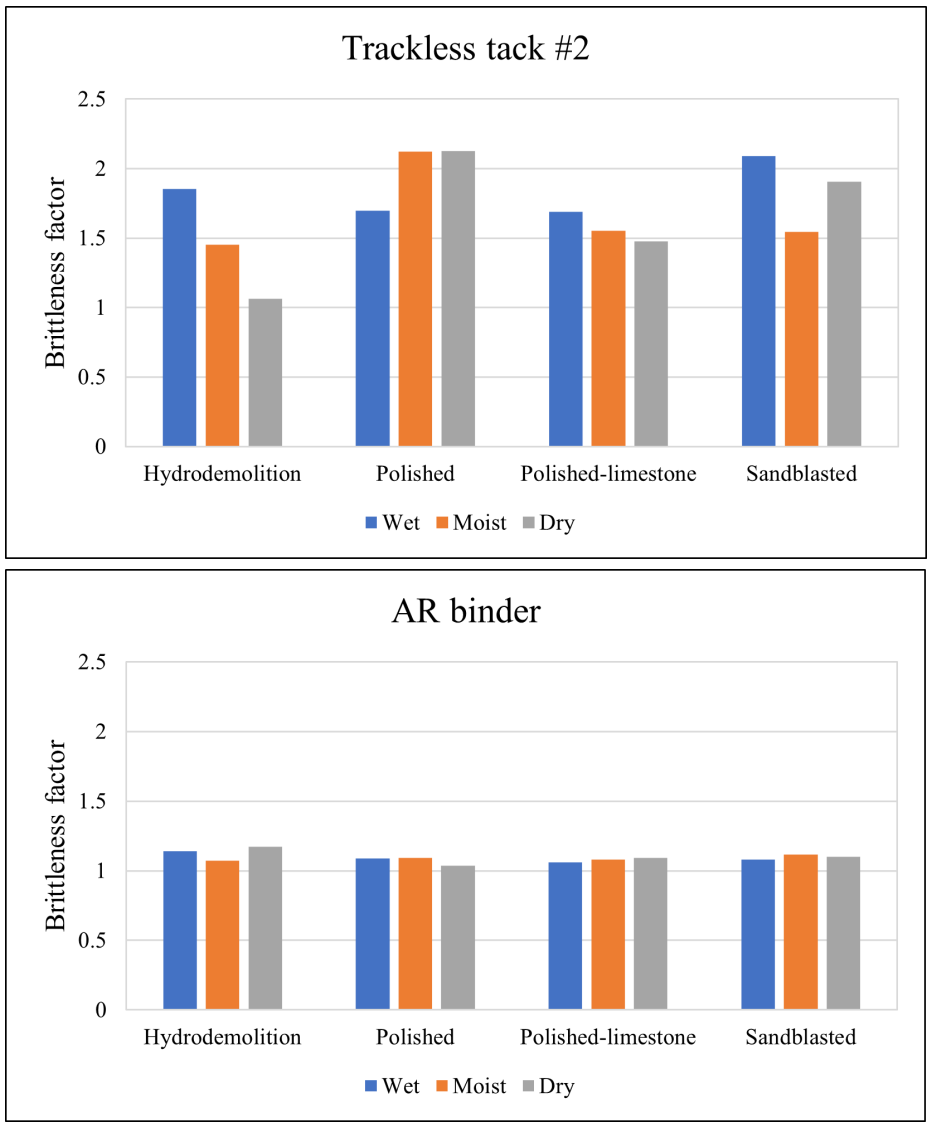

Figure 5.22. Brittleness factor based on surface moisture for different PCC surface textures for two different types of tack coats: (top) Trackless tack #2, (bottom) AR binder

5.7.7 Pull-off strength vs direct shear strength

One of the goals of this task was to compare the pull-off test results with the direct shear test results. Although the pull-off test is not intended for use in the laboratory, the intent of including this test on laboratory samples was to allow for a direct comparison between the direct shear test results and the pull-off test results so that the latter could be used in the field.

Figure 5.23 shows a plot of pull-off strength obtained from the pull-off test against the shear strength obtained from the direct shear test for all the combinations analysed in this study. A good correlation can be observed between the two test methods and results from these test methods. This is expected as typically a tack coat with a higher pull-off strength is likely to also have a higher shear strength. Therefore, this correlation qualitatively validates the data reported in this study and shows the potential of using the pull-off tester in the field to test the PCC-HMA bond.

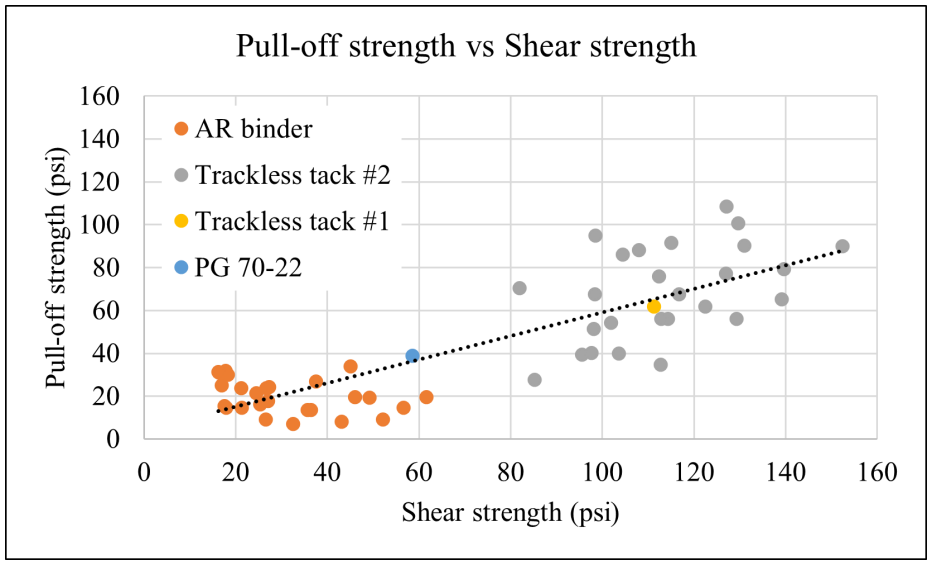

Figure 5.23. Pull-off strength versus direct shear strength for all the combinations of different parameters in this study

5.8 CONCLUSIONS

The following are some of the findings from the direct shear and pull-off testing of the laboratory prepared samples:

1. Trackless tack #1 and Trackless tack #2 have higher pull-off strength and shear strength as compared to AR binder. However, AR binder is more ductile as compared to other tack coats.
2. The influence of application rate on strength is not significant. However, ductility improved for Trackless tack #2 with an increase in application rate.
3. Sandblasting and hydro-demolition are best performing surface texture both in terms of strength and ductility.
4. The influence of PCC surface cleanliness and PCC surface moisture on PCC-HMA bond is not significant . However, good construction practices should be to ensure surfaces of PCC are as clean and dry as possible.
5. A good correlation is observed between shear strength and pull-off strength obtained from direct shear test and pull-off test, respectively. This means that a field pull-off test could be used to ensure adequate bond of the HMA to the PCC.

CHAPTER 6. EVALUATION OF FIELD SECTIONS

The main goal of this part of the study was to identify and evaluate the performance of field sections that have shown issues in the past or sections that have shown no signs of any deformation/delamination after several years of application. Researchers reached out to maintenance engineers at different districts with the intent of identifying tack coat projects and materials combinations that may have resulted in rapid HMA failure or have continued to perform very well over several years. The maintenance engineers were also asked for recommendations on best practices that they carry out to avoid such failures.

6.1 IDENTIFIED SECTIONS

Table 6.1 presents a summary of the identified field sections for this project. Researchers were able to perform the in-situ pull-off test (details on this test is discussed in Chapter 3) on all sections except two. One of the sections (SAT US90) showed significant stripping of the bottom HMA layer resulting in cores that had a severely disintegrated asphalt layer. In the other section (BMT), the HMA debonded from the concrete at all the core locations. Researchers were also able to obtain 6-inch cores from the remaining field sections in order to perform direct shear strength test. Detailed test protocols for these two testing methods can be found in Chapter 3 of this report.

Table 6.1. Identified field sections

Section	Tack Coat Type	Application Rate (gal/sq. yd.)	Asphalt Mix Type	Pull-off test	Direct shear test
AUS-SH130	AR type II (likely as an underseal)	0.55	1.5" PFC	**** ****	****
HOU-IH69	AR Type III (likely as an underseal)	0.55	1" TOM	******* ****	****
HOU-225 repaired area	Non-tracking tack coat emulsion	-	1.5" TY-D	**** ****	*
WAC NB Treated	Hot Applied Trackless Tack	0.18 (residual)	2" Item 341 TY-C PG 76-22	******	-
WAC SB Existing	Trackless Tack Emulsion	0.18 (residual)	2" Item 341 TY-C PG 76-22	****	-
WAC SB No Tr. Spot 1	Trackless Tack Emulsion	0.18 (residual)	2" Item 341 TY-C PG 76-22	****	-
WAC SB No Tr. Spot 2	Trackless Tack Emulsion	0.18 (residual)	2" Item 341 TY-C PG 76-22	****	-
SAT I-410	N/A	N/A	∼2.0"	****	*
SAT I-35	N/A	N/A	∼3.0" multiple layers	**** ****	****
SAT US90	N/A	N/A	∼8.0" multiple layers	deteriorated HMA layer	deteriorated HMA layer
BMT US87	Hot applied trackless tack	N/A	Mill PFC and add 2" Superpave Type-C	HMA layer debonded from concrete	HMA layer debonded from concrete

Note: * indicates number of replicates, * in 2 rows represent two different locations on the same section

6.2 SPECIMEN CORING

Researchers aimed at obtaining a minimum of four 6-inch cores from each identified section in Austin, Houston, and San Antonio. However, the coring failed in one section in Houston (SH225) due to the deterioration of the bond between the HMA and the PCC layer during the operation (Figure 6.1). From this location, the crew obtained one 6-inch and one 4-inch specimen. Also, due to time and traffic constraints in one section in San Antonio (I-410), only one 6-inch specimen was cored. Cores from US90 location indicated deteriorated pavement in the lower 2-3 inch of the HMA. Therefore, no pull-off test or additional 6-inch coring was conducted at this location and the condition was reported to the district. From Figure 6.2 it appears that little or no bonding exists between the HMA layers.

In another section which was in the Beaumont district, debonding between HMA and concrete occurred during coring at all the core locations (Figure 6.3). The causes of debonding may include: 1) the higher pavement temperatures softening the HMA (coring for other field projects was performed in cooler weather) and 2) the concrete pavement had gravel coarse aggregate which was harder to core and produced more heat. Many of the cores also showed that in the milling process, not all the PFC was removed from the concrete. This meant that a tack coat was placed on the remaining HMA and then overlaid with new HMA. This test location did not provide any cores for testing (shear or pull-off) and thus did not provide any additional data.

Figure 6.1. Cores from HOU SH225 with failure at the interface during coring

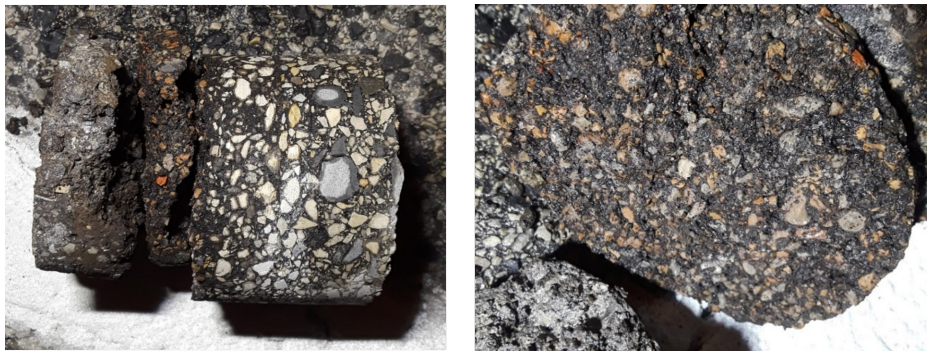

Figure 6.2. Cores from SAT US90 with significant stripping at the bottom of HMA layer

Figure 6.3. Cores from BMT US87 Beaumont district where the HMA debonded from PCC during coring

6.2.1 Procedure

Prior to drilling the 6-inch cores, the direction of the traffic was marked on the designated coring spot. The core barrel was then driven all the way to the bottom of the concrete layer. The full depth cores where then removed with a core extractor and packaged for transportation (Figure 6.4). A cold mix patch was used to fill the holes made from the coring operation. After transporting these cores to the laboratory,

the concrete side of the core was trimmed using a saw to achieve a 3-inch thickness. This was necessary to ensure that the finished specimen fit in the direct shear jig for testing. All cores were allowed to air dry at 25°C for at least 2 days after coring and sawing before they were used for testing. For the 2-inch coring required to perform the in-situ pull-off test, a 9-inch x 9-inch squared area was marked on the pavement and four 2-inch cores were drilled in each area (Figure 6.5). Note that the cores for pull-off tests are not full depth cores and only go approximately 0.125 to 0.25 inch into the concrete layer from the asphalt concrete surface. The shallow depth and smaller diameter make it much easier to create these cores for in-situ testing.

Figure 6.4. Procedure for obtaining 6-inch cores for the laboratory shear test

Figure 6.5. Procedure for obtaining 2-inch pull-off samples for in-situ field test

6.3 HMA-PCC INTERFACIAL LAYER EVALUATION

6.3.1 Test 1: Direct Shear Test

Test 1: Direct Shear - Variation 2: Direct Shear with Normal Stress: Tex-249-F (2019) measured the shear strength between the PCC and HMA layers in the absence of any normal force (Figure 6.6 (a)). However, in the field, shear stresses alone are not developed at the HMA-PCC interface causing the shear failure. In fact, normal stresses are also present due to the confinement and hence it is the combination of shear and normal stresses that causes the shear failure. Figure 6.7 shows a commercially available testing jig that allows for application of a normal stress while conducting the shear strength test. A spring was used to apply the confinement pressure, and a dial indicator was used to read the displacement of the spring. The dial gauge was calibrated to the spring constant and the compression in the spring can be converted the applied normal stress.

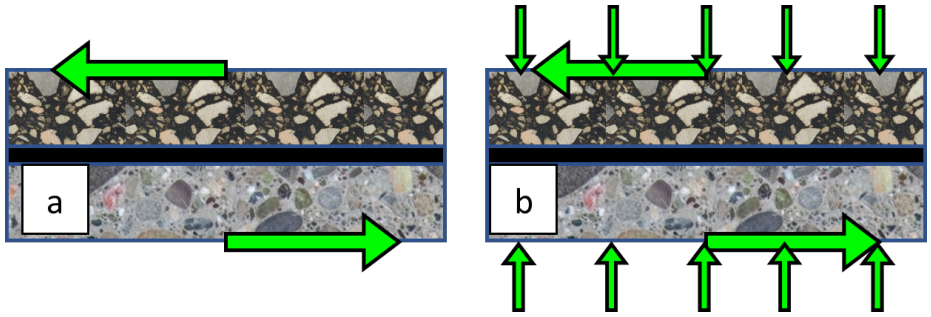

Figure 6.6. Schematic of shear loads applied on 6-inch specimens (a), and combination of shear and normal loads on 6-inch specimens (b)

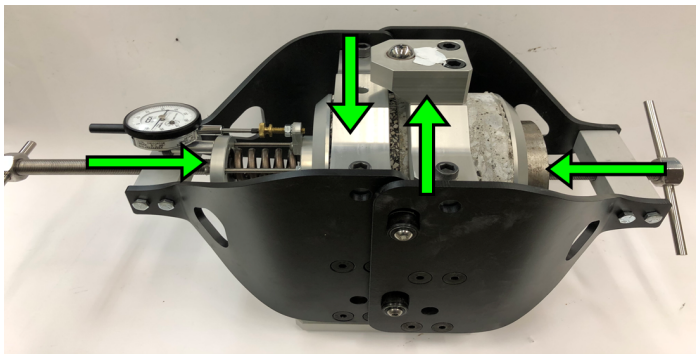

Figure 6.7. Tack coat shear strength tester (Gilson Inc.)

HMA-PCC samples were placed in the direct shear device such that the interface was in the middle of the gap between the two frames. A shear load at a constant rate of load or displacement can then be applied along with a constant confining pressure on the specimens. TxDOT recommends performing the shear test at a constant rate of displacement of 0.2 in./min. AASHTO TP-114 (2018) also specifies a constant rate of 0.1 in./min in the displacement-controlled mode. Several previous studies also conducted the shear test at a displacement-controlled mode. For instance, Song et al. (2018) performed the direct shear test in a displacement-controlled mode (50 mm/min) at 20°C with a normal confining pressure of 20 psi. Mohammad et al. (2002) evaluated the effect of tack coats on interface shear strength by applying a constant load at a rate of 50 lbs/min in the load-controlled mode. In a later study, Mohammad et al. (2010) conducted the direct shear test at a constant rate of 0.1 in./min and a normal confining pressure of 138 kPa (20 psi). Tashman et al. (2006) performed the test at a strain-controlled mode of 2 in./min. Bahia et al. (2019) conducted the test at a constant displacement rate of 0.1 in./min with a confining pressure of 7 psi.

In this study, direct shear test was performed with a constant rate of 0.2 inch/minute with a constant confining pressure of 10 psi. The test was terminated when the displacement reached the maximum allowable displacement of the testing frame. After testing, the load and displacement data was analyzed to obtain the peak shear strength and the area under the load-displacement curve. Additionally, the interface of the HMA-PCC layers was inspected for each specimen.

6.3.2 Test 2: Pull-Off Test

Test 2: Pull-off - Variation 2: Portable Motorized Pull-Off Via HMA layer: In this approach, the pull-off strength of a tack coat is measured by using a motorized portable direct pull-off test device.

Specimens were partially cored from the HMA-PCC pavement to a depth that reached approximately 1/8 inch into the PCC layer to expose the PCC-HMA bonding interface but without fully extracting or separating the core from the PCC base. The top surface of the HMA was glued to a metal plate using high strength epoxy and allowed to cure. A new temperature control system was developed to reduce variability in the pull-off test results. A portable motorized pull-off device was used to conduct a pull-off strength test to measure the tensile strength of the bond between PCC and HMA. The specimen was then visually inspected for the location of failure, whether it occurred at the interlayer, at the HMA layer, or at the glued interface between the metal plate and the HMA layer. Figure 6.8 shows the step-by-step procedure for the pull-off test.

Figure 6.8. In-situ pull-off test procedure (from top-left clockwise: cleaning of cores using an air jet; application of high strength epoxy to glue pull-off plate; use of a temperature control chamber to cure and condition the test specimen; pull-off test being conducted on one of the four replicates; image after completion of all four replicate pull-off tests)

6.4 RESULTS AND DISCUSSION

6.4.1 Direct Shear Test

The direct shear test was conducted on the field cores with a 10 psi confinement stress. After the shear test was terminated, load and displacement data were obtained from the Instron software for each of the 6-inch field cores and the peak interlayer strength was calculated. Figure 6.9 and Figure 6.10 show average shear strength and the average area under the load-displacement curve for all identified sections, respectively.

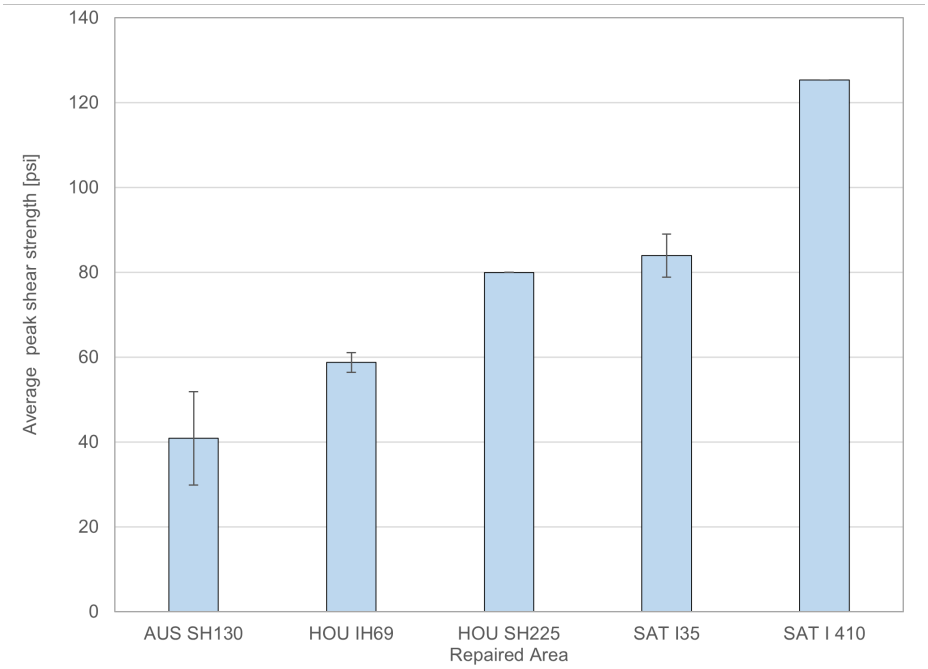

Figure 6.9. Comparison of maximum shear strength for the five identified field sections

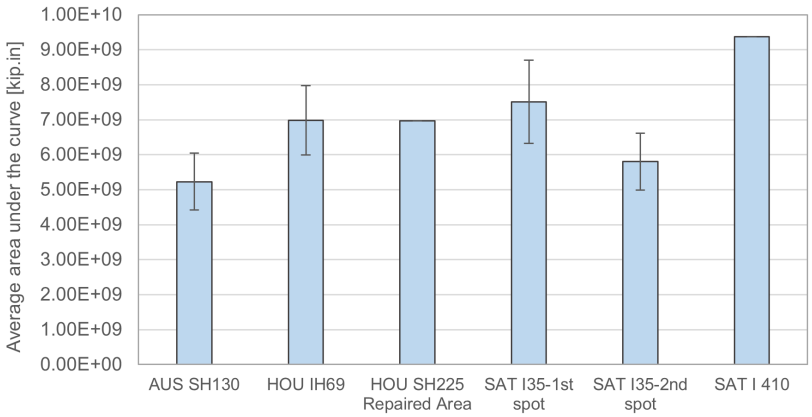

Figure 6.10. Comparison of the area under the load-displacements curves for the five identified field sections

6.4.1.1 AUS SH130

The SH130 field section (Figure 6.11) showed the lowest shear strength and highest variability compared to other sections due to two reasons: (1) This pavement was placed recently, and (2) a 1" TY D level up layer was placed between the PFC layer and the PCC layer, which compromised full bond at the HMA-PCC interface. While visually inspecting the interface after the test, a layer of dust was found on the failure surface of the SH130 cores (Figure 6.12). Also, transverse tining was found on the PCC surface. Although the SH130 cores showed the lowest shear strength, it should be pointed out that physically separating the two layers after the completion of test for the purposes of inspecting the interface required the most effort compared to other specimens.

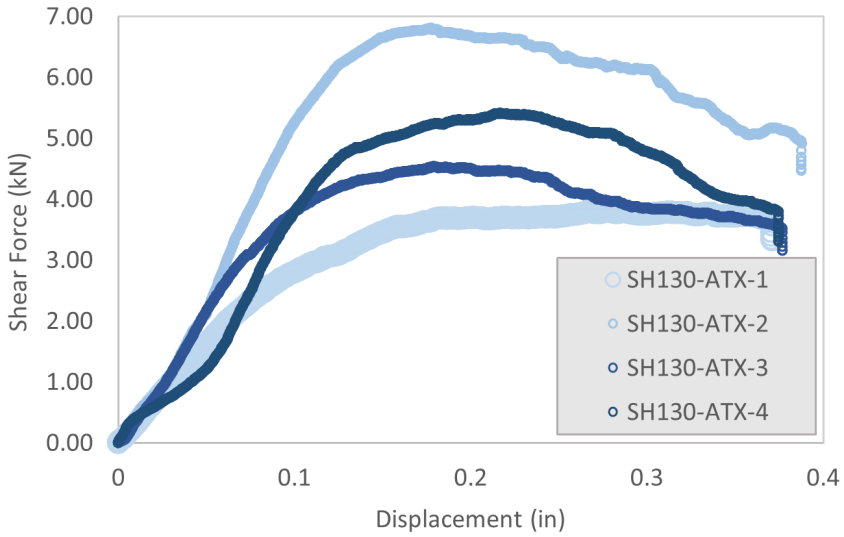

Figure 6.11. Load-displacement curves for AUS SH130 cores

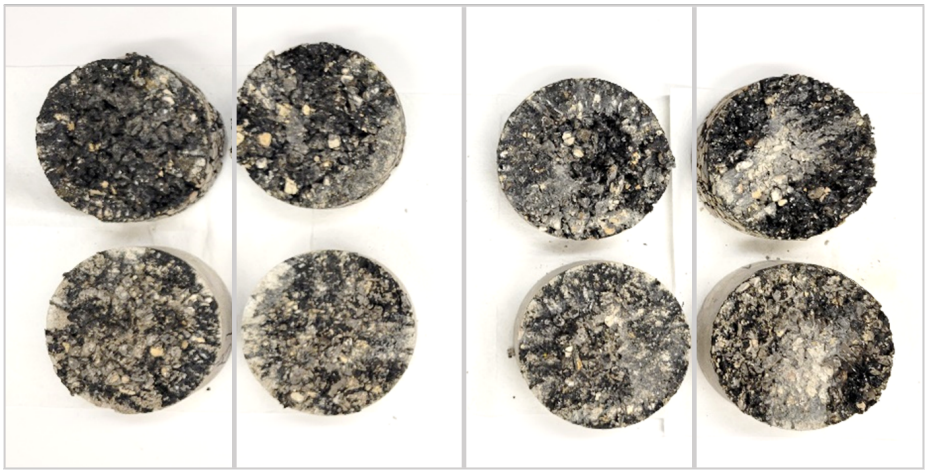

Figure 6.12. Top view from AUS SH130 cores after shear test

6.4.1.2 HOU IH69

The IH69 frontage road was placed between October 2014 and May 2015, and AR Type III was used as the tack coat between the 1" TOM HMA layer and the jointed reinforced concrete layer. After the two layers were separated, a tined texture was found on the PCC layer (Figure 6.14). This section had a variability of 4% (coefficient of variation) in the shear strength among the four collected samples. This was the

least variability in shear strength as compared to the other sections.

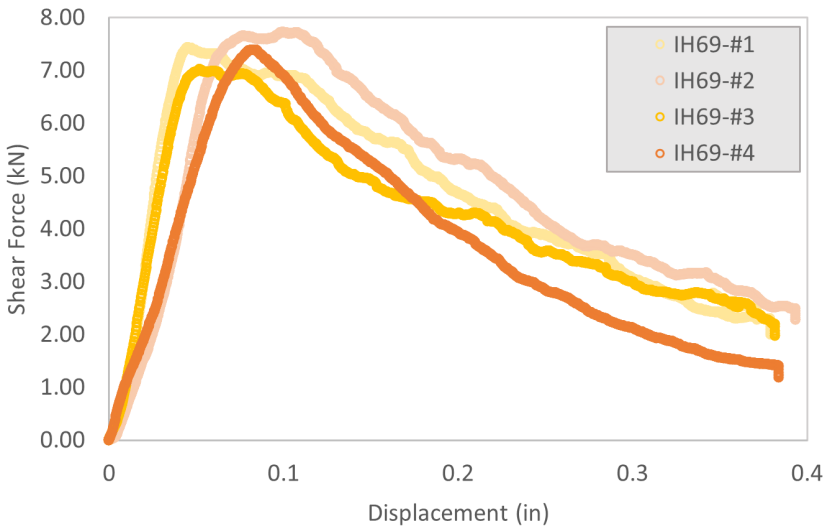

Figure 6.13. Load-displacement curves for Hou IH69 cores

Figure 6.14. Top view from Hou IH69 cores after shear test

6.4.1.3 HOU SH225

The HOU SH225 specimen was cored from a pavement section which was repaired after being flooded. The deteriorated pavement was milled and overlaid with non-tracking tack coat and 1.5" TY D HMA in 2017. When the two layers of this sample were separated, almost no tack coat residue was found on the PCC surface.

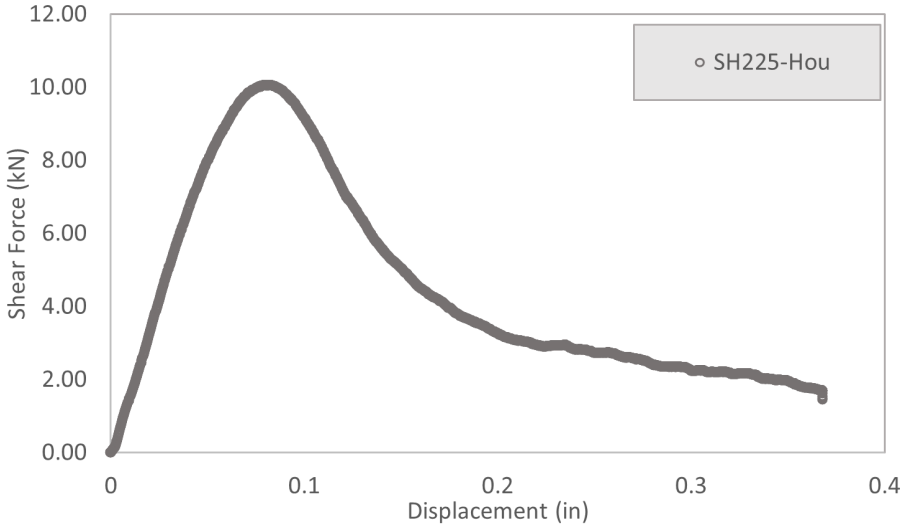

Figure 6.15. Load-displacement curves for Hou SH225 core

Figure 6.16. Top view from Hou SH225 core after shear test

6.4.1.4 SAT IH35

Two locations, 50 ft away from each other, were selected for 6-inch coring on the SAT IH35 field section. Two replicates from each section were tested and load-displacement results were plotted as shown in Figure 6.17. While inspecting the interfacial layer after the test, it was found that cores from the first location had some surface irregularities on PCC surface (Figure 6.19), contributing to the higher area under the load-displacement curves (Figure 6.10).

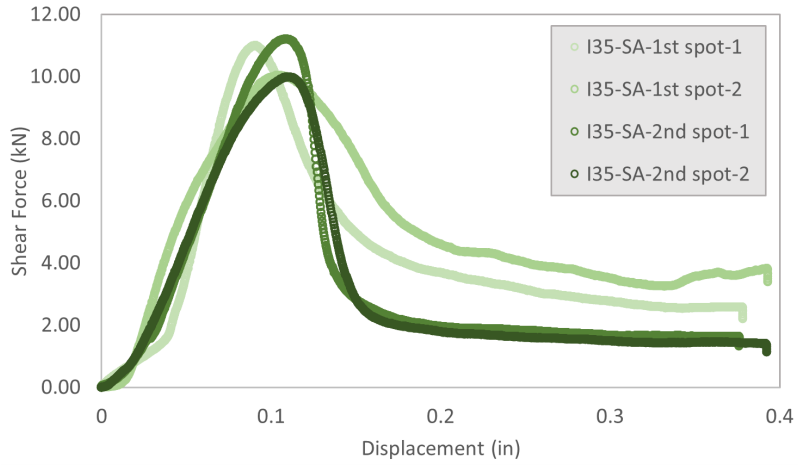

Figure 6.17. Load-displacement curves for SAT IH35 cores

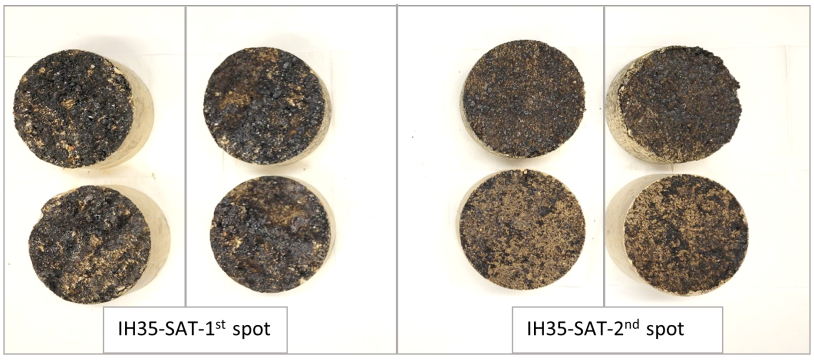

Figure 6.18. Top view from SAT IH35 cores after shear test

Figure 6.19. Side view from SAT IH35 cores after shear test

6.4.1.5 SAT I410

The I-410 San Antonio sample showed the highest shear strength among all the field sections of this project. When this sample was inspected, the concrete surface profile was found to be extremely irregular at the interlayer (Figure 6.21). It is likely that the additional friction caused by the uneven PCC layer, i.e. through mechanical interlocking, contributed to this highest shear strength. No information was provided on the type of tack coat used on this section.

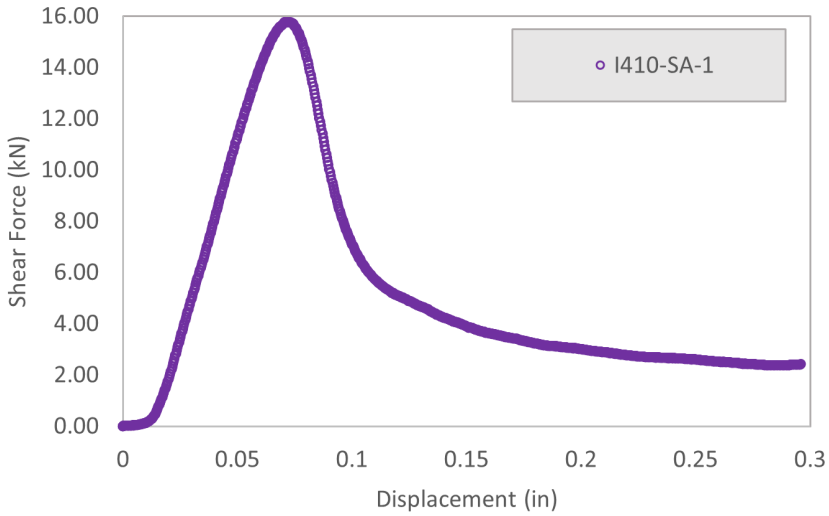

Figure 6.20. Load-displacement curves for SAT I410 core

Figure 6.21. Side and top view from SAT I410 core after shear test

6.4.2 Pull-off test

The in-situ pull-off test results are summarized in Figure 6.22. At least 4 replicates were tested at each location. Results from the Waco bridge deck widening project are also included in this figure. The Hou SH225 repaired area showed the highest pull-off strength among all the samples. This section was repaired with a non-tracking tack coat (emulsion) and a 1.5" TY-D HMA. Similar behavior was observed in the shear test results where HOU-225 performed better than the cores from SH130 and IH69 on which AR Type II and Type III were used, respectively.

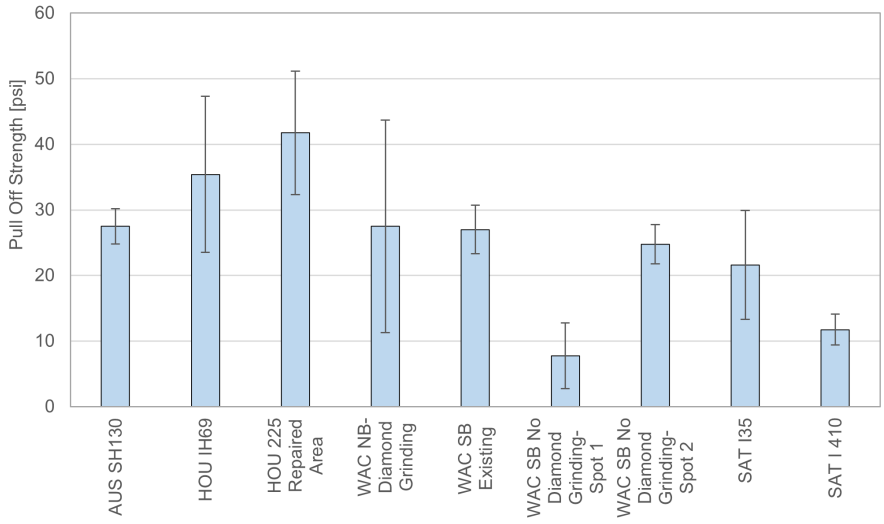

Figure 6.22. Comparison of pull-off strength for the five identified field sections and the Waco project

6.4.2.1 AUS SH130

Pictures from the pull-off test on the SH130 section are shown in Figure 6.23, where an adhesive failure mode was observed for all replicates. The HMA layer was fully separated from the PCC layer at the interface, and the tack coat residue was completely removed from the tines.

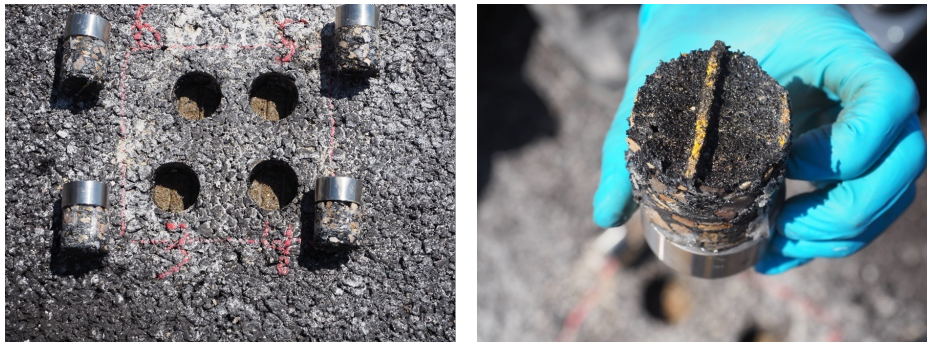

Figure 6.23. Pull-off test on SH130 using AR Type II as tack coat

6.4.2.2 HOU IH69

Pictures from the pull-off test on the IH69 section are shown in Figure 6.24, where a cohesive failure mode was observed. In this section, the HMA layer was not completely separated from the PCC layer, and it is likely that the friction forces contributed to the higher pull-off strength compared to the SH130 section. The AR application rate was similar for both sections.

Figure 6.24. Pull-off test on IH69 using AR Type III as tack coat

6.4.2.3 HOU SH225

Pictures from the pull-off test on the SH225 section are shown in Figure 6.25. This section showed the highest pull-off strength, and the failure mode was mostly adhesive. A non-tracking emulsion tack coat was applied to the PCC layer at this section.

Figure 6.25. Pull-off test on SH225 using trackless tack as tack coat

6.4.2.4 Waco

Pictures from the pull-off test on the Waco section are shown in Figures 6.26 through 6.29. Three test sections were identified at this location. The northbound section, which was finished with diamond grinding to remove the curing compound from a new bridge deck surface, the existing southbound, and the widened southbound with no diamond grinding.

The NB section showed the highest pull-off strength compared to other sections in Waco. The results from NB are comparable to the results from the existing SB, with a slight improvement likely as a result of surface preparation. Also, in this section a hot-applied trackless tack was used as opposed to the trackless tack emulsion in the SB.

Figure 6.26. Waco NB widening section- diamond ground- No Treatment-Hot applied trackless tack

Figure 6.27. Waco SB existing deck with treatment

The SB widening section which was not finished with diamond grinding showed the lowest pull-off strength. Figure 6.28 shows samples from this section which failed in adhesive mode after the test. Figure 6.29 shows samples from another section on the SB which showed partial adhesive failure and a higher pull-off strength compared to the first location.

Figure 6.28. Waco SB widening- no treatment- no diamond grinding- hot applied trackless tack- 1st spot

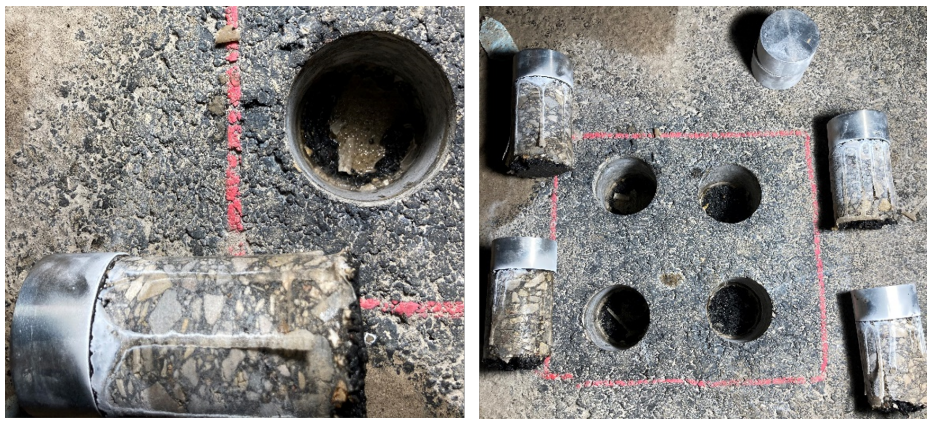

Figure 6.29. Waco SB widening- no treatment- no diamond grinding- hot applied trackless tack- 2nd spot

6.4.2.5 SAT IH35

Figure 6.30 shows the pull-off test samples from I35 section after failure. No information on the type of tack coat and application rate was available for this section. It appears that the samples failed in a cohesive mode.

Figure 6.30. Pull-off test on I35

6.4.2.6 SAT I410

Figure 6.31 shows the pull-off test samples from I410 section after failure. No information on the type of tack coat and application rate was available for this section. This section had the second lowest pull-off strength compared to all other sections, and all five samples failed in a cohesive mode.

Figure 6.31. Pull-off test on I410

6.5 CONCLUSIONS

The main objective of this part of the research was to evaluate the performance of existing pavements for their pull-off and shear strength at the PCC-HMA interface. Interlayer shear strength was measured using a direct shear test device. The interlock between HMA and PCC layers caused by the uneven PCC surface appeared to have a significant effect on the shear strength results. For the pull-off test, the research team developed a direct pull-off test protocol to perform on the identified field sections. With the contribution of the new temperature control system, the repeatability of test results was improved. Most of the identified sections exhibited a pull-off strength higher than 25 psi, which can be used as a frame of reference for acceptable performance.

CHAPTER 7. CONCLUSIONS AND RECOMMENDATIONS

7.1 CONCLUSIONS

The following are the conclusions from this study:

- A good correlation is observed between shear strength and pull-off strength obtained from direct shear test and pull-off test, respectively. This means that a field pull-off test could be used to ensure adequate bond of the HMA to the PCC. The field pull-off test is relatively much easier to carry out compared to obtaining full depth cores, transporting to a lab, trimming, conditioning, and conducting direct shear tests. Further, the pull-off tests can be conducted in locations where it is not feasible to obtain a full depth core such as bridge decks. The field pull-off tests can be conducted at locations that are suspected to have a poor bond strength for forensic purposes and can also be used as a quality assurance measure on newly constructed sections.
- Most of the field sections had a pull-off strength higher than 25 psi, which was found to be true also in the laboratory testing. However, more field sections need to be tested to use the 25 psi as a frame of reference for acceptable performance.
- Trackless tack #1 and Trackless tack #2 have higher pull-off strength and shear strength as compared to AR binder. However, AR binder is more ductile as compared to other tack coats.
- The influence of application rate on strength is not significant. However, ductility improved for Trackless tack #2 with an increase in application rate.
- Sandblasting and hydro-demolition are the best performing surface textures both in terms of strength and ductility. In practice, these methods are not well established among contractors for large scale surface preparation. A field study from WAC indicated that surface milling could be specified and carried out by contractors to achieve a similar effect.
- The influence of PCC surface cleanliness and PCC surface moisture on PCC-HMA bond is not significant. However, good construction practices should be used to ensure surfaces of PCC are as clean and dry as possible.
- Braking forces and overlay thickness were found to be the most influential pa-

rameters on the HMA-PCC interfacial stresses and strains from the numerical simulation.

7.2 RECOMMENDATIONS

7.2.1 Test and limits

This study recommends the modification of the existing direct shear test method to incorporate a newer type of loading jig that has the provision to apply a compressive load while conducting a shear strength test. This study also recommends the use of the field pull-off test for forensic purposes as needed as well as for QA purposes on newly placed overlays.

Data from both laboratory and field components using the shear and pull-off tests suggests the minimum shear strength between the HMA and concrete pavement should be 40 psi and corresponding pull-off strength of 25 psi. Field testing also indicates 20 psi as adequate, but the field tests were not performed on materials where failures had occurred, except in Waco. The results of lab and field studies both point to the use of the pull-off-test for evaluation of the tack coat bond for HMA overlays of concrete pavement in the field.

Both direct shear and pull-off strengths are typically higher when using trackless tack materials as compared to the use of a hot applied binder with aggregates (chip seal type) interface.

7.2.2 Implementation

It is recommended that for an overlay project over concrete pavement, that one of two courses of action be chosen. Refer to the Appendices for the detailed test procedures. The third point is a recommendation on surface preparation for all HMA overlays on concrete pavement.

1. Lab shear and pull-off analysis
   Conduct a lab study to determine the best combination of materials to ensure an adequate shear test and correlate this with the pull off test. This would involve:
   - Construct concrete cylinders with a texture treatment similar to that of the overlay project concrete OR obtain cores from the field that present the real polished surface.

- Apply the selected tack coat materials at the selected rate.
- Use the Superpave gyratory compactor to compact the project-type HMA on top of the sample (construct multiple samples).
- Measure the direct shear on a minimum of two samples using the modified test procedure developed in the project.
- Measure the pull-off strength on a minimum of two samples using the test procedure developed in this project.

The shear strength should be greater than 40 psi. The correlation of shear and pull-off can be used to set a minimum pull off strength in the field. Field pull-off testing can be accomplished to verify tack coat efficacy.

2. Field pull-off test only

   Verify a minimum of 20 psi pull-off strength (a higher limit is recommended for trackless materials) in the field using the test procedure developed in this project.

   The first alternative allows an optimization of the tack coat, while the second should ensure that a minimum tack coat bond is achieved.

3. Surface preparation prior to construction

   The receiving concrete surface must be cleaned and free of debris before placing the tack coat and hot mix asphalt. If the concrete surface is new (as in the case when HMA on new concrete is required to match existing profile during expansion), it is vital to ensure that any curing compounds from the concrete surface are removed.

   The following steps are highly recommended for surface preparation:

   - Diamond grind the deck by approximately 1/16" to remove any contaminants.
   - Pressure wash surface with water and allow the surface to dry or clean with compressed air.
   - Apply tack coat.

References

AASHTO TP-114 (2018). Standard method of test for determining the interlayer shear strength (iss) of asphalt pavement layers.

Abu Al-Rub, R. K., Darabi, M. K., Huang, C.-W., Masad, E. A., and Little, D. N. (2012). Comparing finite element and constitutive modelling techniques for predicting rutting of asphalt pavements. *International Journal of Pavement Engineering*, 13(4):322–338.

Al-Qadi, I. L., Carpenter, S. H., Leng, Z., Ozer, H., and Trepanier, J. (2008a). Tack coat optimization for hma overlays: Laboratory testing. Technical report, Illinois Center for Transportation.

Al-Qadi, I. L., Loulizi, A., Elseifi, M., and Lahouar, S. (2004). The virginia smart road: The impact of pavement instrumentation on understanding pavement performance. *Journal of the Association of Asphalt Paving Technologists*, 73(3):427–465.

Al-Qadi, I. L., Wang, H., Yoo, P. J., and Dessouky, S. H. (2008b). Dynamic analysis and in situ validation of perpetual pavement response to vehicular loading. *Transportation research record*, 2087(1):29–39.

Alae, M., Haghshenas, H. F., and Zhao, Y. (2019). Evaluation of top-down crack propagation in asphalt pavement under dual tire loading. *Canadian Journal of Civil Engineering*, 46(8):704–711.

Ali, B., Sadek, M., and Shahrour, I. (2009). Finite-element model for urban pavement rutting: analysis of pavement rehabilitation methods. *Journal of transportation engineering*, 135(4):235–239.

Alimohammadi, H., Zheng, J., Buss, A., Schaefer, V. R., Williams, C., and Zheng, G. (2021). Finite element viscoelastic simulations of rutting behavior of hot mix and warm mix asphalt overlay on flexible pavements. *International Journal of Pavement Research and Technology*, 14(6):708–719.

Alshukri, A. A., Aziz, F. A., Salit, M. S., Aziz, N. A., and Al-Maamori, M. (2019). Effect of particle size and content of crumb rubber on the dynamic properties of passenger tyre tread using finite element method.

Ameri, M., Mansourian, A., Khavas, M. H., Aliha, M., and Ayatollahi, M. (2011). Cracked asphalt pavement under traffic loading–a 3d finite element analysis. *Engineering Fracture Mechanics*, 78(8):1817–1826.

Assogba, O. C., Tan, Y., Sun, Z., Lushinga, N., and Bin, Z. (2021). Effect of vehicle speed and overload on dynamic response of semi-rigid base asphalt pavement. *Road Materials and Pavement Design*, 22(3):572–602.

ASTM C192 (2015). Standard Practice for Making and Curing Concrete Test Specimens in the Laboratory.

ASTM D6372 (2015). Standard Practice for Design, Testing, and Construction of Microsurfacing.

Bahia, H. U., Sufian, A., Swiertz, D., Mohammad, L. N., Akentuna, M., Bitumix Solutions, L., et al. (2019). Investigation of tack coat materials tracking performance. Technical report, Wisconsin. Dept. of Transportation. Research and Library Unit.

Bai, T., Cheng, Z., Hu, X., Fuentes, L., and Walubita, L. F. (2021). Viscoelastic modelling of an asphalt pavement based on actual tire-pavement contact pressure. *Road Materials and Pavement Design*, 22(11):2458–2477.

Ban, H., Im, S., and Kim, Y.-R. (2013). Nonlinear viscoelastic approach to model damage-associated performance behavior of asphaltic mixture and pavement structure. *Canadian journal of civil engineering*, 40(4):313–323.

Bazi, G., Hajj, E. Y., Ulloa-Calderon, A., and Ullidtz, P. (2020). Finite element modelling of the rolling resistance due to pavement deformation. *International Journal of Pavement Engineering*, 21(3):365–375.

Bekheet, W., Hassan, Y., and El Halim, A. A. (2001). Modelling in situ shear strength testing of asphalt concrete pavements using the finite element method. *Canadian Journal of Civil Engineering*, 28(3):541–544.

Chatti, K., Ji, Y., and Harichandran, R. (2004). Dynamic time domain backcalculation of layer moduli, damping, and thicknesses in flexible pavements. *Transportation research record*, 1869(1):106–116.

Clark, T. M., Rorrer, T. M., McGhee, K. K., et al. (2012). Trackless tack coat materials: a laboratory evaluation performance acceptance. Technical report, Virginia Center for Transportation Innovation and Research.

Davids, W. G. (2001). 3d finite element study on load transfer at doweled joints in flat and curled rigid pavements. *International Journal of Geomechanics*, 1(3):309–323.

Decker, D. S. (2013). *Best Practices for Emulsion Tack Coats*. National Asphalt Pavement Association.

Deysarkar, I. (2004). *Test set-up to determine quality of tack coat*. The University of Texas at El Paso.

Dynatest (2020). Elmod software for pavement analysis.

Eghbalpoor, R., Baghani, M., and Shahsavari, H. (2019). An implicit finite element framework considering damage and healing effects with application to cyclic moving load on asphalt pavement. *Applied Mathematical Modelling*, 70:139–151.

Eslaminia, M. and Guddati, M. N. (2016). Fourier-finite element analysis of pavements under moving vehicular loading. *International Journal of Pavement Engineering*, 17(7):602–614.

Gajewski, J. and Sadowski, T. (2014). Sensitivity analysis of crack propagation in pavement bituminous layered structures using a hybrid system integrating artificial neural networks and finite element method. *Computational Materials Science*, 82:114–117.

Gierhart, D. and Johnson, D. R. (2018). *NCHRP report: Tack coat specifications, materials, and Construction Practices*. Number 20-05/Topic 48-02.

Hachiya, Y., Umeno, S., and Sato, K. (1997). Effect of tack coat on bonding characteristics at interface between asphalt concrete layers. *Doboku Gakkai Ronbunshu*, 1997(571):199–209.

Hadidi, R. and Gucunski, N. (2010). Comparative study of static and dynamic falling weight deflectometer back-calculations using probabilistic approach. *Journal of Transportation Engineering*, 136(3):196–204.

Hamim, A., Yusoff, N. I. M., Ceylan, H., Rosyidi, S. A. P., and El-Shafie, A. (2018). Comparative study on using static and dynamic finite element models to develop fwd measurement on flexible pavement structures. *Construction and Building Materials*, 176:583–592.

Hamim, A., Yusoff, N. I. M., Omar, H. A., Jamaludin, N. A. A., Hassan, N. A., El-Shafie, A., and Ceylan, H. (2020). Integrated finite element and artificial neural network methods for constructing asphalt concrete dynamic modulus master curve using deflection time-history data. *Construction and Building Materials*, 257:119549.

Hu, X. and Walubita, L. F. (2009). Modelling tensile strain response in asphalt pavements: bottom-up and/or top-down fatigue crack initiation. *Road materials and pavement design*, 10(1):125–154.

Hu, X. and Walubita, L. F. (2011). Effects of layer interfacial bonding conditions on the mechanistic responses in asphalt pavements. *Journal of Transportation Engineering*, 137(1):28–36.

Khan, Z. H. and Tarefder, R. A. (2019). A procedure to convert field sensor data for finite element model inputs and its validation. *Construction and Building Materials*, 212:442–455.

Kim, H. and Buttlar, W. G. (2009). Finite element cohesive fracture modeling of airport pavements at low temperatures. *Cold Regions Science and Technology*, 57(2-3):123–130.

Leng, Z., Ozer, H., Al-Qadi, I. L., and Carpenter, S. H. (2008). Interface bonding between hot-mix asphalt and various portland cement concrete surfaces: laboratory assessment. *Transportation Research Record*, 2057(1):46–53.

Leonardi, G. (2015). Finite element analysis for airfield asphalt pavements rutting prediction. *Bulletin of the Polish Academy of Sciences: Technical Sciences*, pages 397–403.

Li, M., Wang, H., Xu, G., and Xie, P. (2017). Finite element modeling and parametric analysis of viscoelastic and nonlinear pavement responses under dynamic fwd loading. *Construction and Building Materials*, 141:23–35.

Li, Z. and Vandenbossche, J. M. (2013). Redefining the failure mode for thin and ultrathin whitetopping with 1.8-× 1.8-m joint spacing. *Transportation research record*, 2368(1):133–144.

Ling, J., Wei, F., Zhao, H., Tian, Y., Han, B., and Chen, Z. (2019). Analysis of airfield composite pavement responses using full-scale accelerated pavement testing and finite element method. *Construction and Building Materials*, 212:596–606.

Mabrouk, G. M., Elbagalati, O. S., Dessouky, S., Fuentes, L., and Walubita, L. F. (2021). 3d-finite element pavement structural model for using with traffic speed deflectometers. *International Journal of Pavement Engineering*, pages 1–15.

Mahmoud, A., Coleri, E., Batti, J., and Covey, D. (2017). Development of a field torque test to evaluate in-situ tack coat performance. *Construction and Building Materials*, 135:377–385.

McDaniel, R. S., Shah, A., and Lee, J. (2018). Tack coat installation performance guidelines.

Mohammad, L., Saadeh, S., Qi, Y., Button, J. W., and Scherocman, J. (2008). Worldwide state of practice on the use of tack coats: a survey. *Journal of the Association of Asphalt Paving Technologists*, 77.

Mohammad, L. N. (2012). *Optimization of tack coat for HMA placement*, volume 712. Transportation Research Board.

Mohammad, L. N., Bae, A., Elseifi, M. A., Button, J., and Patel, N. (2010). Effects of pavement surface type and sample preparation method on tack coat interface shear strength. *Transportation research record*, 2180(1):93–101.

Mohammad, L. N., Bae, A., Elseifi, M. A., Button, J., and Scherocman, J. A. (2009). Evaluation of bond strength of tack coat materials in field: Development of pull-off test device and methodology. *Transportation research record*, 2126(1):1–11.

Mohammad, L. N., Raqib, M., and Huang, B. (2002). Influence of asphalt tack coat materials on interface shear strength. *Transportation Research Record*, 1789(1):56–65.

Monk, P. et al. (2003). *Finite element methods for Maxwell's equations*. Oxford University Press.

Mu, F. and Vandenbossche, J. (2011). Temperature effects on overlay bond characteristics and the overlay response to dynamic loads for bonded pcc overlays placed on asphalt pavements, 7th international dut-workshop on design and performance of sustainable and durable concrete pavements.

Musselman, J. A., Moraes, R., Walbeck, T., West, R., and Director, N. (2020). Methods for addressing tack tracking literature review ncat report 20-06.

Nielsen, C. P. (2019). Visco-elastic back-calculation of traffic speed deflectometer measurements. *Transportation research record*, 2673(12):439–448.

Ong, G. P. and Fwa, T. (2010). Mechanistic interpretation of braking distance specifications and pavement friction requirements. *Transportation research record*, 2155(1):145–157.

Ozer, H., Al-Qadi, I. L., Hasiba, K. I., Wang, H., and Salinas, A. (2013). Pavement layer interface shear strength using a hyperbolic mohr-coulomb model and finite element analysis. In *Airfield and Highway Pavement 2013: Sustainable and Efficient Pavements*, pages 1445–1456.

Ozer, H., Al-Qadi, I. L., and Leng, Z. (2008). Fracture-based friction model for pavement interface characterization. *Transportation Research Record*, 2057(1):54–63.

Ozer, H. and Rivera-Perez, J. (2017). Evaluation of various tack coat materials using interface shear device and recommendations on a simplified device. Technical report, Illinois Center for Transportation/Illinois Department of Transportation.

Park, S. and Schapery, R. (1999). Methods of interconversion between linear viscoelastic material functions. part i-a numerical method based on prony series. *International journal of solids and structures*, 36(11):1653–1675.

Patil, V., Sawant, V. A., and Deb, K. (2013). 2-d finite element analysis of rigid pavement considering dynamic vehicle–pavement interaction effects. *Applied Mathematical Modelling*, 37(3):1282–1294.

Peng, Y., Li, J. Q., Zhan, Y., Wang, K. C., and Yang, G. (2019). Finite element method-based skid resistance simulation using in-situ 3d pavement surface texture and friction data. *Materials*, 12(23):3821.

Raab, C. and Partl, M. N. (2004). Effect of tack coats on interlayer shear bond of pavements. In *Proceedings of the 8th conference on Asphalt Pavements for Southern Africa (CAPSA'04)*, volume 12, page 16. Citeseer.

Saad, B., Mitri, H., and Poorooshasb, H. (2006). 3d fe analysis of flexible pavement with geosynthetic reinforcement. *Journal of transportation Engineering*, 132(5):402–415.

Schapery, R. A. (1974). Viscoelastic behavior and analysis of composite materials. *Mechanics of composite materials*.

Scullion, T., Uzan, J., and Paredes, M. (1990). Modulus: A microcomputer-based backcalculation system. *Transportation Research Record*, 1260:180–191.

Song, W., Shu, X., Huang, B., and Woods, M. (2018). Effects of asphalt mixture type on asphalt pavement interlayer shear properties. *Journal of Transportation Engineering, Part B: Pavements*, 144(2):04018021.

Sufian, A. A. (2020). *Tracking and Bonding Performance of Commonly Used Tack Coat Materials*. The University of Wisconsin-Madison.

Sun, Y., Du, C., Zhou, C., Zhu, X., and Chen, J. (2019). Analysis of load-induced top-down cracking initiation in asphalt pavements using a two-dimensional microstructure-based multiscale finite element method. *Engineering Fracture Mechanics*, 216:106497.

Tang, X. and Yang, X. (2013). Inverse analysis of pavement structural properties based on dynamic finite element modeling and genetic algorithm. *International Journal of Transportation Science and Technology*, 2(1):15–30.

Tashman, L., Nam, K., and Papagiannakis, A. (2006). Evaluation of the influence of tack coat construction factors on the bond strength between pavement layers. Technical report, Washington State Department of Transportation Olympia.

Techbrief (2016). Tack coat best practices.

Tex-241-F (2019). Compacting bituminous specimens using the superpave gyratory compactor (sgc).

Tex-243-F (2009). Tack coat adhesion.

Tex-249-F (2019). Shear bond strength test.

Tran, N., Willis, R., and Julian, G. (2012). Refinement of the bond strength procedure and investigation of a specification. *National Center for Asphalt Technology, Auburn, AL*.

Vandenbossche, J. M., Dufalla, N., and Li, Z. (2017). Bonded concrete overlay of asphalt mechanical-empirical design procedure. *International Journal of Pavement Engineering*, 18(11):1004–1015.

Walsh, I. and Williams, J. (2001). Hapas certificates for procurement of thin surfacing. *Highways & Transportation*.

Walubita, L. F., Faruk, A. N., Lee, S. I., Nguyen, D., Hassan, R., Scullion, T., et al. (2014). Hma shear resistance, permanent deformation, and rutting tests for texas mixes: final year-2 report. Technical report, Texas A&M Transportation Institute.

Wang, H. and Li, M. (2016). Comparative study of asphalt pavement responses under fwd and moving vehicular loading. *Journal of Transportation Engineering*, 142(12):04016069.

Wang, J., Xiao, F., Chen, Z., Li, X., and Amirkhanian, S. (2017). Application of tack coat in pavement engineering. *Construction and Building Materials*, 152:856–871.

Xu, Q. and Prozzi, J. A. (2014). A finite-element and newton–raphson method for inverse computing multilayer moduli. *Finite Elements in Analysis and Design*, 81:57–68.

Xu, Q. and Prozzi, J. A. (2015). A time-domain finite element method for dynamic viscoelastic solution of layered-half-space responses under loading pulses. *Computers & Structures*, 160:20–39.

You, Q., Ma, J., and Qiu, X. (2018). Finite element analysis of effects of asphalt pavement distressrs on fwd dynamic deflection basin.

Zhang, W. (2017). Effect of tack coat application on interlayer shear strength of asphalt pavement: A state-of-the-art review based on application in the united states. *International Journal of Pavement Research and Technology*, 10(5):434–445.

Zhang, Z., Zhang, X., Rasim, Y., Wang, C., Du, B., and Yuan, Y. (2016). Design, modelling and practical tests on a high-voltage kinetic energy harvesting (eh) system for a renewable road tunnel based on linear alternators. *Applied Energy*, 164:152–161.

APPENDIX A. DRAFT TEST METHOD FOLLOWING TXDOT TEMPLATE

Test Procedure for

TENSILE PULL OFF TEST

TxDOT Designation: Tex-255-F

Effective Date: Draft

1. SCOPE

1.1 Use this test method to evaluate the pull off adhesive properties of hot mix asphalt with a tack coat on concrete pavement in the field.

The procedure consists of:

- drilling 2-inch cores through hot mix down to the concrete pavement,
- cleaning the area and adhering pull-off stubs to the top of the core area,
- increase the core top temperature in-situ to accelerate the cure of the adhesive,
- decreasing the temperature of cores in-situ to the test temperature, and
- conducing pull-off testing to measure the tensile strength of the tack coat between the concrete and the hot mix layers.

1.2 The values given in parentheses (if provided) are not standard and may not be exact mathematical conversions. Use each system of units separately. Combining values from the two systems may result in nonconformance with the standard.

2. APPARATUS

2.1 Pull Off test apparatus, including sample metal stubs shown in Figure 1. (Proceq DY-206 has been found to be sufficient)

Figure 1. Pull Off Apparatus

DRAFT

2.2 Temperature control box. Open bottom box with temperature controls and the ability to condition the box atmosphere and the pavement surface the box is place on to 60F +/- XC and 25C +/- YC. The open bottom should be of dimensions to cover the surface of the HMA where cores will be taken (1-foot by 1-foot has been found adequate). See Figure 2.

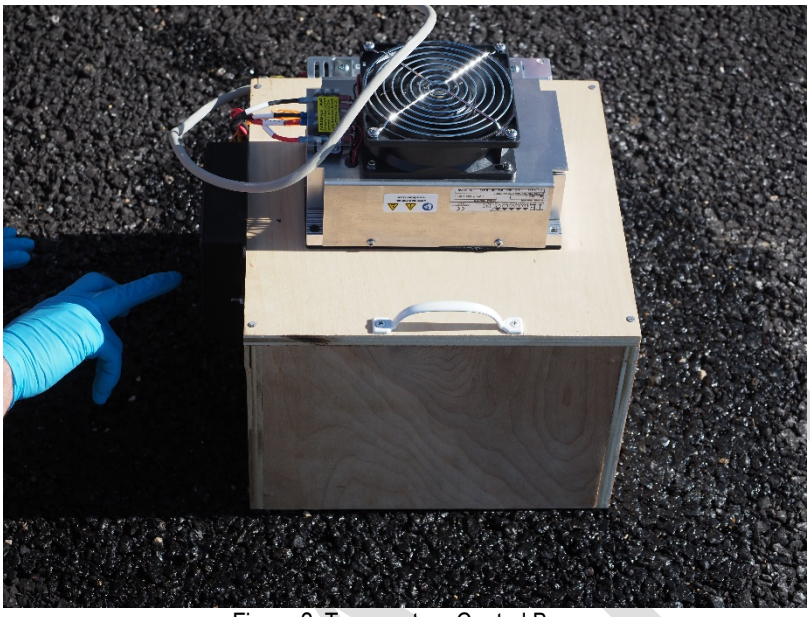

Figure 2. Temperature Control Box.

2.3 Core drill apparatus to drill 2-inch cores. This includes core rig setup, core drill barrel, water tank, hose and water (water is gravity fed to the core drill rig in use). See Figure 3.

Figure 3. Core Drill Apparatus.

2.4 Wet-Dry Vacuum of sufficient capacity to remove water and drill debris from core and core anulus.

2.5 Electric Generator of sufficient capacity to power the core drill, wet-dry vacuum, and the temperature control box.

2.6 Weights, of similar diameter to pull-off stubs, to keep stubs in contact with the core tops while the quick setting adhesive cures.

3. MATERIALS

3.1 Quick setting adhesive. Quick setting 2-component epoxy has been found to work.

4. PROCEDURE

4.1 At the project location, place the temperature control box on the pavement and mark the limits of the bottom on the pavement as shown in Figure 4.

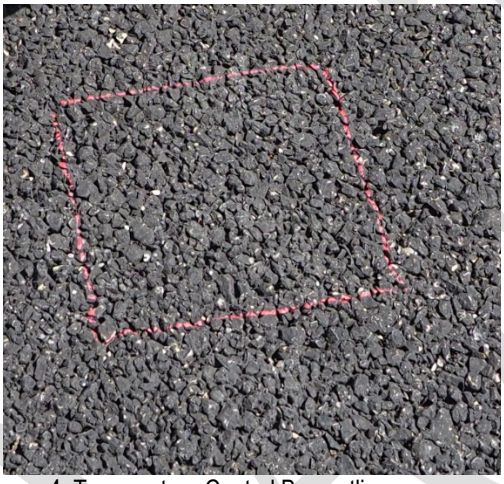

Figure 4. Temperature Control Box outline on pavement

4.2 Inside the temperature box outline, use the core drill apparatus to drill four cores spaced away from each other and away from the box outline to avoid the thickness of the temperature control box sides (the box outline represents the outside dimensions of the box). Cores should extend all the way through the HMA and to the top of the concrete pavement. Use the wet/dry vacuum to remove core cuttings and water from the coring process. See Figure 5.

Figure 5. Cores in box outline

DRAFT

4.3 Using a 2-component quick-setting adhesive, glue four testing stubs to the four core tops and apply weights on top of the stubs to maintain stub-adhesive-pavement contact until the adhesive sets. See Figure 6.

Figure 6. Applying adhesive, test stubs, and weights.

4.4 Place the temperature control box over the core area set at 60C for X minutes to facilitate the setting of the adhesive.

4.5 Change the temperature control setting to 25C and let the temperate equilibrate for Y minutes to come to test temperature.

4.6 Remove the temperature control box and test the pull-off strength of each core with the pull-off tester, See Figure 7.

DRAFT

Figure 7. Conducting Pull-Off test.

Note - Discard any specimens that break in the HMA instead of the HMA-Concrete Pavement interface.

5. CALCULATIONS

Tensile Pull-Off strength = TL (psi)
Where:
TL = Tensile Load (direct readout as measured with pull-off device, based on 2-inch diameter stub area).

6. REPORT

6.1 Report the average of the tests as the pull off strength of the sample. Make note of any samples that do not fail at the concrete pavement – hot mix asphalt pavement interface and do not include these in the average to report.

DRAFT

APPENDIX B. MODIFIED DRAFT TEST METHOD FOR TEX-249-F

Test Procedure for

SHEAR BOND STRENGTH TEST

TxDOT Designation: Tex-249-F
Effective Date: Draft

1. SCOPE

1.1 This test determines the shear strength between two bonded pavement layers. Test with or without normal load confinement. Test bonded, laboratory-molded specimens or roadway cores.

1.2 Measurements on two specimens constitute a single test.

1.1 The values given in parentheses (if provided) are not standard and may not be exact mathematical conversions. Use each system of units separately. Combining values from the two systems may result in nonconformance with the standard.

2. APPARATUS

2.1 Measuring device, such as a ruler or calipers.

2.2 Interlayer Shear Strength Device.

2.2.1 Interlayer Shear Strength Device without normal load confinement, capable of holding the test specimen horizontally and consisting of two parts:

- a fixed sleeve to hold one side of the specimen and to provide a reaction force; and
- a sliding sleeve holding the other side of the specimen that moves perpendicular to the specimen's vertical axis and produces the shear load. While testing, the sliding sleeve must only move vertically.

2.2.1.1 The device must accommodate 6-in. diameter cores.

2.2.1.2 Use core shims when testing cores that are more than 1/8 in. smaller than the target diameter. Shim thicknesses may range from 1/16 to 1/2 in. thick.

2.2.1.3 The gap between the sliding and reaction sleeves should be 1/4 in., and optionally adjust to accommodate larger gaps.

DRAFT

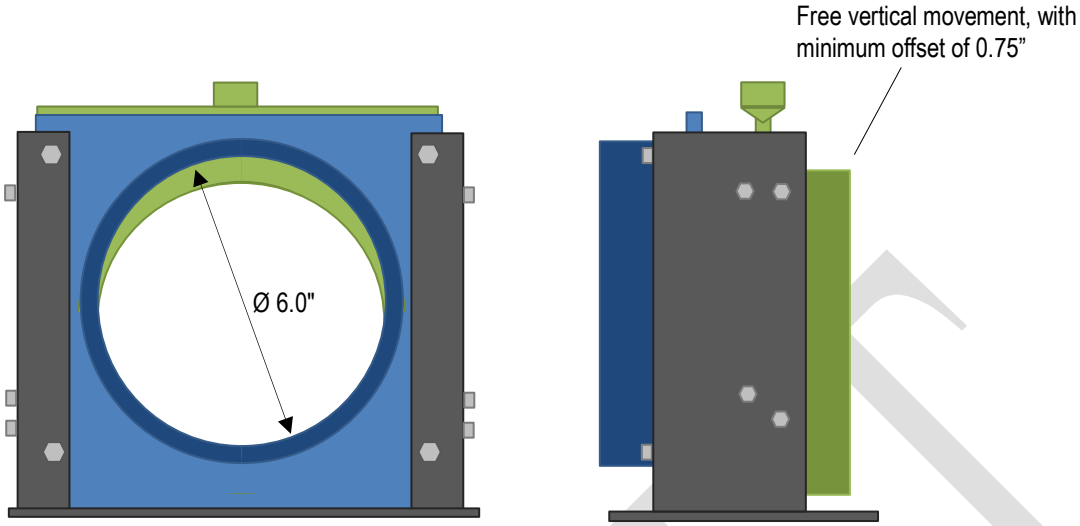

Figure 1—Interlayer Shear Strength Device (Side View)

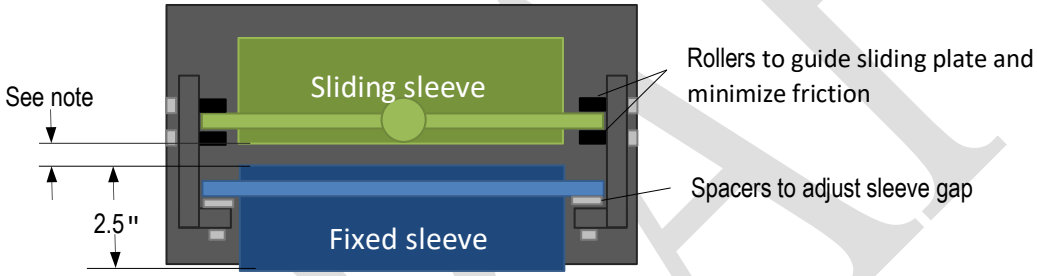

Note: Dimension can be adjusted to 1/4, 3/8, 1/2, and 3/4 in.

Figure 2—Interlayer Shear Strength Device (Top View)

2.2.2 Interlayer Shear Strength Device with normal load confinement meeting the requirements of AASHTO TP 114.

Note: This device is similar to the device described in 2.2, except it can provide lateral confinement.

2.3 Loading Frame, capable of applying a compressive load at a controlled deformation rate of 0.2 ± 0.02 in. per minute. The load cell should have a working range of 200 lb. – 5,000 lb. with an accuracy of 1%. A higher working range—up to 10,000 lb.—may be needed for unique scenarios.

DRAFT

Figure 3—Loading Frame with Shear Strength Device

2.4 2.4 Core Drill and Core Barrel.

2.5 2.5 Temperature Chamber or Heating Oven, capable of maintaining 77 ± 2°F.

3. PROCEDURE

3.1 Preparing Specimens. Specimens can be molded specimens or roadway cores.

3.1.1 Molded Specimens

3.1.1.1 Mold specimens with a Superpave compactor, in two layers with tack coat applied to the first layer before compacting the top layer.

3.1.1.2 Ensure that layers meet any density requirements.

3.1.1.3 Ensure that the specimen thickness meets the requirements of testing as described in this procedure.

3.1.1.4 The bottom layer may be a molded or cored concrete.

DRAFT

3.1.2 Roadway Cores.

3.1.2.1 Obtain two roadway cores with a diameter of 5.5–5.9 in. Obtain cores within three days of paving when testing for specification compliance (new overlay construction).

Note 1— There is no specific density requirement.

3.1.2.2 Mark the direction of traffic on the surface before coring.

3.1.2.3 Core the surface layer and at least 3.0 in. below the bonded interface. Remove the cores carefully to minimize stress to the bond and surrounding layers.

3.1.2.4 **Note 2**—Make a note if any core de-bonds at the interface in question during sampling. Save sample for visual inspection and report shear strength of 0 psi.

3.1.2.5 Trim cores so that the thickness between the bond and either specimen end is no more than 3.0 in.

3.1.2.6 Oven-dry the specimens at 100 ± 5°F to constant weight. Do not leave the specimens in the oven for more than 24 hr.

Note 3 — "Constant weight" is the weight at which further oven drying does not alter the weight by more than 0.05% in a 2-hr. or longer drying interval when calculated in accordance with Section 4.1.

3.2 Test Specimens using either the Interlayer Shear Strength Device without normal load confinement or Interlayer Shear Strength Device with normal load confinement

3.2.1 3.2.1 For each specimen, measure the diameter at four different locations to the nearest 1/16 in. and calculate the average of the readings.

3.2.2 3.2.2 Place the specimens in a chamber or an oven at 77 ± 2ºF for a minimum of 2 hr. before testing.

3.2.3 3.2.3 Slide a specimen into the shearing apparatus and position the bonded interface in question in the center of the gap. Orient core specimens so the traffic direction is vertical. As needed, insert core shims to limit free movement.

Note 4—Clearly mark the bond before placing the specimen in the apparatus to aid in locating the bond.

Note 5—Use shims when needed to ensure that the specimens are firmly held in place within the shear strength device. Ensure that core shims do not interfere with the shearing gap.

Note 6—Tighten the radial bolts on the shear device to keep the specimen from rotating or sliding. Do not overtighten the bolts to avoid damage to the specimen.

3.2.4 If testing with a normal confining load, apply the load desired.

3.2.5 Position the apparatus in the loading frame, apply the shearing load at a constant rate of displacement of 0.2 in. per minute, and stop after achieving the maximum load and the load has decreased substantially.

Note 7—Ensure the sliding half of the shear apparatus does not bottom-out during testing. This will damage the equipment.

DRAFT

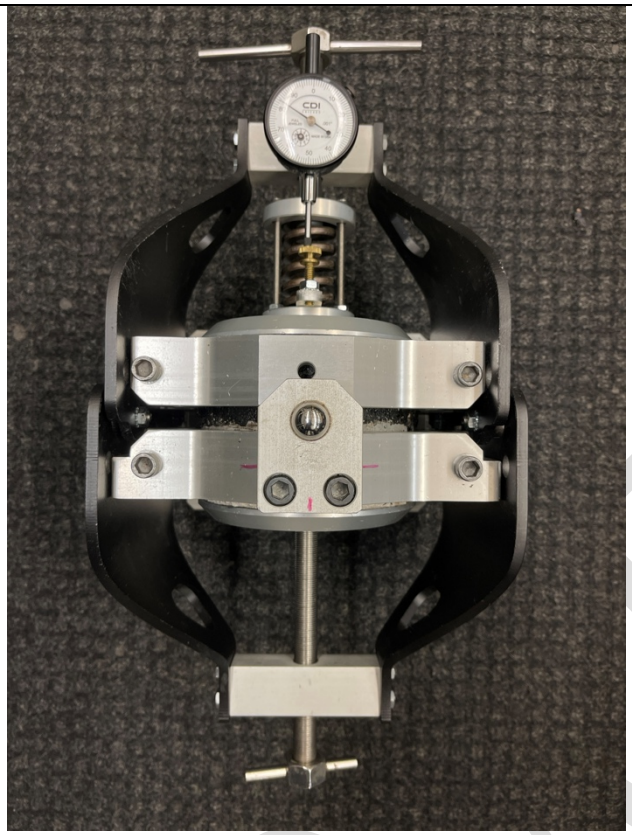

Figure 4— Sample Frame using the Interlayer Shear Strength Device with normal load confinement.

3.2.6 Record the maximum load.

3.2.7 Note the location of the failure (at the bond interface or in the adjacent layers).

3.2.8 Repeat Sections 3.2 for all specimens.

4. CALCULATIONS

4.1 For drying to constant weight, calculate the percent difference in weight:

$$Percent\ Difference = \left(\frac{\text{Initial Weight} - \text{Final Weight}}{\text{Initial Weight}}\right) * 100$$

4.2 Calculate the maximum shear strength of each specimen: $Shear_{max} = 4 * F_{Max}/(\pi D^2)$

Where:

$Shear_{max}$ = Maximum shear strength, psi

F_{Max} = Maximum load, lb.

D = Average specimen diameter, in.

DRAFT

5. REPORT

5.1 Report the following:

- maximum shear strength and location of failure of individual specimens;
- average shear strength of the specimens; and
- additional comments.

5.2 Report the average shear strength of the tested cores to the nearest tenth psi.

DRAFT

APPENDIX C. VALUE OF RESEARCH

PROJECT TITLE

Develop Guidelines and Best Practices for Bonding Hot-Mix Asphalt to Portland Cement Concrete Pavement.

PROJECT STATEMENT

Asphalt overlaid on concrete pavements can result in bond failures that are likely due to one or more factors (e.g. properties of the tack coat, application rate of the tack coat, the type and texture of the concrete layer). The goal of this study was to identify, develop, and validate a test method that can be used on a routine basis to screen and/or field-test the quality of the bond between the asphalt and the concrete layer; use the method to evaluate the impact of various factors on the performance of the bond including but not limited to type of tack coat or membrane, application rate, surface texture (including cost-effective and innovative ways to prepare concrete surfaces), surface moisture, and concrete material type; and propose guidelines for future selection of surface preparation techniques and materials that will meet the requirements for adequate bonding at the interlayer surfaces. Table C.1 presents a summary of the functional areas and benefits from Project 7057.

Table C.1. Functional Areas for Project 0-7057

Benefit Area	Qual	Econ.	Both	Tx-DOT	State	Both
Level of knowledge						
Customer satisfaction	X			X		
Increased service life						
Reduced Construction, Operations, and Maintenance Cost		X			X	
Infrastructure condition						

QUALITATIVE BENEFITS

Level of knowledge

This project conducted an extensive survey of the literature to identify the different process and controls used by other states to ensure lack of failure at the asphalt-concrete interface. The final report from this project will serve as an excellent reference document and knowledge basis for use by area engineers and other relevant personnel in TxDOT. This study also conducted numerical modeling of the stresses at the interface considering several different types of loading scenarios and pavement structures. This part of the study will also serve as a useful resource for pavement design and decision making by engineers within TxDOT and also engineers outside of TxDOT who are involved in pavement overlay design process.

Customer Satisfaction and Infrastructure Condition

Loss of adhesion between the asphalt and concrete overlay can result in shoving and formation of pot holes and other distresses. These distresses not only impact ride quality but also create serious traffic safety issues. Also, typically asphalt on concrete overlays are used in areas with very high traffic volumes. Consequently, the costs of shutting down traffic and repairing the damage can be extremely expensive and result in high volumes of lost time by road users due to congestion during the repair process. Therefore, prevent bonding failures can avoid poor experience by the road users.

ECONOMIC BENEFITS

Increased service life and Reduced costs

This project started on September 1, 2021 and completed on August 31, 2022 with a duration of 2.0 years. The total budgeted cost for this project was $310,076. The project was completed on time and under budget. The total budget includes the budgeted cost for the two agencies that were involved in this study (CTR at UT Austin and UT San Antonio). For the purposes of this analysis and considering full implementation of the recommendations, the following were considered:

- Based on the most recent inventory, TxDOT has approximately 14,000 lane

miles of composite pavement, which is mostly asphalt overlay on a concrete pavement.

- Considering a full design life of 25 years (conservatively high estimate) without any premature failures due to debonding, also conservatively considering that this no growth in this segment of pavements, and considering that these sections were built uniformly over the past 25 years, TxDOT can expect approximately 560 lane miles of asphalt on concrete overlays that will need to repaired and replaced every year.
- Based on recent estimates, the cost of asphalt overlay is approximately $100 per metric ton. Further considering, a typical 2-inch overlay, the material cost of one lane mile of overlay is approximately $75,000. This is again a conservative estimate without including the cost of traffic control, indirect cost impact to roadway users, striping etc.
- Based on the above, asphalt overlays cost approximately $42 million each year. Adoption of the recommended guidelines from this study can prevent or significantly reduce debonding failures. If such failures are estimated in 1% of the cases, then this translates into savings of $0.42 million per year. In fact, during the course of this project and among the six different field sections that were reviewed and used, at least two had reported failures (one was a failure that occurred a few years ago and had to be repaired and repatched) and the other was more recent.

The aforementioned parameters were used to obtain the NPV for this project as shown in Figures C.1 and C.2.

Texas Department of Transportation	**Project #**	0-7070			
	Project Name:	Develop Guidelines and Best Practices for Bonding Hot-Mix Asphalt to Portland Cement Concrete Pavement			
	Agency:	CTR	**Project Budget**	$	310,076
	Project Duration (Yrs)	2.0	**Exp. Value (per Yr)**	$	420,000
Expected Value Duration (Yrs)		10	**Discount Rate**		0%
Economic Value					
Total Savings:	$ 3,469,924	**Net Present Value (NPV):**		$	3,889,924
Payback Period (Yrs):	0.738276	**Cost Benefit Ratio (CBR, $1 : $___):**		$	13

Figure C.1. Parameters used for economic analysis for VOR.

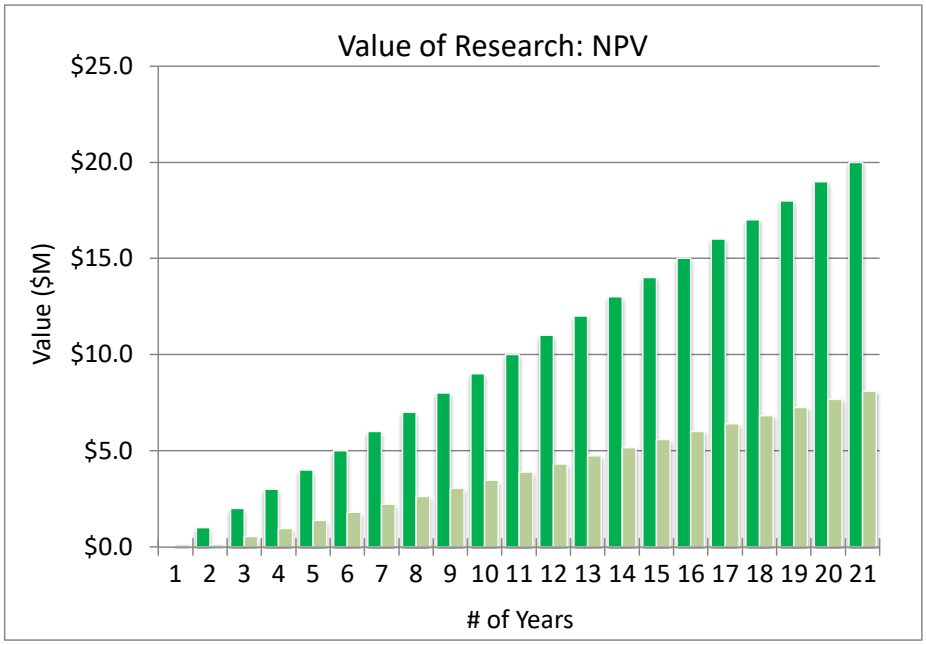

Figure C.2. Illustration of the NPV over a period of 20 years.